UNIVERSITY OF TECHNOLOGY SYDNEY
Faculty of Engineering and Information Technology

Dynamic Spectrum Sharing and Coexistence with Full-Duplex Device-To-Device Communications in 5G Networks

by

Noman Haider

A Thesis Submitted
in Partial Fulfillment of the
Requirements for the Degree

Doctor of Philosophy

Sydney, Australia

2019

CERTIFICATE OF ORIGINAL AUTHORSHIP

I, Noman Haider declare that this thesis, is submitted in fulfilment of the requirements for the award of Doctor of Philosophy (PhD), in the School of Electrical and Data Engineering, Faculty of Engineering and Information Technology at the University of Technology Sydney.

This thesis is wholly my own work unless otherwise reference or acknowledged. In addition, I certify that all information sources and literature used are indicated in the thesis.

This document has not been submitted for qualifications at any other academic institution.

This research is supported by the Australian Government Research Training Program.

Signature: Production Note: Signature removed prior to publication.

Date: 17/09/2019

ABSTRACT

Opportunistic Spectrum Access has recently become the most desirable solution for greatly improving the performance of telecommunication systems. It has proven to be a viable solution to cope with the challenging problem of spectrum scarcity and also it has been widely explored in 5G networks, so that multiple random access technologies can coexist in a cognitive setup. In 5G networks, such secondary technology candidates like Device-to-Device (D2D) communications, and Licensed-Assisted Access are envisioned to opportunistically exploit spectrum opportunities and coexist with primary technologies like LTE or WiFi. Moreover, Full Duplex (FD) technology is envisioned to play a significant role in 5G networks by allowing a user to transmit and receive on the same frequency band.

In this thesis, we present a comparative performance analysis of the spectral efficiency in a heterogeneous system where a cellular network allows the FD-Enabled D2D network to use opportunistically its spectrum while ensuring protection for its transmission/reception through guard zones. The main contributions and emphasis of this work are to explore the spectrum opportunities for secondary users by: firstly, deriving their probability of successful transmissions, deciding the feasible mode of operation (half-duplex, full-duplex or silent); and secondly, incorporating the protection zone for primary users. We assess the overall system performance, analyze the impact of different access mechanisms and propose an efficient mode selection for secondary users.

Such a systematic analysis of the integrated technologies requires a rigorous and critical evaluation of the performance gains and the costs incurred in terms of increased interference. Also, ultra-dense and random network models are envisioned in future networks especially in the urban scenario, hence, pre-deployment average system performance over various deployment scenarios can in fact be advantageous. In this thesis, we use stochastic geometry to model and analyze different coexistence scenarios and spectrum sharing frameworks in 5G networks for multiple radio access

technologies. We also assess different coexistence methodologies for secondary users to fairly and peacefully coexist with primary users while ensuring the interference protection for primary users.

In summary, FD enabled heterogeneous networks have not been critically studied in previous literature, and for this reason a comprehensive study on the use of FD to existing systems is needed. This thesis proposes an innovative FD enabled D2D cognitive setup and carefully studies the improvement in system performance while taking into account the cost of these gains in 5G networks, using stochastic geometry tools.

ACKNOWLEDGEMENTS

First and foremost, I would like to acknowledge that this work has been supported by University of Technology Sydney (UTS), and Macquarie University. I am very grateful for this research opportunity and financial support to complete my studies.

I would like to express my sincerest and deepest gratitude to my supervisor Prof. Eryk Dutkiewicz for his tremendous support, encouragement and kindness during my research work. I acknowledge his helpful and supportive professional advisory role. I also gratefully acknowledge Mr. Ahsan Ali for his continuous technical support, guidance and help throughout this journey. Additionally, I also acknowledge a great technical support, feedback and help from Mr. Cristo Suarez-Rodriguez.

I would like to thank Prof. Ren Ping Liu, Dr. Ying He, Dr. Beeshanga Abewardana Jayawickrama, Shubhekshya Basnet, Meriam Bautista and Hasini Abeywickrama. My sincere gratitude to all UTS colleagues and friends, whose appreciating support will always be remembered.

I acknowledge tremendous support, motivation and love provided by parents, and siblings, especially Dr. Muhammad Imran. Their continuous encouragement and sacrifices has played a key role in the completion of this degree. I also thankfully acknowledge support and motivation from my wife Mrs. Komal Saifullah Khan.

This journey would not be pleasantly memorable without love and care of my friends, who are real asset of my life. I am thankful to Affan Aziz, Amjad Raza, Hassan Faraz, Ijlal Usmani,Raheel Niaz, Nazar Waheed, Tariq Khan and my housemates. Thanks to anybody whom I may have unintentionally missed who deserves a mention.

Noman Haider

Sydney, Australia, 2019.

List of Publications

Journal Papers

J-1. **Noman Haider**, Ahsan Ali, Cristo Suarez-Rodriguez, Eryk Dutkiewicz, "Optimal Mode Selection for Full-Duplex Enabled D2D Cognitive Networks", *IEEE Access*, 2019.

J-2. Cristo Suarez-Rodriguez, **Noman Haider**, Ying He, Eryk Dutkiewicz, "Network Optimisation in 5G Networks: a Radio Environment Map Approach", in *IEEE Transactions on Vehicular Technology*, 2019 (Submitted).

Conference Papers

C-1. **Noman Haider**, Ahsan Ali, Ying He and Eryk Dutkiewicz, "Performance Analysis of Full Duplex D2D in Opportunistic Spectrum Access," 18th International Symposium on Communications and Information Technologies (ISCIT), Bangkok, 2018, pp. 32-37.

C-2. **Noman Haider**, Eryk Dutkiewicz, Diep N. Nguyen, Markus Mueck, Srikathyayani Srikanteswarae, "The Impact on Full Duplex D2D Communication of Different LTE Transmission Techniques," IEEE 85th Vehicular Technology Conference (VTC Spring), Sydney, NSW, 2017, pp. 1-5.

Contents

List of Figures

Abbreviation

2D - Two-dimensional

3GPP - 3rd Generation Partnership Project

BS - Base Station

CA - Carrier aggregation

CS - Carrier Sense

CBRS - Citizen Broadband Radio Service

CSMA - Carrier Sense Multiple Access

D2D - Device-to-Device

EZ - Exclusion Zone

FD - Full-Duplex

GZ - Guard Zone

HD - Half-Duplex

LAA - Licensed Assisted Access

LSA - Licensed Shared Access

LTE - Long Term Evolution

M2M - Machine-to-Machine

MNOs - Mobile Network Operators

MHPP - Matern Hardcore Point Process

OSA - Opportunistic Spectrum Access

PHP - Poisson Hole Process

PPP - Poisson Point Process

PU - Primary Users

RAT - Random Access Technologies

RX - Receiver

SAS - Spectrum Access System

SG - Stochastic Geometry

SIPR - Self-Interference-to-Power-Ratio SU - Secondary Users

TX - Transmitter

UDN - Ultra-dense Networks

WiFi - Wireless Fidelity

Chapter 1

Introduction

The communication systems have transformed wide and distant worlds into one global space. Starting from carrier pigeons (dedicated messengers), to mechanical telegraphs followed by dedicated connections, communication systems finally became wireless. These revolutionary advances and huge strides in technology completely overhauled the communication process, leading to convenience, reliability and timely delivery. In the last few decades, this evolution has yielded one of the most efficient, record performance-based next generation communication systems (5G). This chapter begins with a concise background of wireless communications followed by a discussion of the architectural overview and key enabling technologies of 5G networks. Major enhancements in 5G and significant design changes are discussed followed by the research challenges addressed in this work. Then, the motivation, contributions, and organization of this thesis are presented, followed by the summary of this chapter.

1.1 Background

Recent technological proposals in the field of wireless communication have brought forth many innovative solutions which have kept on improving the service quality, network efficiency and offered services. For instance, 3G offered the internet and multimedia services to users in their handheld devices, 4G further increased the data rates, capacity and bandwidths, and now, 5G is bringing what was deemed impossible a few years back to reality in the next few years. Since Long Term Evolution (LTE) employing 4G started rolling out with incremental improvement to previ-

ous technology and more room in the new spectrum, the visionaries started eyeing a paradigm shift toward 5G with more spectrum opportunities, ultra-dense Base Station (BS) and device densities, spatial Multiple Input Multiple Output (MIMO), Non-Orthogonal Multiple Access (NOMA), Full Duplex (FD) and Network Vitalization (NV) [1].Several key enabling technologies have been explored, researched, and among them successful ideas have been standardized in 5G [2]. This thesis presents work explored in the field of Opportunistic Spectrum Access (OSA) and how it can be exploited by different Radio Access Technologies (RATs) while protecting existing users from induced interference.

1.2 5G Network Design Architecture and Enabling Technologies

The architecture and capabilities of the next generation of both cellular and local wireless networks are driven by the demands and requirements of an increasing number of connected devices. The 5G system aims to provide a single unified platform for integrating all types of communications (existing and new) within a single system.

1.2.1 Architectural Overview

The 5G networks are expected to provide support for all types of communication with adaptable system protocols tuning according to user requirements. Unlike the earlier generation of networks, where control and processing tasks are heavily assigned to the infrastructure side, 5G aims to balance this factor by considering advanced capabilities of M2M devices and smart UEs. It means devices are not just endpoints; they are instead an integral part of overall systems. The cloud-assisted centralized systems and Network Function Virtualization (NFV) in 5G for efficient resource utilization and application management will play a pivotal role in managing

Internet-of-things (IoT) and Machine-to-Machine (M2M) communications. A key to the success of these systems heavily relies on segregation of user and data planes.

The fundamental design aspect of 5G is to bring forth a unified solution in terms of both hardware and software for end users and network operators, appearing as one transparent system integrated with legacy and novel technological components providing seamless user experience. Figure 1.1 manifests legacy and new technological advances which are expected to be an integral part of 5G. These technologies are key enablers for 5G and will be incorporated as a native part of next generation networks. Thus, the question arises: what are those major enhancements which are going to significantly elevate the performance of these networks?

1.2.2 Major Enhancements in 5G Networks

The challenging design objective of 5G is to provide connectivity to more than one trillion devices with diverse characteristics and application requirements. According to a white paper published by Nokia Networks, mobile data volumes may grow up to 1000-fold from 2010 to 2020, while data rates in individual mobile cells are also expected to grow to the peak rates of 1Gbps [3]. Moreover, the number of mobile broadband subscribers will grow by 10% per year and each subscriber will have an average of 25-50% more data per year. At a core router level, total traffic is doubling every 18 months, and mobile data (GSM, LTE) is growing by 92% every 12 months [4]. According to another survey published by CISCO, it presents an annual visual networking index which shows a 13-fold increase in mobile and internet data traffic from 2012 over 5 years time [5]. Moreover, mission-critical M2M applications require minimum latency while applications like smart metering are delay tolerant. Such a broad range of applications with diverse QoS requirements leads to significant enhancements in 5G [6]. The following two major enhancements are foreseen in upcoming 5G networks, which brings into being compatible and integrated support

for complementary technologies within the scope of this work.

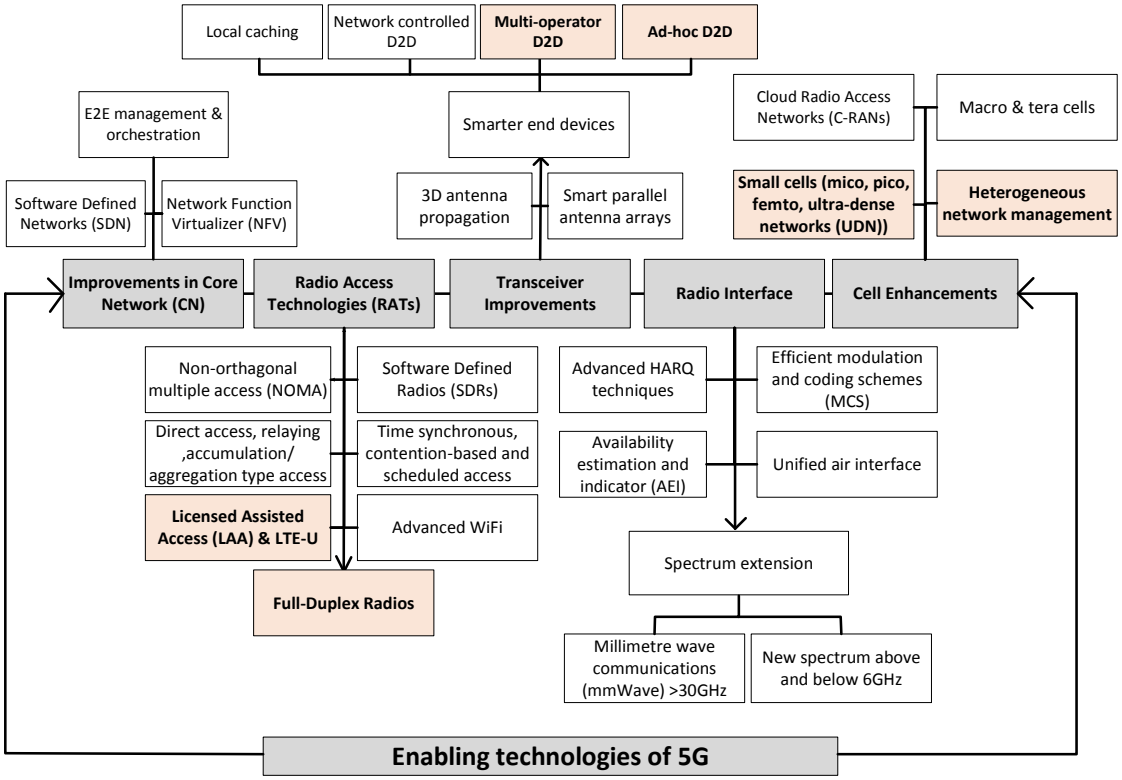

Figure 1.1 : Key enabling 5G technologies (technologies highlighted in orange are the focus of this work).

Spectrum Sharing

Spectrum sharing frameworks have significantly proven their performance advantages and played a vital role in optimizing user capacity and socio-economic benefits of existing communication systems [7]. Among these proposals, Cognitive Radio (CR), TV white spaces, Citizen Broadband Radio Service (CBRS) and Licensed Shared Access (LSA) have proven their worth as effective solutions for spectrum under-utilization. Generally, spectrum sharing methods can be categorized as either centralized or distributed in character. In distributed techniques, the users employ some fair-medium access mechanism to ensure peaceful coexistence with the

other contenders, while users contact a centralized authority for access in a centralized approach. The key aim of sharing methods is to increase spectral efficiency on the basis of a use-it or share-it basis, where, Primary Users (PUs) can share/lease under-utilized spectrum on a short-to-medium or short-to-long term basis with Secondary Users (SUs). This sharing is done based on pre-defined conditions for leaving the spectrum for priority users whenever needed and imposing the least interference on PUs. Spectrum sharing can be done in the time domain (primary user is not transmitting), space domain (primary user is far away) and frequency domain (primary user is transmitting on a different frequency). Different envisioned spectrum sharing frameworks and coexisting multiple random access technologies envisioned in 5G are also shown in Fig. 1.2. In this work, we also investigate the performance of three different coexistence techniques employed by the users in chapter 5.

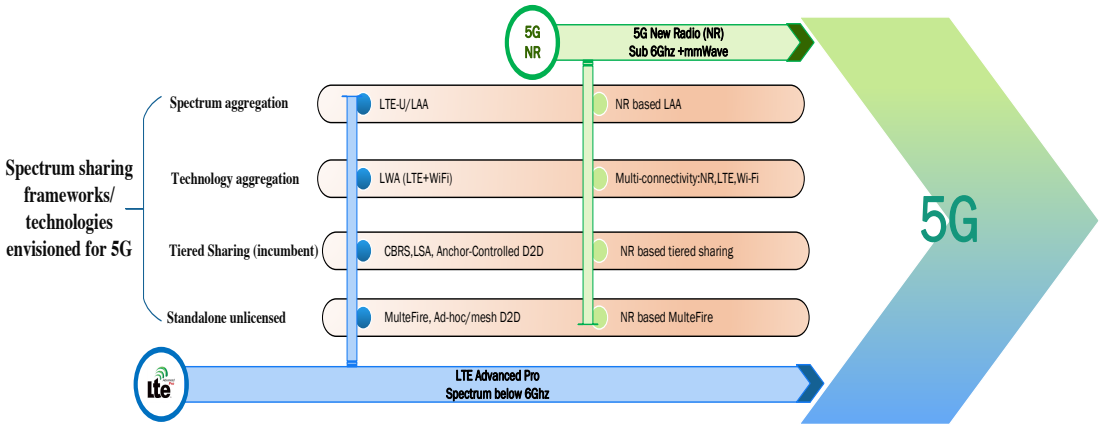

Figure 1.2 : Spectrum sharing frameworks, methods and frameworks envisioned in 5G for different radio access technologies [8].

Device-to-Device Communications

Device-to-Device (D2D) communications emerged from the concept of cooperative communications and came into the spotlight when considered as one of the key enabling technologies in 5G [9]. Previously, in voice-centric systems, connecting

distant users through dedicated network resources was the baseline objective. Over time, data-centric sharing frameworks exhausted the network resources. This lead to new proposals and technologies to off-load the users to secondary networks. For instance, in ultra-dense, congested and co-located environments, it is inefficient to burden the core network where devices can form an ad-hoc mesh network to wirelessly share the content (e.g. pictures, videos, files,) or interact (e.g., video gaming or social networking) [10]. This concept shifted the center of gravity in the context of innovation, investment, and advancement from the core network toward the smarter end devices. The cell-centric architecture shifts to device-centric network design, where devices partially share the control of network resources. The D2D is envisioned to be a promising technology in this direction. We have studied the integration of D2D with other radio access technologies in the context of opportunistic spectrum sharing in this work (Chapter 3).

Full Duplex

In Full-Duplex (FD) communications, an FD transceiver of the device is capable of transmitting and receiving at the same time using the same frequency bands [11]. Previously, due to limitations in antenna design and impracticality of in-band transmissions and reception, FD technology was not considered for mainstreaming. However, recently due to significant advances in minimizing residual self-interference-to-power-ratio (also referred to as self-interference suppression or cancellation), these have paved the way for FD use to double the data rates and are envisioned to increase the capacity of 5G systems [12]. For instance, practically the cancellation capability of 70dB can be achieved using compact/separated antennas at the bandwidth of 100MHz in 2.6GHz band [12]. Thus, in-band FD communications integrated with D2D technology will elevate the spectral efficiency while doubling the data rates [13]. Moreover, recent research has indicated the elevation of

spectral efficiency (up to 100%) in single-cell and single D2D link scenarios as compared to half-duplex (HD) if sufficient residual SIPR reduction is achieved [14–16]. FD communication also captivated the interest of the research community with its advantages and applications in cognitive radios [17–19]. We have investigated the integration of FD technology with legacy systems as envisioned in 5G and performed the feasibility study in terms of comparative performance analysis of the system (Chapters 3-4).

Extension of Radio Spectrum

One of the prominent features of 5G is employing newly available spectrum in licensed and unlicensed bands, while also exploring the unused spectrum in sub6GHz and mmWave bands. Feasibility studies received great interest to test the practicality and scenarios for the use of such new spectrum bands which haven't been used before [20–22]. Fig. 1.3 shows current in-use and prospective frequency bands to be explored around different regions of the world. Such diversity in use of spectrum from different categories is driven by the device's ability to utilize inter and intraband frequencies from different bandwidths using Carrier aggregation (CA) framework. This was proposed in Release 10 of the 3rd Generation Partnership Project (3GPP) [23]. The 3GPP started the study item for LTE deployment in unlicensed bands a few years ago in late 2015. The major challenge highlighted was attaining a fair and peaceful coexistence with other incumbents operating in the same bands as WiFi IEEE802.11x. Two versions of LTE-unlicensed bands were proposed according to regional regulatory requirements and coexistence i.e. LTE-Licensed Assisted Access (LTE-LAA) and LTE-Unlicensed (LTE-U). The LAA requires control signals from traditional licensed bands in macro cells to use unlicensed bands for data services in small micro or picocells. Conversely, LTE-U can be employed as a standalone to support the primary carrier in WiFi like fashion.

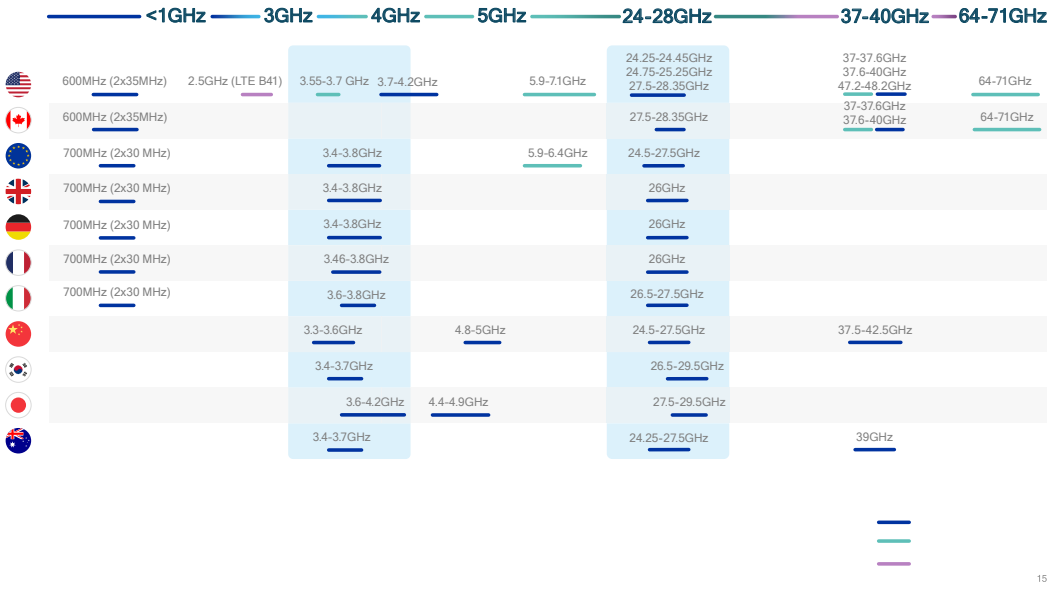

Figure 1.3 : Existing, new and upcoming spectrum for 5G worldwide [8].

The coordinated multi-points among multiple base stations (BSs) and direct device-to-device (D2D) communication also opened up another major research area in 5G, which focuses on advanced interference mitigation and avoidance techniques. This is because interference mitigation directly helps to increase spectrum utilization by allowing frequency bands to be reused [24]. Moreover, the significant amount of spectrum in unlicensed bands can serve to augment network capacity and performance to meet the requirements of 5G systems. For instance, the 5GHz spectrum has several bands available for use globally. The aggregate spectrum available in the 5GHz band is 605MHz in the US and 455MHz in Europe. The amount of this spectrum can be appreciated by noting the total amount of licensed spectrum in the 700-2600 MHz range is approximately 670 MHz in Europe and Asia. In addition to currently available bands, the 5350-5470 MHz band may also potentially become available for use in the US and Europe. In addition to this, the 5350-5470 MHz band may also potentially become available for use in the US and Europe. Thus, 3GPP and Mobile Network Operators (MNOs) are now moving to utilize this spectrum

for mobile data. Fig. 1.4below illustrates the 5GHz spectrum with WiFi channel numbers, DFS requirements and prospective channels which may be available for use as well. As per regional regulations, some channels are obliged to follow DFS requirements [25].

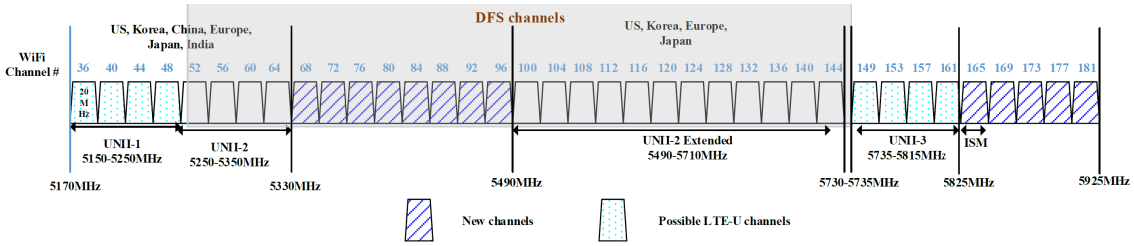

Figure 1.4 : The 5GHz spectrum for WiFi channels, DFS requirements and expected spectrum extension for 5G targeted by LTE-unlicensed.

Cell enhancements

Cell enhancements will play a pivotal role in serving Ultra-Dense Networks (UDN) where a massive number of devices per cell will be competing for limited network resources [26]. For instance, phantom, micro, pico, and femtocells are used as underlying networks for data transmission or reporting by D2D devices along with macrocells. Nevertheless, an interesting concept involving phantom cells for segregation of control and data planes has also shown potential performance improvements. The key idea is to use macrocells for control signaling over microwave or cellular frequencies, while, microcells will be used for data services operating on high frequencies. This use of different frequencies will bring forth a great improvement in terms of spectrum efficiency, network capacity, and coverage through D2D like technologies. More details concerning cell enhancement techniques in different scenarios for LTE-Advances are given in [27]. Further taxonomy of proposed and envisioned technological improvements in 5G are presented in Fig. 1.5.

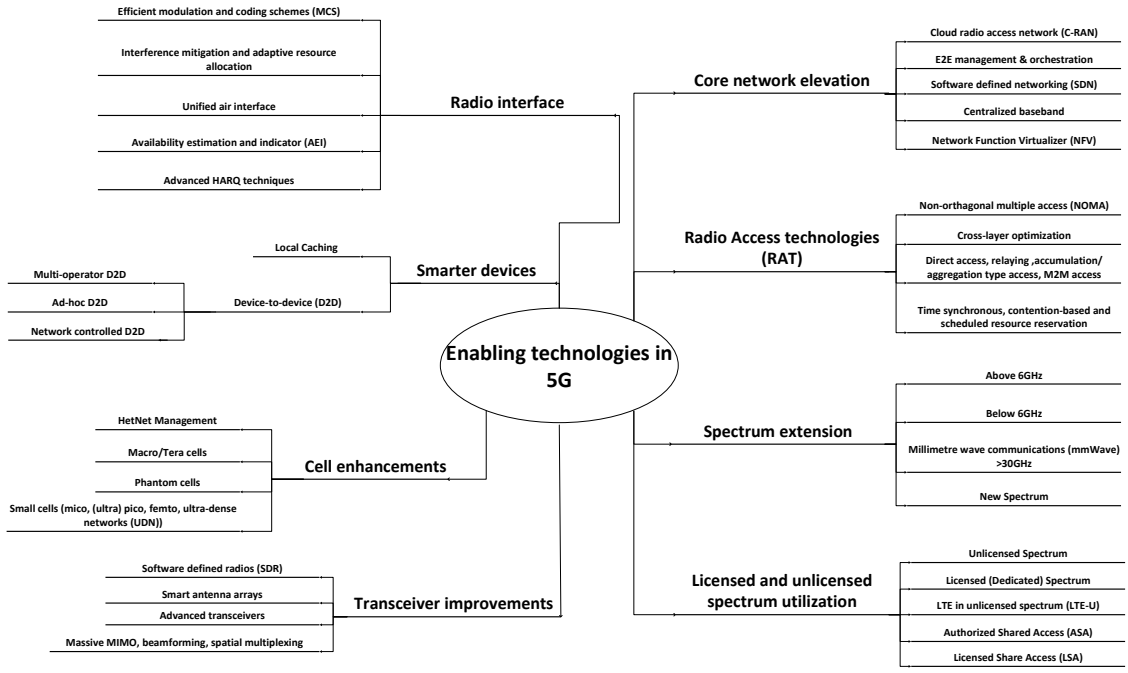

Figure 1.5 : Taxonomy of key enabling technologies and improvements envisioned for 5G.

1.3 Stochastic Geometry for 5G Networks

Stochastic Geometry (SG) and random graph theory have proven to be an effective mathematical platform to model variants of communication networks while characterizing the key network parameters [28]. Due to topological and spatial randomness, SG can successfully yield tractable and in special cases, closed-form expressions that reflect the systems behavior. Alternative methods for performance evaluation of cellular networks include exhaustive simulation scenarios to average out the randomness of different network parameters (base stations, user locations, and fading distributions). However, these methods are time-consuming, prone to errors and require immense funding resources for testing proof of concepts [29]. Therefore, SG provides a supplementary platform to produce baseline results for benchmarking and comparison [29]. The SG model has also proved to be a close approximation

to a grid model, and actual network deployment [30]. SG has widely been accepted to model, design and analyze different technology integrations [31, 32], spectrum sharing methods [33, 34], heterogeneous coexistence [35], cognitive networks [36], and future wireless networks (5G) [37].Inspired by the traditional use of SG tools for the design and analysis of communication systems, we have adopted the SG to assess two things: the integration of different technology aggregation, and spectrum sharing techniques envisioned for 5G.

1.4 Challenges and Objectives

The device-centric architecture and rise of short-distance communication technologies (D2D, M2M, etc.) in 5G for capacity elevation and efficient spectrum utilization required a rigorous feasibility study. The impact of increased heterogeneity in ultra-dense networks on traditional and incumbent users were open research problems. For instance, pushing network operators to lend the underutilized spectrum to secondary network operators on share-it or use-it basis may cause severe disruption of services to primary users. Frequency reuse is a pivotal trait of spectrum sharing in multi-tier networks, yet such reuse induces aggressive interference proportional to the users who are permitted to use the frequency. Hence, the mechanics of spectrum sharing among K-tier users based on an agreed upon set of rules, interference protection, and QoS guarantees require extensive system analysis. Such analysis requires modeling the complex network geometry which closely captures the spatial location of users and inter-dependencies among different tiers.

Motivated by new spectrum sharing frameworks envisioned in 5G along with the new multiple RATs, we aimed to explore the integration of these technologies in legacy systems. Due to a high degree of randomness, ultra-dense deployment scenarios, and heterogeneity, we adopted a well renowned stochastic geometry framework to capture the abstract level performance analysis of different technology integration

and spectrum sharing methods. The key objectives of this work are as follows.

- Proximity based small cell or ad-hoc D2D communications are expected to ease the load from macrocells. We aim to study such a D2D enabled cellular network and how it impacts on the performance of the overall system.
- Since the Full Duplex (FD) technology is still not widely accepted practically for end devices due to a limitation in residual SIPR cancellation, it is interesting to explore what it would cost to achieve the double data rates if FD is used in user devices. When and how should a device select half-duplex or full-duplex modes?
- We aim to investigate the use of FD capable D2D users with a cellular network in a cognitive setup and quantify the gains from FD operation while taking into account its cost.
- Considering the multi-tier cellular network, we use SG to characterize the interference faced by the transmitting/receiving user to find the trade-off between spectrum utilization efficiency and capacity gains offered by a particular spectrum sharing method.
- The CBRS, LSA and similar spectrum sharing models keep on opening the opportunities for spectrum utilization efficiency by conditionally allowing the unlicensed users for temporal use of unused frequency bands. Our aim is to study the impact of such coexistence and how it influences the incumbent users. We study different coexistence methods to test the feasibility and fairness of each method.

1.5 Contributions

The main contribution of the thesis can be summarized as follows,

- We design, model and evaluate a stochastic geometry model for FD enabled D2D cognitive network, where a primary user has guaranteed interference protection from a secondary user (FD D2D). Interference protection is ensured by drawing a guard zone around the primary user. The developed model also proposes an optimum mode selection (FD, HD or Silent) for D2D users in the vicinity of the primary users guard zone in such a way to elevate the capacity of secondary users while protecting the primary users communication. We critically study the trade-off to harvest the gains of FD equipped D2D and the induced interference faced by the primary user. Furthermore we incorporate the impact of imperfect residual SIPR to overall induced interference when the D2D link operates in FD mode. The performance of a primary user is assessed through extensive simulations which are validated with theoretical results.

- Considering the Rayleigh fading channel, the coverage probability of D2D users is evaluated. We assess the capacity of FD enabled D2D to operate as secondary users in an ad-hoc manner while LTE users are transmitting. Using SG tools, we analyze the average successful transmissions for D2D links which exploit opportunistic spectrum access. Multiple concurrent cellular and D2D transmissions are simulated for an aggressive interference scenario and flexibility for which D2D users can still find the spectrum opportunities.

- We investigate the impact of different transmission techniques proposed for versions of LTE-unlicensed spectrum with other technology candidates in unlicensed spectrum. The trade-off between the benefits of transmission techniques and their impact on the performance of competing technologies in the unlicensed spectrum is critically analyzed. We use SG, Monte-Carlo simulations and discrete link level ns3 simulator to simulate the network realization for multiple RATs competing for channel access. The feasibility of such a coex-

istence is thoroughly investigated by characterizing the interference fields and calculating the average success probability for each type of user. Moreover, the impact of imperfect to perfect residual SIPR is studied.

1.6 Thesis Organization

This chapter presented the context of the topic, discussed the research problems addressed and contributions of the presented work. The thesis organization and scope of each chapter is illustrated in Fig. 1.6. The rest of the thesis is organized as follows.

In Chapter 2, we present the literature review on the scope of this work. In section 2.1, we summarize the key enabling technologies, frameworks and standardization activities envisioned for future networks (5G). Section 2.5 presents a taxonomy of the literature review in the context of state-of-the-art SG tools for modeling, design, and analysis of similar communication networks. Section 2.4 summarizes the key spectrum sharing frameworks, methods, and network models for licensed, unlicensed and cognitive setups. The key features of the related works are listed and short-comings are noted, which lead to the motivations for doing the work presented in Chapters 3,4 and 5.

Chapter 3 presents the SG model of a FD enabled D2D cognitive network. Building on the brief introduction in section 3.1, followed by the closely related works in section 3.2, we present our system model, a methodology of analysis and performance metrics in section 3.3. Analytical modeling for optimal mode (silent, HD or FD) selection for a D2D link is given in section 3.4. Finally, simulation results validated with theoretical results are presented in section 3.6, followed by the summary in section 3.7.

In Chapter 4, the SG-based success probability for FD and HD users is evaluated

based on the interference experienced by a D2D communication link. Section 4.1 outlines the introduction of the chapter, followed by discussion on related literature in section 4.2. Section 4.3 presents the system model considered for the simulation setup. Interference characterization for a D2D link using SG tools is evaluated in section 4.4. Section 4.5 presents key findings from simulations results, followed by the summary of the chapter presented in section 4.6.

In Chapter 5, section 5.1 presents the introduction and related work for dynamic spectrum sharing in the unlicensed spectrum. Section 5.2 evaluates the impact of different LTE transmission techniques on the FD enabled D2D cognitive network. This is followed by section 5.3 which presents ns-3-based results and analyses for the coexistence of LTE-unlicensed and the most dominant incumbent in unlicensed WiFi. Section 5.4 briefly summarizes the key features of the chapter.

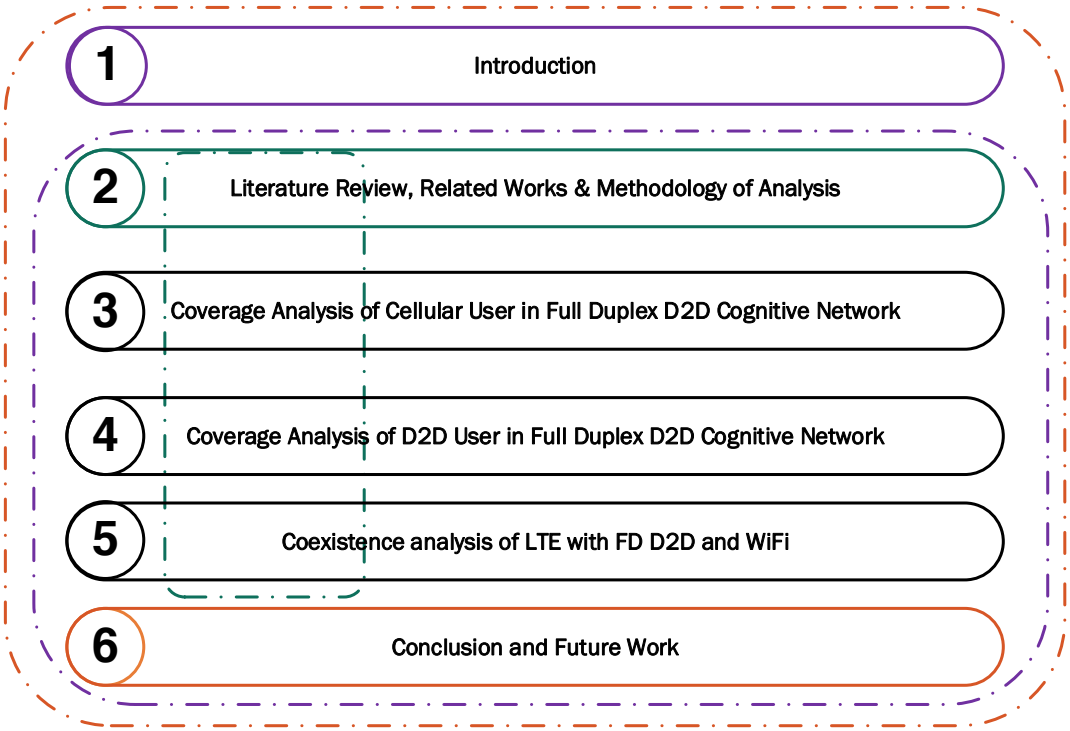

Figure 1.6 : Thesis organization and scope of each chapter.

Finally, Chapter 6 concludes the dissertation by presenting the key features of this research work and possible future research directions.

Chapter 2

Literature Review

Based on the dynamic spectrum sharing in 5G, this chapter presents the relevant works published in literature. In section 2.1, we summarize the key enabling technologies, framework and standardization activities envisioned for future networks (5G). It also includes an introduction and taxonomy of stochastic geometry methods which are used for modelling, design and analysis of telecommunication networks in section 2.5. Then, most relevant recent works which explore performance of key enabling technologies in 5G with the help of stochastic geometry are discussed. Section 2.4 summarizes the key spectrum sharing frameworks, methods and network models for licensed, unlicensed and cognitive setups. The key features of the related works are listed, short-comings are noted which lead to the motivations of the work presented in Chapters 3,4 and 5. Some content included in this chapter have been published in our work in [38].

2.1 5G Networks and Key Enabling Technologies

2.2 Dynamic Spectrum Sharing

The ideal solution to augment the capacity of mobile networks is to add licensed spectrum, which is becoming an in-feasible and costly solution due to the scarcity of the licensed spectrum. Exclusive licensed spectrum allocation has proven to be beneficial but also has its shortcomings. Existing licensed spectrum is congested and over utilized, which has pushed communication industry to optimize the spectrum utilization by peacefully and harmoniously sharing it with other users. As a result,

Dynamic Spectrum Sharing (DSS) has gained significant interest from governments, industry, regulators, vendors and all the stakeholders involved as it has also hinted at several profitable business models. Contrary to fixed long-term leasing of spectrum to one operator, DSS opens new horizons for short-term spatial use of spectrum to secondary users/operators with agreement of the primary licensee. DSS has proven its significant potential previously and is heavily tried, tested and included in various heterogeneous coexistence models in 5G. It has also paved the way for new short-term licensing solutions, either for commercial uses or for unlicensed use. Due to multiple radio access technologies (RATs) for the same spectrum, it is very critical and sensitive to assess the performance of such systems beforehand to assess their practicality because of harmful interference. Therefore, a critical investigation into different system models and coexistence of multi-RATs was needed to assess the factual performance gains of DSS. Following were some of the key findings during this study in the context of DSS:

- The licensed spectrum can peacefully be shared with secondary users by agreeing to interference protection, spatial use of spectrum and terms of contract between primary and secondary operator.
- The peaceful and fair coexistence of new technologies like LAA, multi-FIRE, D2D and IoTs can be made possible by exploring different medium access mechanisms, which ensures equal resource allocation to all users.
- Depending on channel sensing and access mechanism, incumbents share of the channel may become affected by new technologies if not properly studied and tested beforehand.
- Government regulators have to offer incentives to long-term licensed users to drive them toward DSS on a short-term basis.

Thus, DSS paved the way for emerging technologies, users and services to opportunistically access the available spectrum by conforming to conditions set by primary users.

2.3 Opportunistic Spectrum Access

The demand for ubiquitous connectivity and high data rates have motivated network providers and vendors to come up with an optimum use of existing resources (spectrum) and integration of new technologies (Full Duplex, D2D). The development and testing of such solutions is also one of the driving factors for future generation (5G) of mobile networks. Among these proposals, Cognitive radio, TV white spaces (TVWS), Citizen Broadband Radio Service (CBRS), Spectrum Access System (SAS), Licensed Shared Access (LSA) and multi Radio Access Technologies (RATs) have proven to be effective solutions for spectrum scarcity.

The key idea behind spectrum sharing is the use-it or share-it rule, where primary licensed users can share underutilized spectrum with secondary unlicensed users conditional on interference protection from secondary users. This sharing is done based on pre-defined conditions for leaving the spectrum for priority users whenever needed and imposing the least interference to primary users. Spectrum sharing can be done in the time domain (primary user is not transmitting), space domain (primary user is far away) and frequency domain (primary user is transmitting on a different frequency). For detailed benefits of dynamic spectrum sharing and heterogeneous device coexistence, readers are referred to [9].

The D2D communication has significantly shown its potential to elevate the user experience and efficiently improve the network capacity by traffic off-loading from the main network. It is also one of the key enabling technologies in future wireless and cellular networks [39]. D2D is a good technology candidate for opportunistic dynamic spectrum sharing without producing harmful aggregate interference to other

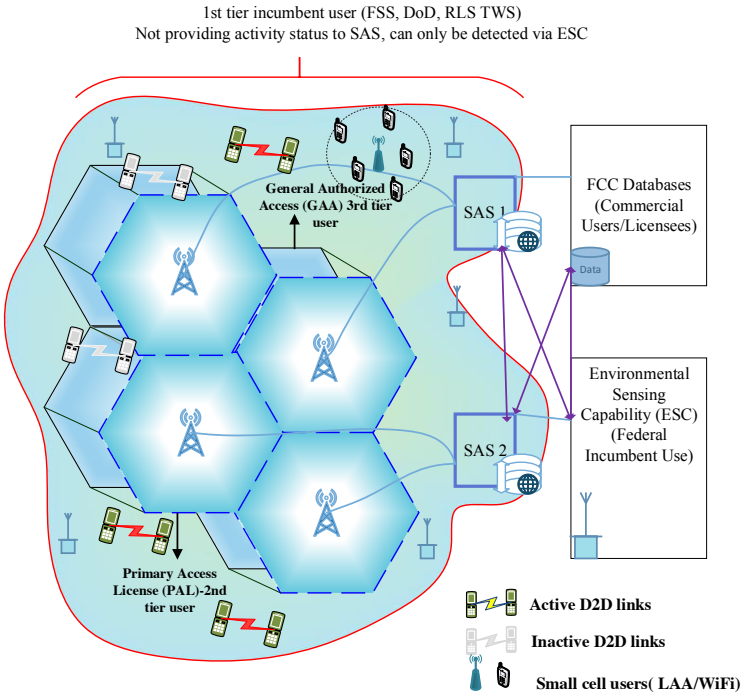

Figure 2.1 : A typical illustration of CBRS system with incumbents (tier-1 user), priority access licensed (tier-2 cellular) and general authorized access (D2D and small cells tier-3) users.

devices (due to shorter link distances and lower transmit powers). In this thesis, we propose D2D technology as a tier-2 (SU) technology candidate and model the system by characterizing the interference and success probability [33]. Due to strict interference threshold conditions which SU has to comply with for PU transmission protection, D2D has more potential as compared to LTE-LAA and WiFi as the D2D users can communicate in a near distance of Exclusion Zones (EZ). The D2D network has performance advantages as compared to other small cell technologies due to limited interference and near-distant communication between transmitters (TXs) and receivers (RXs). For instance, a CBRS system and active/inactive D2D links based on their location and proximity to EZ of PU are shown in Fig. 2.1.

2.4 Spectrum Sharing Frameworks

This section presents the spectrum sharing architecture and technologies coexisting and sharing the same frequency bands. The taxonomy of the spectrum sharing framework is mainly done on the basis of how spectrum is allocated i.e. licensed access or unlicensed access. The licensing policies may vary on regional, political and economical factors. Fig. 2.2 presents an abstract level taxonomy of the spectrum sharing framework.

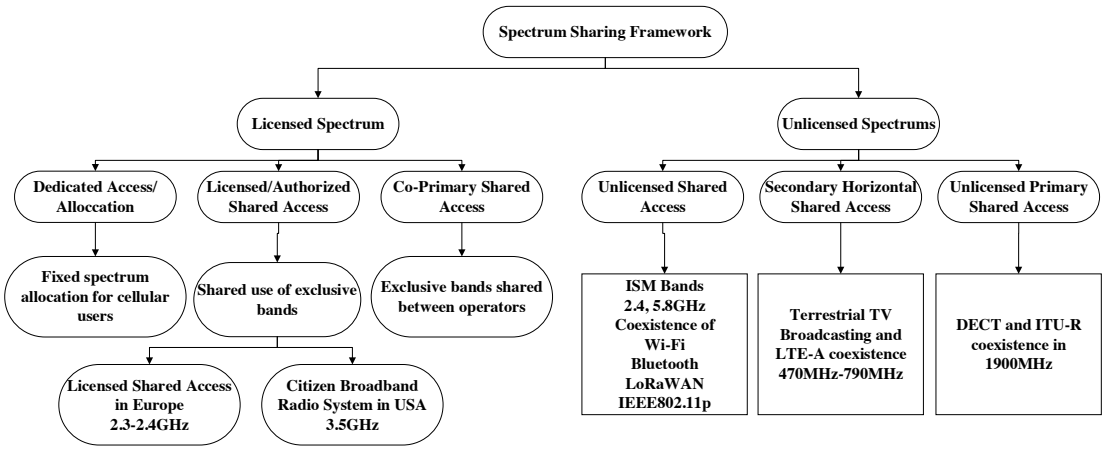

Figure 2.2 : Taxonomy of spectrum sharing frameworks/methods in licensed and unlicensed bands [40]

.

2.4.1 Sharing in Licensed Spectrum

The government regulatory body auctions/sells frequency bands from available spectrum exclusively to one party (mobile operator). Only the licensed party can use these frequency bands in time, frequency and spatial domain. Following are the spectrum access and sharing policies for licensed spectrum.

Dedicated Access

One operator is allocated an exclusive access for specific frequency bands in exchange for higher license fees. The license holder has full access/control of the licensed bands and they have guaranteed Quality of Service (QoS). The operator has guaranteed interference protection as no other user will operate on these frequency bands. Such kind of access is favorable to operators which require secrecy, privacy and confidentiality of their users and data from the public. Also, such access offers all time guaranteed access which is mostly needed for military grade communication and other Government agencies. However, it comes at the cost of spectrum utilization inefficiency as spectrum is not in use all the time, over all spatial domains. Such spectrum opportunities are targeted in 5G to find innovative ways through which this spectrum utilization can be optimized and licensed access users are given incentives to sublease/share the licensed spectrum chunks with other users. The challenging factor here would be guaranteed interference protection and ubiquitous access for the licensed user while sharing it with the other users.

Licensed/Authorized Shared Access

This type of sharing is done on the basis of mutual agreement between the sharing stakeholders. Depending on the licensing polices by respective authorization regimes, such sharing is formulated into the following access systems.

Authorized Shared Access (ASA): ASA is a regulatory framework which conditionally permits licensed sharing of underutilized spectrum between incumbents and secondary users through individual authorization scheme. European (EU) regulatory framework for electronic communications, is pushing regulators for ASA which has significant potential due to recent technological advancement which can guarantee peaceful coexistence between incumbents and secondary users. The potential bands in sight for ASA are 2.3GHz (in the U.K.) and 3.8GHz (in the U.S.).

Licensed Shared Access (LSA): LSA proposal has been tabled by the European Telecommunications Standards Institute (ETSI) as an extension of ASA which offers comparatively higher gains in performance and also improves spectrum efficiency. The idea is to facilitate the sharing of underutilized frequency bands for mobile communications in a harmonious and protective manner for incumbents. The advantage mobile operators have is of comparatively low licensing fee but they have to abide by the certain transmit power and interference requirements. Only the licensed users have guaranteed access to leased frequency bands in the absence of incumbents so therefore, it is more favorable to mobile operators.

The initial targeted frequency bands were between 2.3-2.4GHz, but LSA is expected to be implemented in other bands and also for non-cellular uses as well. Fig. 2.3 presents the LSA architecture and key entities to ensure harmonized technical and regulatory conditions. The detailed technical aspects of LSA system, defined by ETSI Technical Specification (TS) can be studied in literature [41, 42]. The incum-

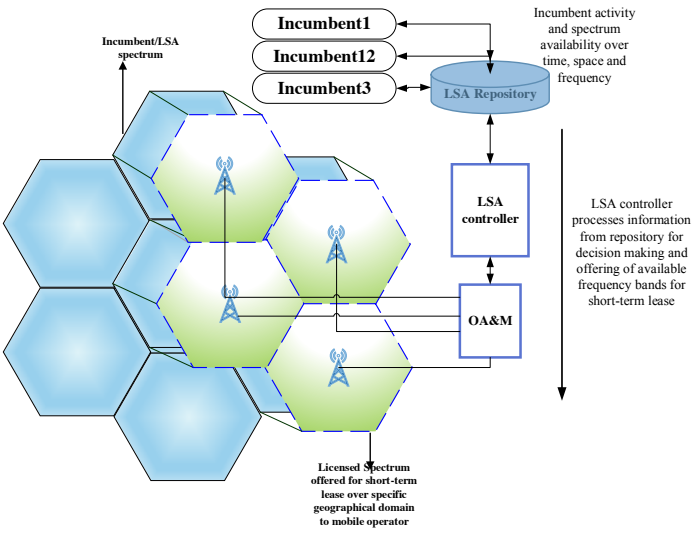

Figure 2.3 : Operational mechanism of LSA architecture

bents may report the availability of spectrum to the LSA repository for short-term

licensing to cellular operator on condition of guaranteed access and interference protection. **LSA repository** is an intermediary relay between incumbents information and LSA controller. Depending on the incumbents sensitivity to sharing the details, LSA repository may contain the incumbents spectral activity from geographical, temporal and frequency domains. Based on information from LSA repository, **LSA controller** processes the information for spectrum offering to mobile operators. As the LSA repository contains very sensitive information regarding incumbent activity and LSA controller is responsible for offering frequency bands, it is expected that these two units of LSA architecture will be governed by a third party to ensure the compliance of agreed upon conditions. **OAM** (Operation, Administration and Management) entity is responsible for relaying control information between LSA controller and the licensed mobile operators. The notable feature of LSA is that the secondary licenses for short-term use are leased to mobile operators and only licensed operators can use the allocated frequency bands. They have tier-2 level guaranteed access from other users and interfere-rs in the same band. Followed by extensive discussion in ETSI forums, the potential of LSA's performance efficiency was conduted using live trials of LTE in 2.3GHz bands [43]. Another recently published proof-of-concept for LSA implementation using Virtually Shared Spectrum Access (ViSSA) is published in [44]. The economical aspects, possible business models for incumbents in LSA are presented in [45].

Citizen Broadband Radio System (CBRS)

The limitation of LSA (no generalized access) is a distinctive feature in Spectrum Access System or also known as Citizen Broadband Radio System (CBRS) in literature. FCC tabled this proposal for DSS in 3.5GHz band to be implemented in the US. SAS offers three-tier spectrum access. The first tier is for **Incumbent Users** special government/military users with priority access to spectrum and interference

protection from all other users all the time. The second tier is for **Priority Access Licensee (PAL)**, which are Mobile operators who lease spectrum (of ∼10MHz) on a short-term to medium-term (three years) basis in time, frequency and space domain (census tract). PALs have to abandon the frequency bands if incumbents activity is detected and have to switch to different frequency bands. The third tier is for **General Authorized Access (GAA)** users, which are allowed to conditionally use the available frequency bands but they must protect PAL's transmission under strict interference conditions. Fig. 2.1 shows a typical illustration of SAS system model with all three-tier access level users.

2.4.2 Sharing in Unlicensed Spectrum

In an unlicensed spectrum, complying users, or service providers can use the available spectrum opportunistically without any license but must follow a peacefull, fair and equal priority channel access mechanism. All users must comply and follow regulatory frameworks to ensure peaceful and fair coexistence of a diverse set of users in respective frequency bands. A range of new technologies have also targeted these bands to optimize spectrum efficiency while ensuring fair coexistence. As there are no QoS, access guarantees or interference protection to users, channel access mechanism/protocol plays a vital role in harmonious and fair coexistence of multi-RATs. Extensive literature work has been done for coexistence of users in unlicensed bands in the context of CRNs. The DSS and OSA are also widely explored in literature.

LTE in Unlicensed Spectrum

Existing licensed spectrum is congested and over-utilized, so mobile communication is moving toward unlicensed spectrum (5GHz). The cellular system (LTE) with the support of unlicensed spectrum has the capability to achieve data rates of multi-gigabits per second. Considering the 5GHz frequency range is only slightly

used, and more spectrum is expected to be available soon, opportunistic utilization of this spectrum for cellular technologies is an interesting idea.

The Carrier Aggregation (CA) framework introduced in Release 10 of 3GPP paved the way for LTE to step into an unlicensed spectrum. The idea is to keep all control and signaling data in licensed spectrum by using primary anchor carrier, while, a secondary carrier in unlicensed spectrum supplements data rate whenever available. However, WiFi (IEEE802.11 n/ac/ax) is the dominant incumbent technology operating in the same unlicensed spectrum. The effectiveness of LTE in unlicensed spectrum relies on its harmonious and fair co-existence with WiFi. Therefore, design objectives for LTE operation in unlicensed spectrum include fair co-existence and obeying regional regulatory requirements for using unlicensed spectrum. Recent literature studies shows that multiple wireless technologies have more performance efficiency and success probability then limiting them to WiFi only [46]. Due to the differences in the MAC and PHY layer protocols of LTE and WiFi, compatible channel access mechanisms (CAM) are required. LTE is a scheduled system with eNB controlling UE access for transmission, whereas WiFi is a distributed contention-based system. Due to robust physical design, LTE is spectrally efficient and tolerant of interference more than WiFi and receives assistance from licensed spectrum for control signaling as well. However, LTE deployment in unlicensed spectrum without any protocol modifications is disastrous for WiFi transmissions. Deploying LTE and WiFi in the same location and frequency bands negatively impact WiFi communication because LTE interference levels are higher than the threshold used by WiFi to detect channel vacancy (sensing thresholds in CSMA/CA). In this thesis, we provide an extensive taxonomy of proposed coexistence techniques for LTE with their potential benefits and limitations. Moreover, recommendations based on critical analysis of these approaches is made to assist future research.

One of the initial proposals allowing LTE operation in unlicensed spectrum in-

cludes discontinuous transmissions via muting subframes [47]. This method is referred to as LTE-U and it requires small modifications to existing infrastructure [48]. LTE-U is backward-compatible with Release 8 and 9, and it uses an idea of Almost Blank Subframes (ABS) for a muting portion of LTE transmissions. The sensing-based methods for LTE in unlicensed use the Listen-before-talk (LBT) mechanism before initiating its transmission, thus exhibiting polite behavior. Such methodologies are referred to as Licensed-Assisted Access (LAA) LTE in 3GPP [49]. The LBT flavor of LAA inspired from CSMA/CA showed greater potential for optimum throughput of WiFi and LAA while maintaining fair and peaceful co-existence among them. Currently, DL only mode of LAA is under consideration, but LAA bi-directional operation is also possible using TDD. Three modes for LAA have been identified based on communication in an unlicensed spectrum; Supplemental Downlink (SDL), Carrier aggregation TD-LTE and standalone LTE-U [49]. SDL complements existing networks to boost throughput and capacity by carrying DL data in unlicensed spectrum, whereas uplink and control channel remain in licensed spectrum. In CA TD-LTE mode, an unlicensed spectrum can be used for both uplink and downlink data traffic, but control signals remain in licensed spectrum. Standalone LTE-U mode allows autonomous operation by allowing control and data traffic for unlicensed spectrum. Fig. 2.4 shows different wireless Radio Access Technologies (RATs) operating in unlicensed spectrum along with LTE.

The true potential LAA offers to legacy network ultimately relies on its impact on incumbent systems operating in the same unlicensed spectrum. LTE in unlicensed spectrum should behave as a polite neighbor, which is possible in a peaceful, fair and polite CAM. A metric of fairness defined by development bodies is that LTE should not impact the performance of WiFi more than any other WiFi. In this section, we categorize coexistence techniques proposed for LTE operations in unlicensed spectrum, based on their methodology.

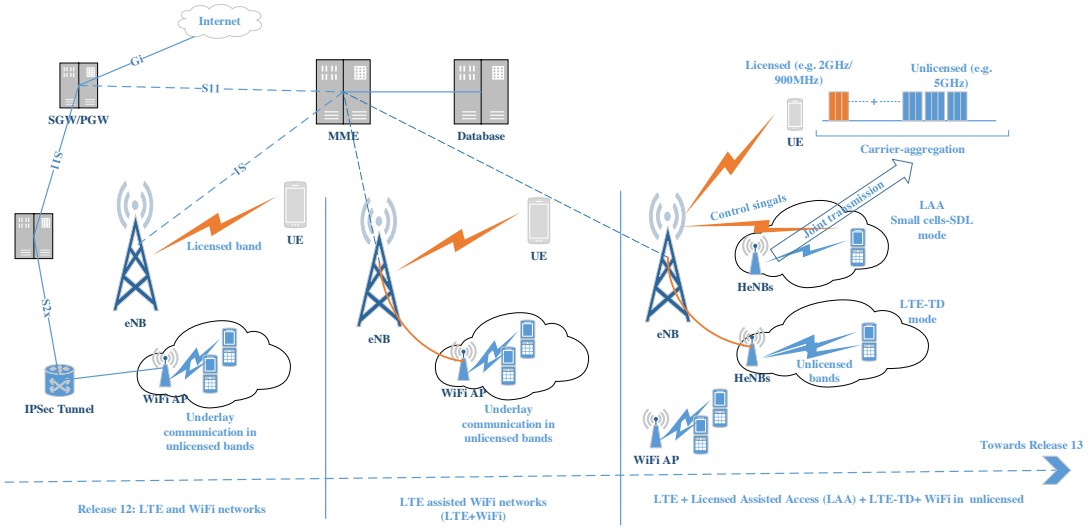

Figure 2.4 : Proposed architecture models, coexistence and evolution of LTE in licensed, LTE-LAA and WiFi in unlicensed coexistence toward Release 13.

WiFi and LTE in Unlicensed Spectrum

The WiFi has proven to be an efficient and dominant system for indoor use in unlicensed spectrum. There has been an enormous upsurge in WiFi technology deployment to cater for an exponential increase in network capacity. Cellular systems also have greatly benefited from WiFi for data offloading. WiFi use CSMA/CA for channel access to avoid collisions and causing interference to other devices in the vicinity. CSMA employs a clear channel assessment (CCA) sensing mechanism before starting its transmission. For instance, communication at 20MHz carriers in IEEE802.11x, a channel is considered to be busy if a CCA slot exceeds the CCA-ED threshold of -62dBm or measured energy from another AP or station in the preamble detection exceeds the CCA-CS threshold of -82dBm. In the case of a busy channel, a transmitter uses random backoff until the channel becomes idle again. If any device operating on the same channel does not use a similar CAM, then WiFi efficiency severely degrades unless it uses a CSMA/CA like protocol, which ensures

fairness.

After initial proposals and demand from industry forums to bring LTE to unlicensed spectrum, 3GPP started a Study Item (SI) in September 2014 for LAA operation study and completed it in June 2015. The SI focused on the 5 GHz spectrum for this purpose and to develop a global solution that can work across all regions. The SI evaluated the feasibility of LTE deployment in unlicensed spectrum, defined requirements for any modifications needed and conducted fair coexistence analysis with main incumbent technologies i.e. WiFi [47]. 3GPP renamed LTE-U as LAA to highlight an important point to government spectrum regulators that the use of an unlicensed carrier is accompanied and controlled by a primary licensed carrier. Licensed spectrum is used for a performance boost while unlicensed spectrum will provide a speed boost for users by carrying additional data payloads. The main idea is to aggregate carriers in licensed and unlicensed bands using the CA framework. One deployment scenario is a heterogeneous network where an underlay of low-power nodes (e.g. picocells, femtocells, etc.) is introduced into the macrocell. Small cells operate on unlicensed bands while macro cells use primary licensed bands. A UE can only gain access to the unlicensed bands (secondary cells) via control signals from the licensed bands (primary cells). Moreover, LAA considers regional regulatory requirements for using unlicensed spectrum to avoid interference with existing technologies and radar signals. LAA also will meet ETSIs LBT requirements as it considers deployment in regions like Europe and Japan.

LTE is a scheduled system, while WiFi is a contention based system. Therefore, LTE has no intra-system contention while operating in the multi-operator environment. Regarding control signals (CS), LTE has better CS optimization than WiFi. LTE also has support for seamless handover and service continuity when a user leaves one cell and joins another. The WiFi has fixed bandwidths while Release 8/9 offers carrier bandwidths of 1.4, 3, 5, 10, 15, and 20 MHz for LTE. Moreover, LTE

has a centralized architecture where eNB controls channel access decisions, while a WiFi system relies on the distributed channel access mechanism based on the CSMA protocol.

Coexistence protocols/mechanisms in ISM bands

Recently, coexistence methods for LAA attracted great attention from the research community and MNOs. Extensive investigation of WiFi and LTE coexistence methods is done by using diverse simulation scenarios [50], typical analytical methods [34], [51] and real-time experiments [52]. Based on the methodology, proposed techniques can be categorized as coordinated (centralized) or non-coordinated (distributed). We present a novel taxonomy of distributed schemes based on the channel access method, which is either time-hopping, frequency hopping or channel-sensing. Fig. 2.5 shows a feature-based extensive taxonomy of the co-existence techniques proposed for LTE deployment in unlicensed spectrum.

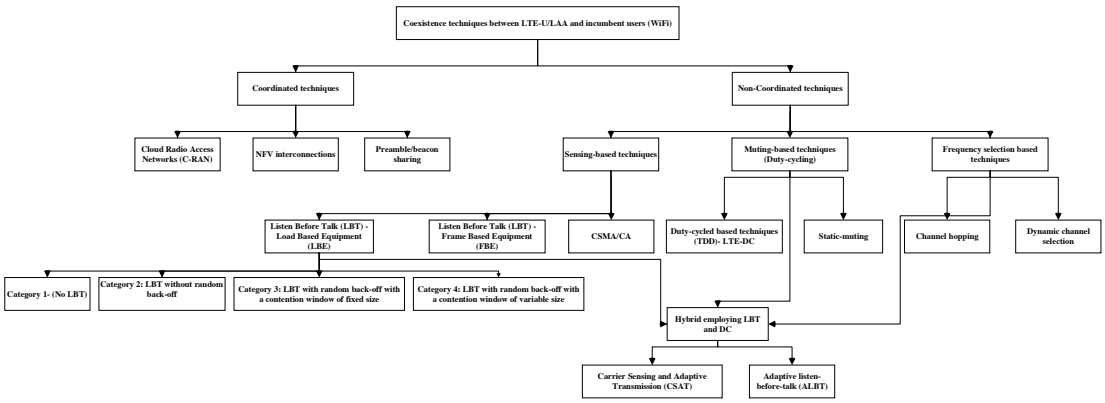

Figure 2.5 : Taxonomy of proposed co-existence methods for LTE operation in unlicensed spectrum

Coordinated techniques: The coordinated techniques have centralized control of medium access and spectrum sharing for LAA and WiFi devices. Using Network Function Virtualization (NFV) and cloud-based central cooperative manage-

ment, it is easier to distribute equitably shared resources among candidate devices. Such central control of spectrum and common resources also eliminates the need for LBT/CSMA and efficiently manages co-channel interference. For instance, authors in [53] proposed a virtualized core network which enables coordinated management of spectrum and medium sharing for WiFi and LTE-U coexistence.

The idea is to segregate control and data planes for efficient utilization of resources via centralized coordinated management. The user data is forwarded in a distributed manner among access points and users. Such an approach not only allows meeting large data rate requirements with limited spectrum but also improves spectral and operational efficiency. The challenging task is to inter-connect control and management planes among the virtualized TWAG (vTWAG) and the virtualized EPC (vEPC). This method improves control signal adaptability and robust connectivity considering the available spectrum for the existing users. Another coordination-based network architecture for higher frequency communications is proposed in [20]. The idea is to enhance further capabilities of core backhaul network by introducing load-centric backhauling (LCB), multiple-frequency transmission, and intelligent control techniques. Such adaptive and feedback-based learning backhauls are much more efficient than fixed backhauls. Fig. 2.6 shows cloud-assisted centralized management of a diverse set of wireless RATs operating in the same unlicensed spectrum.

The other form of coordinated techniques require devices to collaborate on coexistence parameters (such as time, frequency or spatial domains) and agree on common policy to ensure harmless coexistence. Advantages of such centrally controlled systems may reduce complexity and eliminate the need for a distributed channel mechanism; however, limitations lie in scalability and collaboration among different technologies (LTE and WiFi). Also, devices operating in unlicensed spectrum other than WiFi and LAA also need to be compatible with the central backhaul

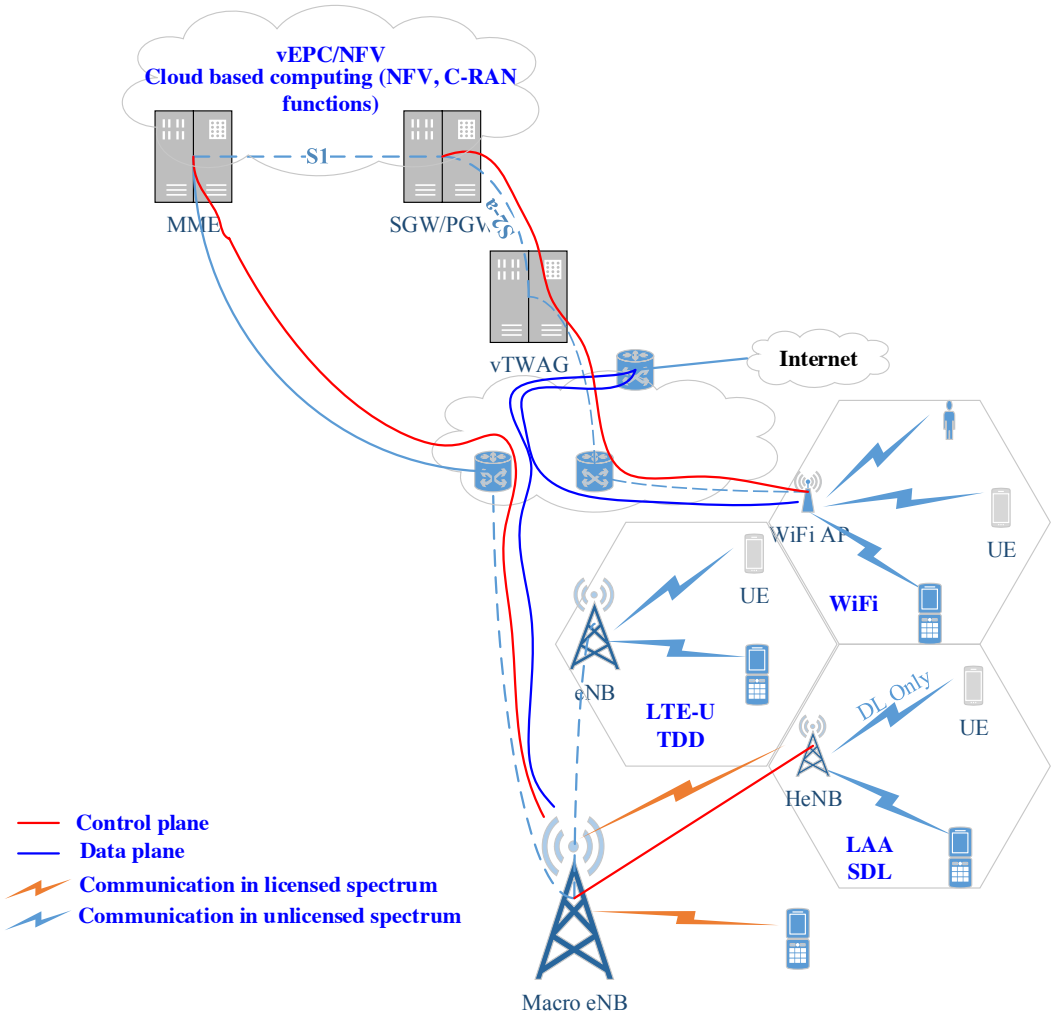

Figure 2.6 : Centralized cloud-assisted model of different wireless RATs

infrastructure. This architecture is more suitable for localized small networks but may not become a practical solution for wide area networks. The challenge will be integration of plug and play based Internet-of-things (IoTs) technology. Moreover, limitations in terms of scalability are also an issue in centralized techniques. Therefore, distributed or non-coordinated techniques have attracted more attention from the research community.

Non-coordinated techniques: In non-coordinated (distributed) co-existence

techniques, each device operating in the same unlicensed spectrum must use compatible and fair channel and medium access mechanism. The metric of fairness is to provide equal opportunity to all the devices in the medium to access the sharing channel. The existing distributed techniques can further be categorized based on the medium sharing method i.e. sensing based, time or frequency based sharing as shown in Fig. 2.7.

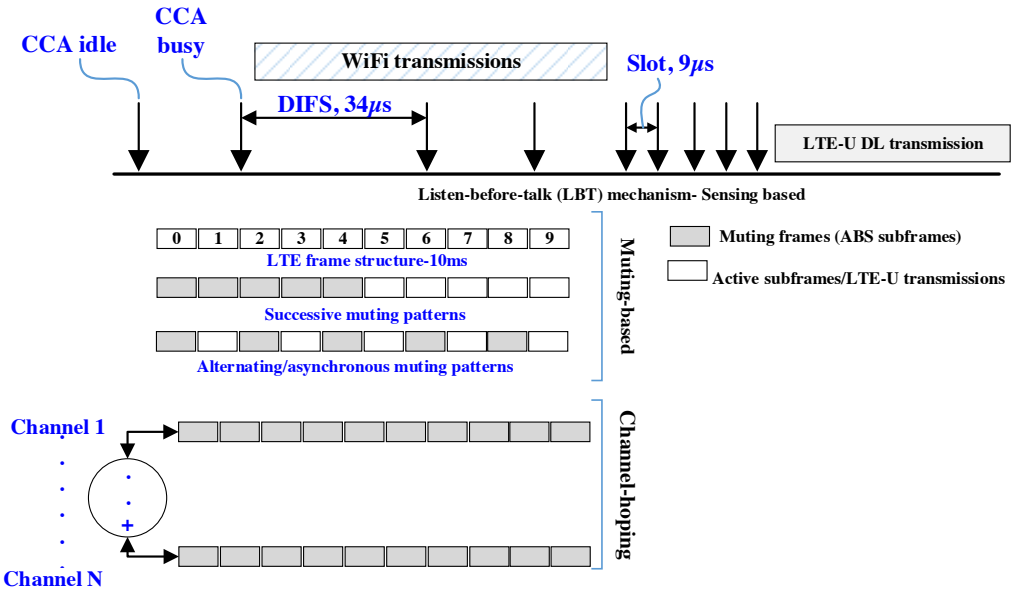

Figure 2.7 : Centralized cloud-assisted model of different wireless RATs.

Sensing based: Among sensing-based techniques, the legacy CSMA/CA has proven to be an efficient method, and LAA also must adopt a similar protocol to coexist peacefully. However, due to PHY and MAC layer differences among WiFi and LTE, CSMA/CA may undermine the efficiency of LTE features and limit their performance. According to European regulations, devices operating in an unlicensed spectrum of 5GHz must use the LBT mechanism like CSMA or LBT with frame based equipment (FBE) or load based equipment (LBE) [54]. The difference lies in channel sensing periodicity; FBE senses the channel status every fixed period

known as the fixed frame period (FFP). On the other hand, LBE detects channel state whenever there is a packet to transmit. The majority of co-existence techniques for LAA extends potential benefits of LBT-LBE by proposing different backoff and contention window size. 3GPP categorized sensing-based LBT schemes based on the results, findings, and discussions with different vendors and telecom industries. In category 1 (No LBT) systems, a device immediately transmits packets without sensing the channel for any on-going transmission. This solution is impractical due to its destructive repercussions for neighboring devices operating on the same channel. However, it can be used as a baseline for evaluation of optimized approaches.

Category 2 techniques listen to the channel before transmission by employing the simplest form of LBT without using any random backoff. A device makes a transmission decision based on the fixed duration of the time the channel is sensed to be idle. Due to the lack of back off before starting LTE transmissions, some of the WiFi packets which have not been received at destination may result in error due to collision. This shortcoming is well considered and dealt within Category 3 approaches, which employ LBT with a random backoff period from the contention window of a fixed size. Every device follows CAM; it draws a random number N from the contention window of a fixed size specified by the minimum, and maximum values of N. A decision to start a transmission is taken if the channel is sensed idle for the duration of time N. Such schemes outperform especially in dense network deployments where the number of devices competing for channel access is high.

The category 4 LBT co-existence schemes are closely related to the CSMA approach as they employ a contention window of a random size. Unlike category 3 LBT, in category 4 techniques a device can dynamically adjust the size of the contention window for a minimum, and maximum values of N. Thus, category 4 type LBT schemes are more likely to provide fair, globally acceptable inter-operator co-existence for the shared medium. Also, these techniques are reported and discussed

in evaluations of the 3GPP technical report and outperform Category 1-3 approaches regarding performance efficiency.

Muting-based: This method uses duty-cycle for LTE in unlicensed spectrum to allow WiFi interference-free transmissions. An essential muting feature proposed in Release 10 of 3GPP for enhanced inter-cell interference coordination (eICIC) inspired this co-existence solution for LTE-U. The idea is to use ABS with a minimized downlink transmission power or activity for coordination among macro and pico eNBs in heterogeneous deployments. The effectiveness of TDM for channel access among LTE-U and WiFi is shown in [20]. This concept is further extended by introducing static/dynamic or adaptable muting patterns for LTE-U frames according to interference and traffic scenarios. The same thing is also referred to as tunable co-existence gaps (TCG). The shortcoming of exclusive TDM based techniques is the lack of politeness for on-going transmissions as a device does not sense a channel for any packets in the air.

Frequency selection based techniques: The key idea is to shift from channels being extensively used by neighboring devices to avoid interference, as a plethora of other channels are available in unlicensed spectrum. Similar to TDM based channel sharing, a device using shared unlicensed spectrum can use channel hopping to avoid interference on a particular channel for a longer time. Devices may switch among different channels available in shared unlicensed spectrum. Such channel hopping and dynamic frequency selection (DFS) are one of possible co-existence methods. However, such methods alone without any duty-cycling or channel sensing cannot ensure fairness for all devices, especially in dense deployments. By combining this with other channel sharing techniques like TDM and LBT, potential advantages can be achieved.

Hybrid co-existence techniques: Potential benefits of LBT and shortcom-

ings of TDM and frequency hopping based schemes lead to the emergence of hybrid coexistence techniques. Such methods use LBT for channel sensing and also use adaptable duty-cycle periods to balance the metric of fairness in medium access. For example, carrier sensing and adaptive transmission (CSAT) as the name suggests, use both LBT and TDM approaches. CSAT senses channel activities for a longer duration then LBT/CSMA and based on an intelligent algorithm it gates off/on LTE transmission proportionally [55]. CSAT decides duty-cycle for LTE communications in small cells based on the knowledge of channel activities in a longer sensing period. Duty-cycle defines the proportion of time LTE transmits and remains silent otherwise. CSAT provides fair and peaceful co-existence, with the impact of LTE-U on WiFi AP not more than any other neighboring WiFi. During an LTE-U off period, a small cell measures WiFi medium activity and then accordingly adjusts the on-off duty cycle. Such an approach better suits real-time densely deployed networks with multiple LTE-U and WiFi stations. Another approach in [56] uses FD based mode adaptation techniques for WiFi and LTE-U coexistence by employing transmit and sense (TS mode) operation simultaneously.

The real-time adaptive nature of hybrid approaches potentially works well in dense networks with changing traffic and load conditions. Another hybrid approach with the flavor of frequency hopping or dynamic frequency selection is introduced along with LBT. The Adaptive LBT (ALBT) [53] performs channel assessment to monitor WiFi activities in an LBT duration and applies co-existence gaps in the DL operations to exhibit fairness for channel access. ALBT has a pool of all available channels in operating unlicensed spectrum, and it switches channels among this pool to avoid occupying a single channel for an extended period. Such a method enables WiFi and other devices in the vicinity to utilize that channel. For instance, ALBT uses idle channel 1 for a limited duration and then performs multi sub-frame DL while searching for other unused channels. On the identification of a new idle

channel, LTE-U shifts to this channel N while leaving co-existence gaps following DL at channel 1. Such flexibility, adaptability and voluntary releasing of channels are favorable for WiFi to co-exist friendly with LTE-U. However, other systems in the vicinity will be affected for a certain portion of the time. Table 2.1 lists state-of-the-art coexistence methodologies with their potential advantages and limitations.

2.5 Spatial Geometry and Wireless Networks

To evaluate the performance of a communication system and its entities (users and base stations), Signal to Interference Ratio (SIR) or Signal to Interference and Noise Ratio (SINR) are the key performance metrics. For any given user/link, SINR is the ratio of strength of desired signal from intended transmitter (in down link) or from intended receiver (in up-link) to the strength of all the unwanted signals from other interferers plus the noise power. To calculate SIR/SINR for a specific user, we need transmit power, channel gains, path-loss and antenna characteristics. Now, channel gains and path-loss are functions of users location which could be anywhere in a given region. In mathematics, such randomness can be captured through random point processes and locations can be modelled with the help of spatial geometry. The ground-work for mathematically modelling such macro-cell base stations originated with grid-based hexagonal model. This became the most commonly used network model especially for simulation purposes. However, due to randomness of base stations deployment in real-world, this model over simplifies the base station deployments and is also analytically intractable.

The initial benchmark models for theoretical performance analysis of a communication system considered extreme simplifications but laid the foundations for evolution of mathematically emulating the real-world communication models. For instance, in the 1990's the Wyner model [71] considered only one or two interfering cells or assumed fixed channel gains from all the interferers in the network. Another

Table 2.1 : Taxonomy of basic coexistence techniques with their advantages and limitations, a comparative analysis and trade-offs

Technique	**Advantages**	**Shortcomings**
Coordinated/Centralized [20, 53, 57–59]	No need for LBT, segregated control and data planes, feedback and learning based intelligent/smart backhaul network, adaptable according to frequency and interference conditions	Scalability, significant delays and single point of failure
Muting-based/silent or blank subframes [60–62]	No inter-RAT interference, channel/medium sensing not required, full access to medium in dedicated time/frequency or spatial slots, does not require sophisticated upgrades to existing systems.	Does not suit in dense, high-traffic or urban scenarios, longer delay/waiting-time before access to medium/channel, inefficient resource utilization in case of non-bursty traffic.
Channel-hoping/switching [63–65]	Less co-channel interference, avoids congestion on single channel, improved spectrum utilization in dense networks, compatible for existing RATs.	Does not perform well in bursty traffic conditions with high user load, fair coexistence not guaranteed, higher inter-RATs interference.

Technique	**Advantages**	**Shortcomings**
LBT with frame based equipment (FBE) [66, 67]	Periodic channel detection/sensing, less detection complexity	No back-off/contention window in case of unstable channel or high bit error rate, longer delays for contending users, channel access inefficiency in urban, dense and bursty traffic scenarios
LBT load based equipment (LBE) [66,67]	Efficient channel utilization in high-load scenarios, backoff in case of unstable channel or high bit error rate, simple implementation	Higher processing and power consumption at user end, fair-coexistence not guaranteed, less immune to high level of interference.
CSMA/LBT (sensing based) [68–70]	Peaceful coexistence among multi-RATs, fair coexistence for all contenders, back-off in case of unstable channel or high bit error rate, opportunistic resource utilization, scalable and simple	WiFi version not suitable for LTE-U, hidden node problems, performance degrades for urban, highly dense scenarios, performs differently for different energy detection/channel sensing thresholds, inter and intra technology interference from contenders.

model in [72] tries to characterize the interference using a single random variable and then empirically fit it to some probability distribution, such as log-normal. A few other models such as in [73,74] take into account fixed distances of interferers to probe user, which is quite contrary to the estimated distance distribution in real network scenarios. Thus, such models can be accepted from an information/theoretic point of view due to tractability but can not exactly be used for real-world scenarios which depict a high degree of randomness especially in dense deployments.

Over the years, with the evolution of communication systems from macro only cells to heterogeneous and densely populated small cells, mathematical models also advanced significantly to more closely and accurately capture the key network features. Recently, Stochastic Geometry [75] has captured the interest of the research community to analyze wireless networks properties and has proven to be a compelling analytical modelling tool [76]. Despite numerous random factors (such as user locations, fading, power, antenna gains.), stochastic geometry tools under reasonable assumptions can provide abstract level performance of entire network in terms of success/coverage probability, area spectral efficiency and data rates. In Stochastic Geometry, a generalized analytical model is developed which gives expressions for key performance metrics and is applicable for all possible network realizations [77]. For instance, if we want to study FD enabled D2D cognitive network then the developed model gives us general performance analysis, design insights, and dependencies for all possible network realizations. In this section, we provide the detailed overview on the models, and tools that can be used for performance analysis of wireless networks. The first thing to map network realization to spatial geometry would be the location of users (UEs) and the base station. This is done by mapping one of the suitable point processes according to expected user/BS locations under consideration.

2.5.1 Point Processes

Informally, a point process (PP) is a random collection of points scattered in some spatial region. PPs are used to realize events/data in space and time. For instance, a random pattern of points residing in an n-dimensional Euclidean space, $\mathbb{R}^n$ can be denoted as $\Psi = X_i, i \in \mathbb{N}$. A useful interpretation of finite PP is through random counting measure, where all the points residing in the finite region, set or space (B) are counted, while $B \subset \mathbb{R}^n$. So, the total points in set or region B can be denoted as ,

$$\Psi(B) = \sum_{X_i \in \Psi} \mathbb{1}(X_i \in B) \tag{2.1}$$

where, $\mathbb{1}$ is an indicator function only valid for the points X_i that reside in B, or alternatively counts the points which belong to B. Taking all the possible different realizations for $\Psi(B)$, it can completely capture all realizations of Ψ. Such counting measure is typically and in this thesis is also denoted by $\mathbf{\Lambda(B)}$. Each PP also has intensity of users over specific area, commonly denoted by λ.

PPs exhibit certain properties which make the analysis easier. A few important properties of PP are found in [28],

- A PP is known to be ***simple*** if multiplicity of all points is at most one i.e.

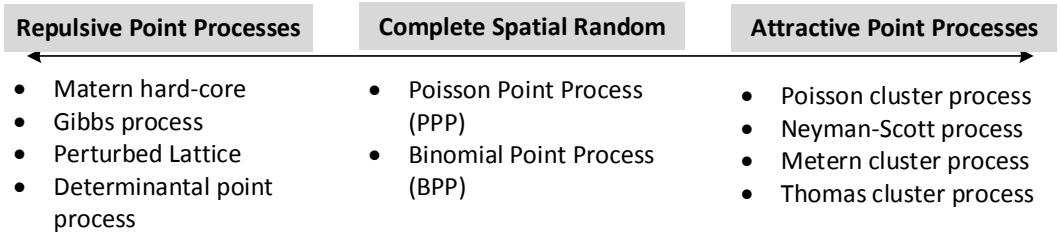

Figure 2.8 : Taxonomy of point processes based on inter-dependency and correlation between the points [78]

(no two points have the same location).

- A PP will be ***stationary*** if law of PP holds or is invariant by translation of PP. Stationarity property holds for a PP when it is shifted with some constant parameter in space or time.

- A PP is known to be ***isotropic*** if law of PP is invariant or independent of direction of PP. Isotropy property holds for a PP when it is rotated in any direction in space.

- A PP is said to be ***motion invariant***, if it is both stationary and isotropic.

Following are some of the commonly used and important statistical measures of a PP,

- The ***Expectation measure*** of a PP gives the mean value or mean number of points in any given set. For instance, for a set B, the expectation measure would be the mean number of points residing in B. Typically denoted as,

$$\mu(B) = \mathbb{E}[\Psi(B)] \tag{2.2}$$

- The ***Lebesgue measure*** is a systematic way of assigning a measure to subset of n-dimensional Euclidean Space ($\mathbb{R}^n$). For instance, for $n = 1$, the Lebesgue measure of subset $|B|$ in Euclidean Space of interest coincides with the length of interval , for $\mathbb{R}^2$ it is the area of the subset and for $\mathbb{R}^3$ it is the volume of the subset.

- The ***Palm distribution*** is the probability of an event or characteristics of PP by placing a point at a specific location in given space. It is the view of PP from the perspective of that point in PP. For instance, if point $x \in \Psi$ is added at a specific location on $\mathbb{R}^n$, then conditioned at point x, the conditional distribution of PP would be the Palm distribution. This property greatly

helps to study the overall properties of PP from x, such as closest point to x in PP (which could be strongest interferer in wireless networks) and the average/mean number of points in a disc centered at x with radius r denoted by $B(x, R)$. Most commonly in SG, this point is added at origin (o, o) for $\mathbb{R}^2$ and Palm probability then can be denoted as P^{x_o} or P^o. The ***Palm probability*** P^o of stationary PP is then the probability measures of events when a point is conditioned at origin for a PP.

- The ***reduced palm distribution*** is the distribution of the PP when point $x \in \Psi$ (on which PP is conditioned on), is removed from the PP [76]. Hence, the reduced Palm probability $P^{!x_o}$ of a PP is the probability of event/s being studied once the point x_o is removed from the origin.

- The ***mark of point in PP***, informally speaking, is a quantity associated with with each point $x \in \Psi$. Such property of PP is also referred to in literature as marked PP [29] and is also used in this work in chapter 5. This mark is a feature of each point and follows this point when the PP is mapped by a global translation operation [28]. For instance, for every transmitter $X_i \in \Psi$, a receiver is assigned at a fixed distance from X_i, denoted by Y_i, then marked PP can be referred to as $\Psi_{Tx,Rx} = \{X_i, Y_i\}$.

- The ***Laplace Transform*** of pdf of a random variable I at s is defined as,

$$\mathcal{L}_I(s) = \mathbb{E}\{^{-sI}\} \tag{2.3}$$

Now, we will highlight the relation between PPs and spatial locations of users/base station in communicating networks.

2.5.2 Point Processes and Spatial Locations

From modeling real-world user/base station locations with PPs, it is a widely acknowledged assumption that users are distributed randomly. Especially in urban

scenarios, small cells and K-tier heterogeneous wireless networks exhibit a high degree of randomness. Thus, to model spatial locations of communications system entities (transmitters and receivers), random PPs are used for different network realizations usually in two-dimensional space ($\mathbb{R}^2$). Various works have previously established tightness of results for key performance metrics among real-world deployments and through PPs network abstractions. For instance, authors in [30] established and observed how closely accurate are the results from real-world 4G deployment networks when compared to the results for the same networks abstraction using random PPP. This paved the way for PP based network models and performance evaluations with tractable results.

Depending on correlation and dependency between points, authors in [78], PPs have been categorized into attractive and repulsive PPs. The reference point of this taxonomy is the simplest PP with no dependency between the points and completely random known as PPP, also referred to as Complete Spatial Random (CSR). PPP is the most widely and well known PP model used to model the locations of user/base stations due to its mathematical tractability, availability of generalized expressions and high degree of randomness depicted in real-world cellular networks. PPP is a baseline CSR process but it also serves as the baseline process toward the evolution of other attractive and repulsive PPs. Fig. 2.8 categorizes the commonly used PPs based on correlation and dependence between the points. For more detailed study on PPs, readers are referred to [76] and [79]. In this thesis, we also mostly use PPP to model spatial locations of users. The next section highlights key features, and properties of PPP.

2.5.3 Poisson Point Process and Key SG tools

A PP is said to be ***Poisson Point Process (PPP)*** if it exhibits the following two properties,

- For all disjoint subsets $B_1, B_2, B_3, ..., B_n$, the numbers of points in each subset are independent of each other and are random variables.

- The number of points in each subset $\Psi(B)$ follows Poisson distribution with mean $\mu(B)$.

The basic feature of PPP is that for any given set B, the number of points inside $\Psi(B)$ are independent of each other. The most commonly used, well known and baseline PPP in literature to map the locations of users/device in cellular network is homogeneous PPP. A homogeneous PPP is a PPP with fixed intensity of points distributed over given space i.e. $\lambda(x) = \lambda$.

The formal definition can be written as,

$$\mathbb{P}(\Psi(B) = n) = \exp(-\mu)\frac{\mu^n}{n!} \tag{2.4}$$

which gives us the expected number of points in subset B. Considering homogeneous PPP, the mean ($\mu(B)$) can be equated to $\lambda|B|$ as the intensity of users is fixed. From this, a very useful expression of ***void probability for PPP*** can be derived, which states that subset $|B|$ is empty or $k = 0$ in Eq. 2.4. So, the null/void probability of homogeneous PPP will be $\exp(-\lambda|B|)$ [37]. Similarly, PPPs inherit some important properties along with already derived expressions for important measures, which results in tractability of analysis, simplified and closed-form expressions. Some of these properties which have also been used in this work are listed below,

- A homogeneous PPP will be ***motion invariant*** if it is both stationary and isotropic. This property helps in evaluating location-independent performance analysis of a system.

- The ***independent thinning*** of a PPP also results in a PPP but with different intensity. For instance, if all the points in Ψ with intensity λ are randomly assigned with independent marks from probability $q, 1-q$. Then, all the points

with probability q are retained to form another PPP with intensity $q\lambda$ and, removed points also form another PPP with intensity $(1-q)\lambda$.

- The ***displacement*** of points X_i in PPP independently with some random law or Markov kernel $K(X_i, .)$ also results in a different PPP.

- The ***superposition*** of two or more independent PPPs with intensities $\lambda_1, \lambda_2, ..., \lambda_k$ results in a new PPP with intensity $\lambda = \lambda_1 + \lambda_2 + ... + \lambda_k$.

These properties allow systematic manipulation of PPP with the help of transformations, thinning and marking to be used for evaluation of key performance metrics for network realization mapped to PPP. As, in the end, analysis comes down to the intensity of points in particular subset of considered space. To evaluate the expression for performance metric of interest, the PP is captured as either expectation over a random sum (or random product) of points. Now, interestingly, PPP offers two main following techniques to capture this randomness.

- ***Campbell Theorem:*** The Campbell's theorem converts expectation over sum of PP to integral. For instance, Ψ be a homogeneous PPP with intensity λ in $\mathbb{R}^n$ and $f : \mathbb{R}^n \to \mathbb{R}$ is measureable function. Then, Campbell theorem states that [29],

$$\mathbb{E}\left\{\sum_{X_i \in \Psi} f(X_i)\right\} = \int_{\mathbb{R}^n} \lambda f(x) dx \tag{2.5}$$

  The simple and generic application of Campbell theorem to compute the mean interference in a cellular network is given in [29].

- The ***Probability generating functional (PGFL)*** converts expectation over random product of PP to integral, hence, simplifying the mathematical analysis. The PGFL of homogeneous PPP is [29],

$$\mathbb{E}\left\{\prod_{X_i \in \Psi} f(X_i)\right\} = \exp\left(-\lambda \int_{\mathbb{R}^n} (1 - f(x)) dx\right) \tag{2.6}$$

Laplace transform is mostly used among PGFL and Campbell theorem to characterize the interference seen by the typical user (x_o) at the origin. Thus, the Laplace transform of random interference $\mathcal{I} = f(X_i)$ at s over random sum and random product can be written as [29],

$$\mathcal{L}_{\mathcal{I}}(s) = \mathbb{E}\{^{-s\mathcal{I}}\} = \mathbb{E}\left\{-\sum_{X_i \in \Psi} sf(X_i)\right\} = \mathbb{E}\left\{-\prod_{X_i \in \Psi} sf(X_i)\right\} \tag{2.7}$$

- The ***Slivnyaks theorem*** is the foundation of SG analysis and use for a wireless communication system. This theorem states that conditioning PPP with point at x, removing this point does not change the distribution for the rest of PPP because of Independence of points in PPP. Thus, reduced Palm probability ($P^{!x_o}$) of PPP Ψ is also the distribution of the Ψ itself and can be written as ($P^{!x_o} = P$) [28]. This striking property for PPP gives freedom to place/remove a point at a certain location, perform the analysis and the analysis would equally be applicable for the entire PPP. Typically, this test/probe point is added at origin (o, o) and is referred to as ***typical point*** in literature and in this work as well. The laws/properties seen from analysis of typical point holds for the entire PPP, thus leading to simplified and tractable analysis with mostly closed-form expressions for key performance metrics.

Above mentioned SG tools and baseline knowledge of PPs allows us to characterize the key performance metrics for communication systems with different properties. Table 2.2 summarizes the state-of-the-art tutorials and surveys published in literature which provide basics for using stochastic geometry for design of wireless networks. Readers are referred to [80] for more comprehensive taxonomy of Stochastic geometry based works based on PPs, approximation techniques and network types.

Table 2.2 : The Summary of state-of-the-art tutorials/surveys on stochastic geometry for wireless networks

Work, type, year	**Key features/expressions using stochastic geometry**
[81], Book, 1995	Applications of stochastic geometry for applied sciences and engineering. PP's, models of stochastic geometry, statistical theory of different shape models and applications.
[82], Paper/Chapter, 1995	Intensity measures of PPP, user association, traffic modelling. Stochastic geometry modelling of basic telecommunication systems through homogeneous PPP, statistical distribution of number of users in a cell, Moments of functional of performance metric.
[83] Survey/Tutorial	Taxonomy of transmission capacity results, interference cancellation and suppression, direct-sequence versus frequency-hopping spread spectrum, use of sub-bands conditioned on rate constraint, use of multiple antennas, power control, optimum channel-strength
[84], Tutorial, 2005	The density function of n-nearest neighbour in uniformly distributed networks over $\mathbb{R}^m$.
[85], [79] Book, 2009/2010	Theoretical derivations for basic stochastic geometry tools for performance analysis of wireless network design, interference characterization, user distributions, and [79] for applications of these formulations to assess different performance metrics in wireless communication and networking
[28], Tutorial/Survey Paper, 2009	Use of stochastic geometry and theory of random graphs for interference modeling, SINR expressions, and LT of interference. Outage probability, throughput expressions and percolation theory for user connectivity.

Work, type, year	**Key features/expressions using stochastic geometry**
[86], Tutorial Paper, 2009	Mathematical framework for characterizing network interference, employed fading/shadowing (Nakagami-m fading and log-normal shadowing). Interference modelling for cognitive networks, SINR formulation, spectral outage probability (SOP) and coexistence study and dependence of users among UWB and NB systems.
[87], Tutorial Paper, 2010	Important formulations on transmission capacity (TC) of ad-hoc (decentralized) wireless networks. TC with random channels (shadowing/fading) and upper/lower bounds for TC from outage probability. Applications for analysis of power control, scheduling, and multiple antennas.
[30], Tutorial Paper, 2011	General and one of the pioneer stochastic geometry framework for multi-cell SINR for cellular networks, also tractable expressions for mean data rates, coverage gain (from frequency reuse) are presented and validated with grid based, Poisson based and actually 4G deployed models.
[88], Tutorial, 2012	Stochastic geometry framework for modelling, design and analysis of k-tier heterogeneous cellular network (HCN). Interference modelling for micro, pico and femto cells. Probability of coverage and average rate via SINR expression with Rayleigh fading.
[80], Survey, 2013	Survey on stochastic geometry models for single/multi-tier. cognitive, cellular and ad-hoc wireless networks. Comparative analysis and taxonomy of previous work based on PPs, network model and performance metrics.

Work, type, year	Key features/expressions using stochastic geometry
[35], Tutorial Paper, 2015	Macro and Pico cell based heterogeneous network modelling with PPP and PHP. Inter-dependency among points and base station is employed for formulations of outage probability, per-user capacity, area spectral efficiency and key performance metrics.
[13], Tutorial, 2016	Stochastic geometry framework, modelling and design for FD enabled cellular network (underlay) in up-link. Outage probability and rate expressions for cellular and D2D users.
[29], [77], Tutorial, 2016	Tutorials on pioneer stochastic geometry tools for modelling, analysis, and design of cellular networks. Key performance metrics expressions for single/multi-tier in up-link/down-link modes. Interference characterization for different network configurations.
[89], Tutorial, 2017	Fitting analysis of heavily and lightly loaded cellular networks with Poisson and Ginibre PPs. Mean cell vacancy/occupancy area and pair correlation functions are characterized from user/base station point of view.
[90], Tutorial, 2018	Analytical and approximate expressions for density of active users satisfying certain outage constraint for Poisson bipolar networks with ALOHA. Exact closed-form expressions using stochastic geometry tools for spatial outage capacity (SOC).
[91], Tutorial, 2018	Stochastic geometry formulation of Spatial Spectrum Sensing (SSS) based D2D enabled cellular network while guaranteeing QoS to cellular users. ASE and outage probability of D2D users is characterized.

2.5.4 Analyzing Metrics

Equipped with SG tools and knowledge of PP properties, we can now proceed to define the key network statistical properties.

Signal to Interference and Noise Ratio (SINR)

Design, modelling and analysis of cellular networks using SG tools involve capturing the interference experienced by typical receiver at origin (in down link analysis) from all the other transmitters except the intended transmitter (tagged base station). The ***tagged base station*** is referred to as either the nearest base station to a typical receiver or with highest signal strength. This leads to a powerful expression for key performance metric to evaluate the performance of any communication system i.e. Signal to Interference and Noise Ratio (SINR). Considering the downlink analysis, lets assume all the base stations are distributed according to PPP Ψ of intensity λ in Euclidean space $\mathbb{R}^2$. Denote locations of base stations with y, such that $y \in \Psi$. Base stations are transmitting with power P and signal attenuation follows standard distance-based path-loss propagation model with path-loss exponent $\alpha > 2$. Assume random channel gains with $h(x, y_i))$, which is channel gain between the receiver at x and transmitter y_i. The ***probability density function (PDF)*** of nearest base station (tagged base station y_o) for typical receiver (x_o) is the well known result ,

$$f_R(r) = 2\pi\lambda \exp(-\lambda\pi r^2) \tag{2.8}$$

which means the nearest base station follows Rayleigh distribution and no other base station is closer than the tagged base station y_o, derived from the null-probability of PPP in $\mathbb{R}^2$. Let us assume the tagged base station is at distance R, and taking leverage of Slivnyaks theorem by placing test receiver (x_o) at origin (o, o), then we

can write the SINR expression for typical receiver at origin (x_o) as,

$$SINR_{x_o} = \frac{p_{rx}(x_o, y_o)}{\mathcal{I}_{x_o, y \setminus \mathcal{C}(x_o, r)}} = \frac{Ph(x_o, y_o)R^{-\alpha}}{\sum_{y_i \in \Psi \setminus y_o} Ph(x_o, y_i)||y_i||^{-\alpha} + \sigma^2} \tag{2.9}$$

where, p_{rx} is the received power from tagged base station to typical receiver, $\mathcal{I}_{x_o, y \setminus \mathcal{C}(x_o, r)}$ is the interference seen by typical receiver from all other base stations except tagged base station y_o, $\mathcal{C}(x_o, r)$ represents circle with center at x_o and radius of distance to tagged base station r, and σ is the noise power. The notation $\mathcal{I}_{x_o, y \setminus \mathcal{C}(x_o, r)}$ and $\mathcal{I}_{x_o, y \setminus y_o}$ are used interchangeably to identify all interference field for a typical user conditioned on tagged base station y_o. The interference field $\mathcal{I}_{x_o, y \setminus y_o}$ is a stochastic process which has two random variables, the location of interferers $y_i \in \Psi$, and channel gains $h(x_o, y_i)$. Depending on the system design and analysis, further randomness is also dealt with in performance evaluation. For instance, in the case of uplink analysis, the transmit power could be another factor of randomness. Thus, different system configuration parameters as required by the analysis are mapped to suitable PP and final expressions are derived using SG tools. The Laplace transform of pdf of interference field from certain nodes is evaluated using Eq. 2.7. Some classical results including Laplace transform of pdf of interference are well known in literature and follow taking expectation of random sum or product, and then applying either Campbell theorem or PGFL. Readers are referred to [29] for detailed steps, the Laplace transform of interference field for $\mathcal{I}_{x_o, y \setminus y_o}$ will be ,

$$\mathcal{L}_{\mathcal{I}_{x_o, y \setminus y_o}}(s) = \exp\left(-2\pi\lambda \int_r^\infty \left(\frac{1}{1 + (sp)^{-}1x^\alpha}\right) x dx\right) \tag{2.10}$$

Success or Coverage Probability

The cellular user can communicate successfully if received signal (in downlink) is stronger than the interference power i.e. $p_{rx}(x_o, y_o) > \mathcal{I}_{x_o, y \setminus y_o}$. From this, we can define probability of successful communication (success probability) and/or coverage probability for a typical user at origin as in [29],

- the probability that typical user can achieve target $SINR$ threshold (T) needed for successful communication,
- the average number of users in considered area of interest who can successfully communicate by achieving target $SINR$ threshold T,
- the average segment of area that is within coverage at any time.

Mathematically, we can define this performance metric as ,

$$p_s(T, \lambda, \alpha, \Psi) \triangleq \mathbb{P}(\text{SINR}_{\mathcal{X}} > T), \tag{2.11}$$

where, $\mathcal{X}$ is randomly chosen user, commonly typical user at origin.

Similarly, the other relevant key network performance metrics depend on $SINR$ and their expressions are well known in literature e.g. Area spectral Efficiency (ASE), Data Rate, Outage Probability.

2.5.5 Interference Characterization Using Stochastic Geometry Tools

The SG analysis helps statistically measure the interference averaged with respect to a number of interferers in a spatial domain. The interferers are distributed according to one of the point processes and interference is characterized using Laplace transform of pdf of the interference or also using its cdf. Typically, simplified expressions are available for large scale wireless scale networks. These expressions are derived either using Laplace transform, characteristic function (CF) or moment generation function (MGF) of pdf of interference. These expressions have been derived already in detailed steps in previous literature. Readers are referred to Table 2.2 for taxonomy of key stochastic geometry tutorials, surveys and books which discuss these concepts and formulation techniques in detail. For simple PPP, these expressions are well known in literature. However, for different cases,

depending on the system design and modelling, mostly the interference characterization and expression for performance metrics becomes a complicated task due to the high degree of randomness and inter-dependencies of pdf's of different random variables. Hence, different techniques or approximations are used to either derive the upper/lower bounds or approximate expressions for performance metrics.

2.6 Summary

In this chapter, we have presented the basic concepts of next generation networks of LTE and relevant key enabling technologies related to this dissertation. Then, we have categorized different dynamic spectrum sharing frameworks commonly used in literature and also relevant works employing these frameworks. The last section presents key concepts of stochastic geometry and important tools used to formulate some performance metrics of wireless networks. We have then presented a summary of important stochastic geometry tutorial and survey works.

Chapter 3

Coverage Analysis of Cellular User in Full Duplex D2D Cognitive Network

This chapter presents SG model of FD enabled D2D cognitive networks. Building on the brief introduction in section 3.1, followed by the closely related works in section 3.2, we present our system model, methodology of analysis and performance metrics in section 3.3. Analytical modelling for optimal mode (silent, HD or FD) selection for a D2D link is given in section 3.4. Finally, simulation results validated with theoretical results are presented in section 3.6, followed by the summary of the chapter in section 3.7. Parts of the work described in this chapter resulted in Publication [92].

3.1 Introduction

The gigantic increase in the number of connected users and devices to the internet complemented by significant growth in mobile applications has aggressively challenged the capacity of existing communication systems and demanded multi-gigabits per second data rates. To cope with such increase, advancements in all aspects from access to the core network are required along with the performance elevation of key network resources. The capacity of existing and future telecommunication systems is highly reliant on effective spectrum utilization. This is because spectrum is a key resource or carrier which connects users to the internet. In recent years, optimization of spectrum usage among sharing stakeholders has played a vital role in the evolution of Next Generation Networks (5G). Along with the addition of new spectrum space for mobile systems in 5G [20], innovative proposals have been

made to employ different spectrum sharing options to further elevate the system capacity [93].

Spectrum sharing frameworks have significantly proven their performance advantages and played a vital role in optimizing the user capacity and socio-economic benefits of existing communication systems [7]. Among these frameworks, Cognitive Radio (CR), TV white spaces, Citizen Broadband Radio Service (CBRS) and Licensed Shared Access (LSA) have proven to be effective solutions for spectrum under-utilization. The key aim is to increase spectral efficiency on the basis of use-it or share-it basis, where Primary Users (PUs) can share/lease underutilized spectrum on a short-to-short or short-to-long term basis with Secondary Users (SUs). This sharing is done based on pre-defined conditions for leaving the spectrum for priority users whenever needed and imposing the least interference to PUs. The spectrum sharing can be done in the time domain (primary user is not transmitting), space domain (primary user is far away) and frequency domain (primary user is transmitting on a different frequency). For detailed benefits of dynamic spectrum sharing and heterogeneous device coexistence, readers are referred to [9].

The key enabling technology candidates in 5G further paved the way for higher gains in improving spectrum efficiency using Dynamic Spectrum Sharing (DSA) [39]. Among these technologies, Device-to-Device (D2D), massive MIMO, Full-Duplex (FD) radios, millimeter wave and Terahertz band, multi-Radio Access Technologies (multi-RATs) and Network Virtualization are spotlight candidates. The performance gains offered by these enabling technologies can be multifold after thorough feasibility studies for their practicality to be integrated into cellular systems [1]. Such technologies have complemented and elevated significantly machine-type communications in pursuit of accelerated automation and industrial revolution [38].

3.2 Related Works and Motivation

The recent significant advancements in self-interference-to-power-ratio (SIPR) reduction have paved the way for the use of full-duplex radios to double the data rates at the cost of induced interference. For instance, practically the cancellation capability of 70dB can be achieved using compact or separated antennas at the bandwidth of 100MHz in 2.6GHz band [12]. Thus, in-band FD communications integrated with D2D technology will elevate the spectral efficiency while doubling the data rates [13]. Moreover, recent research has also indicated toward the elevation of spectral efficiency (up to 100%) in single-cell and single D2D link scenarios as compared to half-duplex (HD) if sufficient SIPR reduction is achieved [14–16]. However, without considering the impact of induced interference from FD mode, it may cause more harm than benefit. Thus, an interesting research problem needs further work to find a feasible trade-off between the use of FD radio while limiting the induced interference, which is also the motivation behind this work. In this work, we study the use of FD equipped D2D devices as secondary users and propose mode switching between half-duplex and full-duplex based on interference faced by primary users. The recently published and closely related work in [91] presented detailed insight into Spatial Spectrum Sensing based D2D enabled cellular networks, where a HD D2D network was modelled as Poisson Hole Process (PHP) and relevant interference characterizations along with upper and lower bounds were well studied; however, we consider FD enabled D2D setup in this work.

We use Stochastic Geometry (SG) analysis which has proven to be an effective mathematical platform in previous works to model variants of communication networks while characterizing the key network parameters [28]. For instance, the authors in [94] present stochastic geometry analysis of coverage and performance of D2D network from a user association model based on multiple simultaneous re-

quests in homogeneous systems and ultra-dense small networks. Due to topological and spatial randomness, SG can successfully yield tractable, and in special cases, closed-form expressions that reflect the system behavior. The alternate methods for performance evaluation of cellular networks include exhaustive simulation scenarios to average out the randomness of different network parameters (base stations, user locations and fading distributions). However, these methods are time-consuming and prone to errors. Therefore, SG provides a supplementary platform to produce baseline results for benchmarking, and comparative performance analysis [29].

The comprehensive tutorial on SG modeling, design, and analysis for multi-tier and cognitive cellular networks is presented in [36] and more are summarized with key features in Table 2.2. Interference characterization and relevant analytical tools are comprehensively discussed. Another related work in [95] characterized D2D throughput based on social interaction and distance distribution in the context of spectral efficiency. Moreover, link-distance based mode selection along with link-distance distribution in different social scenarios was proposed to decrease the communication probability density.

Authors in [96] proposed SG-based modeling of carrier sensing based multiple access schemes for cognitive radio networks. Protection zones were considered among PUs where SUs will not be retained and are not allowed to transmit. The baseline work for coverage and rate analysis in cellular networks was published in [30], which also highlighted tractability of SG tools and comparative performance analysis with a SG model, a grid model, and actual network deployment. Another work [97] studied the stochastic geometry of thinned nodes to capture the knowledge of the post-MAC geometrical distribution of nodes, as thinning mechanisms alter the spatial distribution. Circular Guard Zones (GZs) were drawn around the intended receiver to protect its reception by inhibiting close-by transmissions. A similar concept is adopted in this research work to protect PUs reception and it was investigated if

SU should switch to HD, FD or silent mode.

Moreover, the SG analysis for interference characterization and expressions for network performance metrics for K-tier heterogeneous cellular networks is presented in [88]. One of the closely related works [98] modeled PUs and cognitive users (CUs) as independent Poisson Point Processes (PPPs). Exclusions zones (where cognitive cannot transmit) were drawn around PU such that CUs form PHP. Due to inter-dependence between PUs and CUs along with overlap of protection zones (PZs), the interference upper and lower bounds were given along with the practicality of implementing Poisson cluster process on such networks. Most of these works have employed SG analysis and modeling of PUs and SUs with HD only; however, in this study, we assess the impact of FD D2D enabled SUs while guarding PUs reception in up-link and characterize the interference for mode selection (HD, FD or silent). Another related work recently published in [99] characterizes aggregate interference using SG tools for TVWS cognitive networks. The PDF aggregate interference is characterized and closed-form expressions are given for different path-loss values. Similarly, the SG based analysis to characterize the aggregate interference for primary user in cognitive radio systems is presented in [100]. The emphasis is kept on the performance analysis of the primary network, where the secondary users are Poisson distributed in a finite area between radii of two circles. MGF's, cumulants of relative interference from SU are derived and PDF is given for different path-loss exponents. However, the focus of this work is on TVWS/cognitive networks and does not consider FD enabled D2D system.

In the context of dynamic spectrum sharing, recently SG modeling and analysis of CBRS are done in [33]. Authors present a tractable performance analysis of CBRS by employing PZs for priority access licensed (PAL) users, while general authorized access (GAA) users operate using the contention-based channel access mechanism (CSMA). A similar approach of employing guard zones (GZ) has been used in [101],

SG analysis for co-existence of contention-based (WiFi) and scheduled based (LTE) networks is presented in [34].

SG analysis of FD D2D has also been recently studied and performance trade-offs have been assessed in [32]. The initial SG analysis for throughput of wireless networks equipped with FD capability and imperfect SIPR was done in [102]. Another SG approach presented signal to interference and noise ratio (SINR), transmit-power and mode switching (HD/FD) for FD D2D for cellular networks [13]. Authors in [32] presented performance analysis of FD in cache-enabled D2D networks but the emphasis was kept more on the content caching, sharing and delivery, whereas, our work focuses more on cognitive type setup with FD D2D users.

The key motivation of this work is driven by the fact that critical mode selection analysis of adjacent secondary users while protecting primary user receptions would elevate the spectral efficiency alongside making more space and opportunities for ultra-dense networks in future urban scenarios. As this work focuses especially on the secondary users lying in the vicinity of the edge of PUs GZ, the analysis will study the limits to which a secondary user can still communicate while near to the boundary of PUs GZ. Such opportunistic lending of spectral resources benefits both network operators (licensed operators), and license-free service providers. To the best of our knowledge, none of the existing works proposes the mode selection for FD enabled secondary users to protect the primary users receptions in the context of SG.

3.2.1 Contributions

In this work, a SG framework for an optimal mode selection for D2D users enabled with half-duplex and full-duplex capabilities is proposed, while protecting receptions of primary users. Specifically, each primary user reception is protected and D2D users opt for a mode based on their proximity to primary users. The main

contributions of this work are summarized as follows:

- The induced interference from FD use of D2D devices and overall aggregate interference is characterized using SG tools. The trade-off between interference introduced by FD operation and spectral efficiency due to FD is critically investigated.

- We propose a novel mechanism for mode selection by D2D devices depending on receivers vicinity to PUs guard zones while ensuring it does not impact the PUs reception for dynamic spectrum sharing frameworks. The proposed mode selection mechanism encourages primary licensees to allow SU operation either in HD or FD modes as long as SUs provide agreed-upon interference protection to PUs.

- The research work presents quantified performance gains for opportunistic spectrum use complemented by FD radios in terms of probability of successful receptions by both cellular and D2D users. Using the expressions for coverage probabilities, we also present insights into different GZ radius values and their impact on SUs communication.

3.3 System Model

We consider a heterogeneous wireless network, where the primary user (cellular operator) allows secondary users (D2D) to opportunistically use the spectrum conditioned on interference protection for cellular users. The leased spectrum is segregated into small chunks; we assume PU is operating on one of these selected frequency bands for downlink reception. The second-tier users can be inferred as ultra-dense small networks dynamically sharing spectrum with tier-1 users. Specifically, we focus on D2D users as secondary users (SU), enabled with Full-Duplex (FD) transceivers, which opportunistically use cellular spectrum conditioned on preset

Interference Protection. The analysis is equally applicable for similar technologies which can operate as SUs with FD capabilities. The D2D users can opportunistically share incumbent's spectrum outside of the GZs. Moreover, these FD enabled D2D transceivers can switch between the modes depending upon the induced interference to PUs. The self-interference leakage in FD links is considered to be imperfect with a residual self-interference-to-power-ratio factor β. The value of β ranges from 0 to 1, from perfect to imperfect SIPR cancellation, respectively. The link-state of the D2D communication pair is half-duplex, full-duplex or silent.

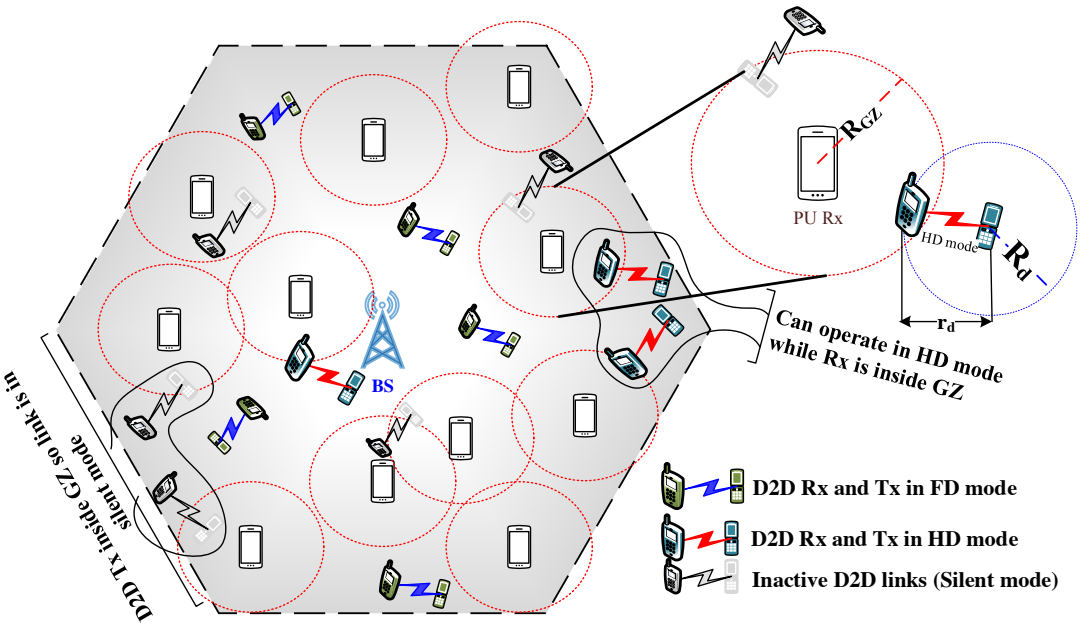

Figure 3.1 : Realization of considered network model in single cell scenario with circular guard zones and D2D links (silent, HD and FD mode). [92]

3.3.1 Spatial Locations and Distance Distribution

We consider a two-tier wireless network, in which the full-duplex enabled D2D users can opportunistically share the spectrum with tier-1 cellular users, also referred to as primary users (PUs). The locations of all the cellular users are modeled via

an independent homogeneous PPP Φ_c with an intensity of λ_c in a single cell, while, the D2D transmitters are modeled via another homogeneous PPP which we denote as Φ_d, with intensity of λ_d. The PU's communication (reception in our model) must be protected from any harmful interference of SUs as required in most of Dynamic Spectrum Sharing (DSS) systems. In order to protect the reception of PU, we employ circular GZs of radius R_{GZ} centered at the locations of cellular users i.e. $x \in \Phi_c$. We denote this circular GZ around a cellular user located at x with radius R_{GZ} by $C_{x,R_{GZ}}$. The total area covered by all these circles with radius R_{GZ} can be expressed as [103],

$$\mathcal{A}_T \triangleq \bigcup_{x \in \Phi_c} C_{x,R_{GZ}}. \tag{3.1}$$

To protect the reception of cellular users from harmful interference of D2D transmitters, we delete the D2D Txs (points) from a ground PPP i.e. $y \in \Phi_d$ which lie inside the GZs of the primary users. Hence, the resulting point process of retained points will be Poisson-Hole Process (PHP) denoted by φ_d,

$$\varphi_d = \left\{ y \in \Phi_d : y \notin C_{x,R_{GZ}} s.t. x \in \Phi_c \right\}, \tag{3.2}$$

which states that for a point $y \in \Phi_d$ to be retained in $y \in \varphi_d$, y should not be inside any of the circular GZ around primary receivers ($C_{x,R_{GZ}}$). The resulting intensity of φ_d is the number of points outside the GZs given by $\tilde{\lambda}_d$ [33],

$$\tilde{\lambda}_d = \lambda_d \exp(-\pi \lambda_c R_{GZ}^2), \tag{3.3}$$

Now, the D2D transmitters outside GZs (in Eq. 3.2) can transmit and form a communication link with receivers. To model the location of the D2D receivers for these transmitters $y \in \varphi_d$, we assign a mark m_y which is uniformly and randomly distributed on the circumference of a circle of radius r_d centered at D2D Tx. The D2D communication link formed between transmitter y and receiver m_y has distance of r_d. The mark m_y can also be represented as, $m_y = y + r_d(\cos(\theta), \sin(\theta))$, where

Table 3.1 : Notations, Symbols and Description

Notation	**Description**
Φ_c, λ_c	PPP for cellular users, and its intensity
Φ_d, λ_d	PPP modeling of D2D transmitters, and its intensity
$\varphi_d, \tilde{\lambda}_d$	PHP of D2D transmitters from ground PPP of Φ_d, and its intensity
$\varphi_{m_d}, \tilde{\lambda}_{m_d}$	Marks (RXs) of D2D transmitters, and their intensity
$C_{x,R_{GZ}}$	Circular guard zone centered at $x \in \Phi_c$ with radius R_{GZ}
θ	The angle between D2D transmitter y and receiver m_y
$b(o, R)$	Circular disc of Radius R centered at origin $(0, 0)$
$\mathcal{C}_1$	Annulus area of interest in ring formed by region $b(o, R_{GZ}) \cap b(o, R_{GZ} + R_d)$
$F_{o,\kappa}$	Channel fading at origin from user $\kappa = x, y, m_y$
α_c, α_d	Path-loss component for primary and D2D users
β	Residual self-interference-to-power ratio (SIPR) for FD nodes
T	SIR threshold for successful communication
R_{GZ}	Radius of guard zone around primary users
r_d, R_d	Random and fixed distance for D2D communication link
R_c	Fixed distance between typical cellular user and tagged base station
R_p	Radius of the area of the plane (i.e. total area of interest under consideration)

the angle θ is independently and uniformly distributed on $[0, 2\pi)$. These marks (m_y) form another point-process which we denote by φ_{m_d}. It should be noted here that m_y may lie inside the GZ of the cellular user, but it will not impact the reception of PU as the Tx (y) of D2D is still outside. However, its probability to go into

half-duplex or full-duplex mode may change depending upon its location and angle θ. We will discuss this in detail in Section 3.4. The realization of the considered system model is presented in Fig. 3.1.

3.3.2 Propagation Model

Random wireless channel effects are taken into account for performance analysis. We assume that each link in a considered wireless network described above experiences an i.i.d Rayleigh fading denoted by $F_{o,\kappa} = \exp(\mu)$ i.e. fading at typical receiver located at origin (o, o) from any point κ, which can can take values from, $x \in \Phi_c, y \in \varphi_d, m_y \in \varphi_{m_d}$. Also, we use notation $l(d)$ generically for path-loss of a communication link with distance d. For large scale fading we assume a distance based path loss model i.e. $d^{-\alpha_c}$ $(d^{-\alpha_d})$ for cellular and D2D links. Similarly, the transmit power will be P_c (P_d). For the typical cellular receiver the received power from the tagged base station (x_{BS}) located at a fixed distance of R_c can be written as:

$$P_r(x_o, x_{BS}) = P_c F_{x_o,x_{BS}} l(x_o, x_{BS}), \tag{3.4}$$

while, $l(x_o, x_{BS}) = R_c^{-\alpha_c}$, represents the distance based path loss which is given by $l(x_o, x_{BS}) = ||x_o - x_{BS}||^{-\alpha_c}$, while, $||.||$ is Euclidean norm operator and $F_{x_o - x_{BS}}$ is the respective channel gain.

3.3.3 Performance Metrics

The typical receiver (at the origin) can successfully receive from a tagged (intended) transmitter if SIR requirement is met at the receiver. The SIR success probability of a typical receiver is the probability of achieving the target SIR threshold T,

$$p_s(T) \triangleq \mathbb{P}(\mathrm{SIR}_{\mathcal{X}} > T), \tag{3.5}$$

where, $\mathcal{X}$ represents the probe receiver under consideration for analysis which is either a cellular (x_o, as in this chapter) or D2D user (m_o, as in chapter 4.3). Now, the SIR at a typical receiver is the ratio of the intended received signal power to total interference power from the rest of users. The SIR of probe receivers in the case of a cellular link is given as follows,

$$SIR^{c}_{x_o} = \frac{P_c F^{c}_{x_o,x_{BS}} l\left(x_o, x_{BS}\right)}{\mathcal{I}_{x_o,y} + \mathcal{I}_{x_o,m_y} \mathbb{1}^{FD}_{m_y,y}}, \tag{3.6}$$

where, the first interference term ($\mathcal{I}_{x_o,y}$) in the denominator is the interference experienced by a typical user from all D2D transmitter and the second term ($\mathcal{I}_{x_o,m_y}$) is the interference from D2D receivers if the D2D link is in FD mode, indicated by indicator function ($\mathbb{1}^{FD}_{m_y,y}$).

3.3.4 Methodology of Analysis

We have followed the standard practice of stochastic geometry analysis and have used key stochastic geometry tools/expressions given in the literature. These techniques have been discussed and presented in section 2.5 in general and in subsection 2.5.3 in specific for PPP. Without loss of generality, we can assume that our probe receiver x_o is located at the origin which is permissible due to Slivnyak's theorem for PPP [76]. The conclusions drawn from the analysis of the system model described above is equally applicable to all the other users in the network due to the stationarity of PPP, explained in subsection 2.5.3. Symbols, definitions and corresponding simulation values are listed in Table 3.1. We will begin with the mode selection probability of D2D users based on their vicinity to the primary receiver. The intensity of D2D links in either (HD or FD) mode is going to impact on the performance of the primary receiver. The next subsection defines the criteria for the mode selection of D2D links.

3.4 D2D Mode Selection

In this section, we derive the probability of the communication mode for a D2D link to be in silent, half-duplex or full-duplex mode based on its transmitter's distance to nearby cellular user GZ. The main objective is to protect cellular user reception from harmful interference of the D2D link. As the interference is mainly dependent on the distance of nearby interferers, the reception mode of the D2D receiver primarily depends on its distance from the primary user, the angle θ on a disk of radius r_d and how much inside it is in the guard zone.

D2D Link Distance Distribution: In the context of a D2D communication link distance distribution (r_d), it depends on the underlying application and social interactions among the users. For instance, in the case of the congested audience in a stadium, this would result in smaller r_d, and it would be higher in a typical urban scenario. One of the trivial distance distributions for D2D users is formulated in [104]; based on power-law communication probability ($0 \leq \vartheta < 2$), the PDF of D2D communication distance r_d is given by,

$$f_{r_d}(v) = \frac{(2-\vartheta)v^{1-\vartheta}}{R_{dmax}^{2-\vartheta}}, \tag{3.7}$$

where v is a Random Variable (RV) representing D2D link distance r_d, R_{dmax} is the maximum communication distance of the D2D link and ϑ is the control parameter for the contact distance distribution (depends on social interaction of D2D users). Setting the value of $\vartheta = 0$ will make $f_{r_d}(v)$ independent of social-interaction and will result in a uniform distribution of D2D Rx in a circle of radius R_{dmax}, centered at D2D Tx as in [105]. The CDFs for different D2D link distances and θ values are shown in Fig. 3.2. As we start increasing the value of ϑ, the CDF of the D2D link distance approaches 1 as ϑ approaches to 2. Thus, ϑ can be set according to social-interaction scenarios depending upon the density of D2D users ($\tilde{\lambda}_d$). The receivers (m_y) are uniformly distributed inside a disc of radius r_d taking values from

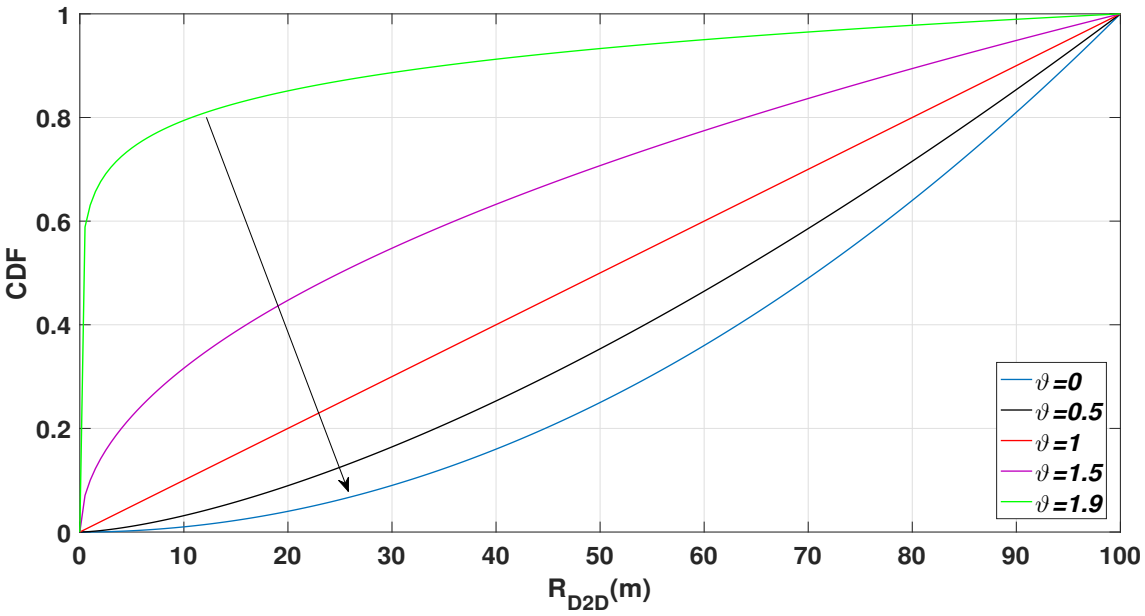

Figure 3.2 : CDF of D2D Link Distance for different values of ϑ (social interaction parameter) as a function of D2D link-distance

pdf (f_{r_d}), where maximum possible distance can be R_{dmax}. In this work, we have considered fixed D2D link distance, R_d to reduce the mathematical complexity and closed-form expressions for the key performance metrics.

Let's consider cellular user x_o located at origin (o, o), also referred to as a typical cellular user, connected to base station x_{BS} at distance R_c. Now, we are interested to analyze the impact of the distance of x_o to nearby D2D transmitter y, referred to as $r_{x_o,y}$. From Fig. 3.3, depending on the distance ($r_{x_o,y}$) between the location of the primary user (i.e. center of its GZ) and the D2D transmitter (with Rx on a disk of radius R_d and angle θ), the communication modes for the D2D link can then be chosen safely to protect x_o reception. All the possible case scenarios which may emerge based on distance ($r_{x_o,y}$) are illustrated in Fig. 3.3 and discussed in detail in the following subsections.

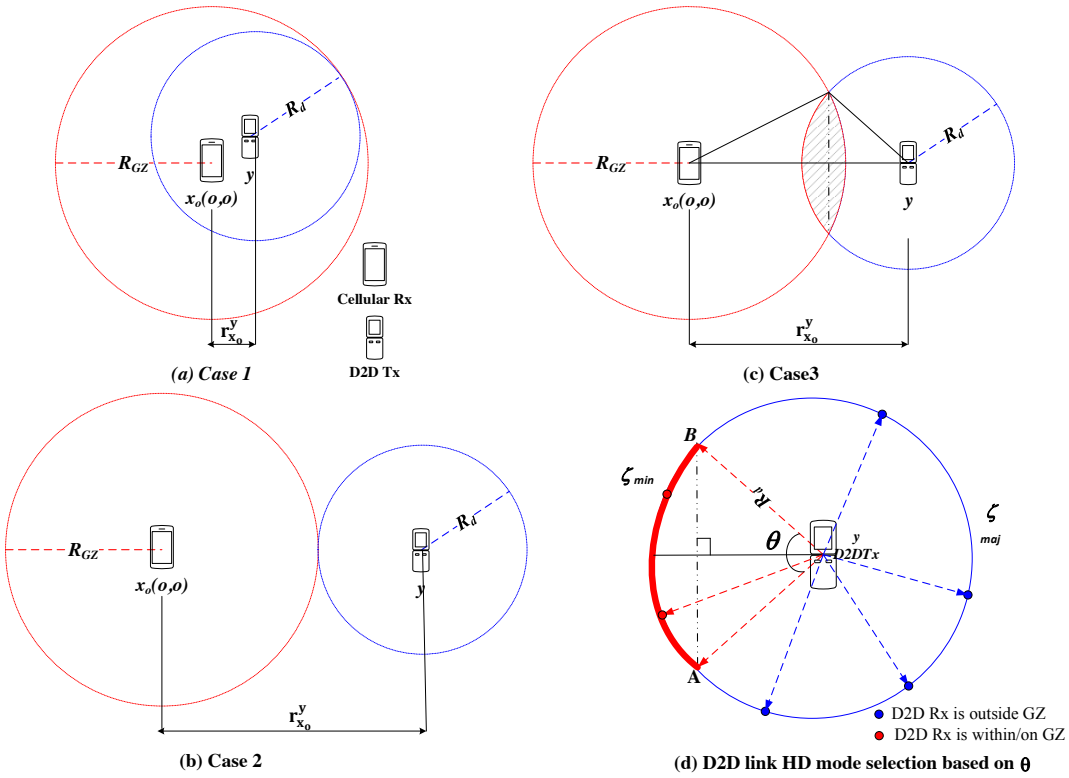

Figure 3.3 : Illustration of possible case scenarios for D2D communication pair based on the distance between D2D transmitter and guard zone of cellular receiver

3.4.1 Case 1: D2D users in Silent mode

In this case, the D2D communication pair is inside the GZ of cellular receiver (x_o), then as per the interference protection conditions, x_o's reception must be protected and the D2D pair will not be active (remain in silent mode). This case was also used for D2D transmitters thinning in the system model in Eq. 3.2 where users inside the GZs were deleted. Alternatively, the D2D link will remain silent if the following distance-based condition is met,

$$r_{x_o,y} < R_{GZ} \tag{3.8}$$

This scenario is also shown in Fig. 3.3 (a). We can represent the counting measure of D2D Txs in silent mode using random set formalism, where $\Phi_d \subset \mathbb{R}^2$

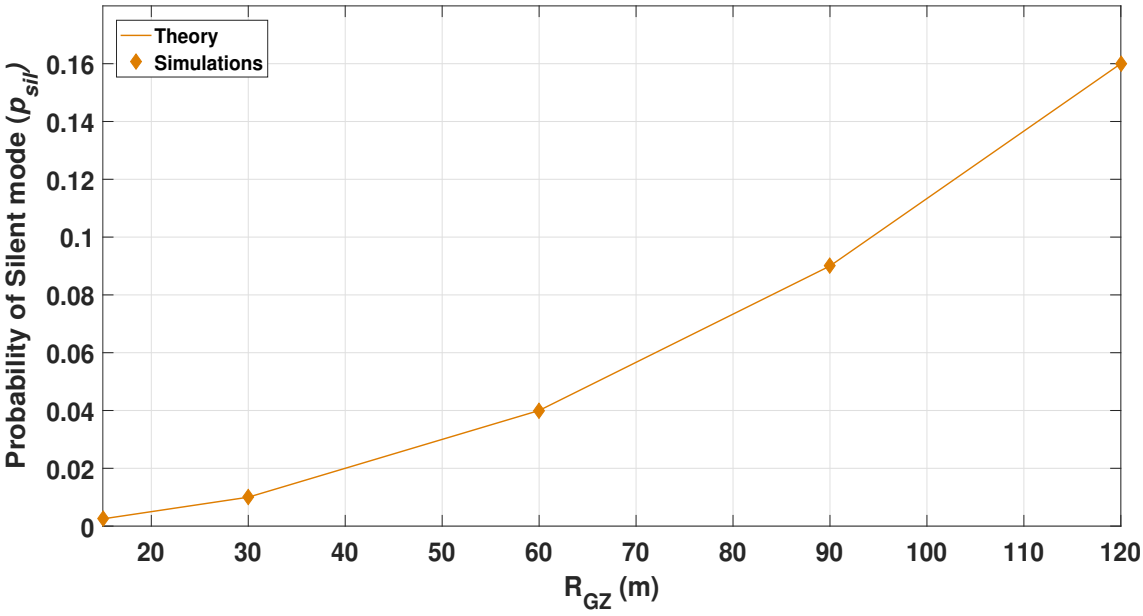

Figure 3.4 : Probability of Silent D2D links as function of R_{GZ} from Lemma 1 and simulations

over an area of interest $|A|$ is a countable random set of D2D transmitters,

$$\Lambda_{sil} = \sum_{y_i \in \Phi_d, 0<||Y_i|| \leq R_{GZ}} \mathbb{1}(y_i \in |A|) = \pi \lambda_d R_{GZ}^2 \tag{3.9}$$

Lemma 1: Considering disk $b(o, R_{GZ})$ of radius R_{GZ} at origin o, the probability of any D2D communication link to be in silent mode can be expressed as,

$$p_{sil} = \frac{\pi \lambda_d (R_{GZ})^2}{|A|} \tag{3.10}$$

Proof: Assuming points are uniformly and randomly distributed by PPP, let $|A|$ be the total area/bounded set ($|A| < \infty$) of the plane where all D2D points are distributed with intensity λ_d. Also, if B is a circular disk of radius R_{GZ} at origin (o), then the probability of D2D points being in $B \subset A$ will be,

$$p_{sil}\,(y \in B) = \frac{|B|}{|A|} \tag{3.11}$$

Now, the expected intensity measure of points in B will be ,

$$\mathbb{E}\left\{\Lambda_{|B|}\right\} = \mathbb{E}\left[\sum_{y_i \in \Phi_d} \mathbb{1}_{(0<||Y_i||\leq R_{GZ})}\right] \stackrel{a}{=} \lambda_d \int_0^{\infty} \int_0^{2\pi} \mathbb{1}_{(0<||y_i||\leq R_{GZ})} d\theta dr$$
$$\stackrel{b}{=} 2\pi\lambda_d \int_0^{R_{GZ}} r dr = \pi\lambda_d R_{GZ}^2. \quad (3.12)$$

where (a) is derived from Campbell's theorem for PPP and (b) is derived from applying the integrals for polar coordinates. Putting above expression into $p_{sil}\,(y \in B)$ completes the proof. Fig. 3.4 presents the analytical and simulation results of p_{sil}. The number of D2D users to be inactive directly depends on the radius of the guard zone, which ensures strong protection for the cellular receiver; however this decreases the intensity of active D2D links.

3.4.2 Case 2: D2D receivers in half-duplex mode

The critical scenario is where a D2D receiver is either on the boundary of GZ or inside GZ (shaded area in the overlap region in Fig. 3.3 (c) and a D2D transmitter is outside GZ. The D2D link will be in the HD mode if m_y is inside GZ or on the guard zone to ensure protection for cellular receivers and will be in the FD mode if m_y is outside GZ (3.4.3). Such a scenario can analytically be expressed as,

$$R_{GZ} < r_{x_o,y} < R_{GZ} + R_d. \quad (3.13)$$

while, m_y is inside GZ.

Now, we will evaluate the probability of the D2D link to communicate in the half-duplex mode. The important region which impacts the cellular user's reception greatly is the ring-shaped overlap region between circle $b(o, R_{GZ})$ and $b(o, R_{GZ}+R_d)$, denoted by $\mathcal{C}_1$ and shown as the highlighted region in Fig. 3.5. In region $\mathcal{C}_1$, the D2D links are segregated based on the angle (θ) and location of receiver m_y on circle $b(y, R_d)$ of radius R_d. Based on the angle $\theta(y, m_y)$, the probability of the D2D link to be either in the half-duplex or full-duplex mode can be derived.

Lemma 2: Given cellular user located at the origin with guard-zone $b(o, R_{GZ})$ and a D2D transmitter inside region $\mathcal{C}_1$, the D2D link will be in the half-duplex mode if receiver m_y exists on the minor arc (ζ_{min}) of the overlapping area between $b(o, R_{GZ}) \cap b(y, R_d)$,

$$\zeta_{min} = 2 \arcsin \left(\frac{\sqrt{4r_{x_o,y}^2 R_{GZ}^2 - \left(r_{x_o,y}^2 - R_d^2 + R_{GZ}^2\right)^2}}{2R_d r_{x_o,y}} \right). \tag{3.14}$$

Proof: Assume a typical receiver is at the origin (o, o), with guard zone circular

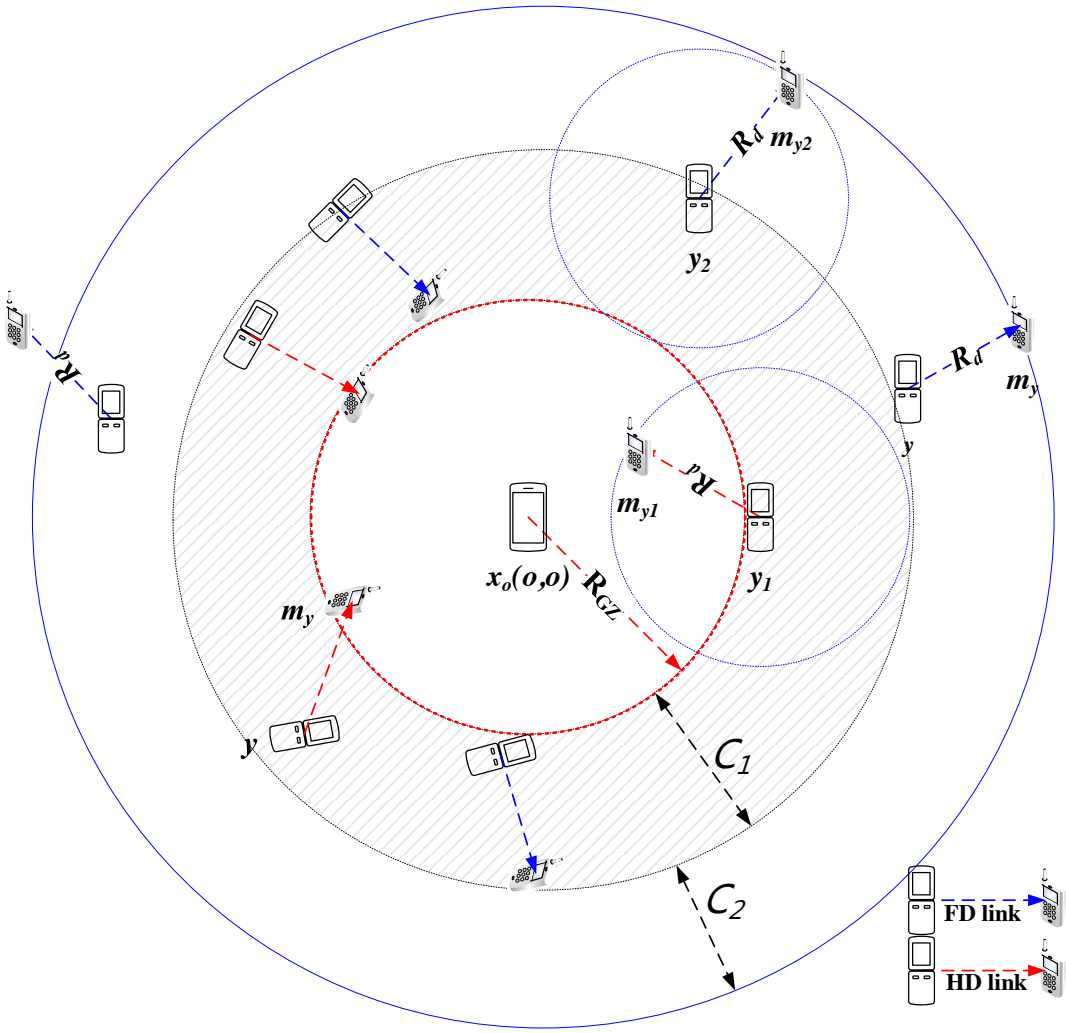

Figure 3.5 : An area of interest where D2D communication link can be either in half-duplex or full-duplex mode depending on the angle (θ) of the receiver (m_y)

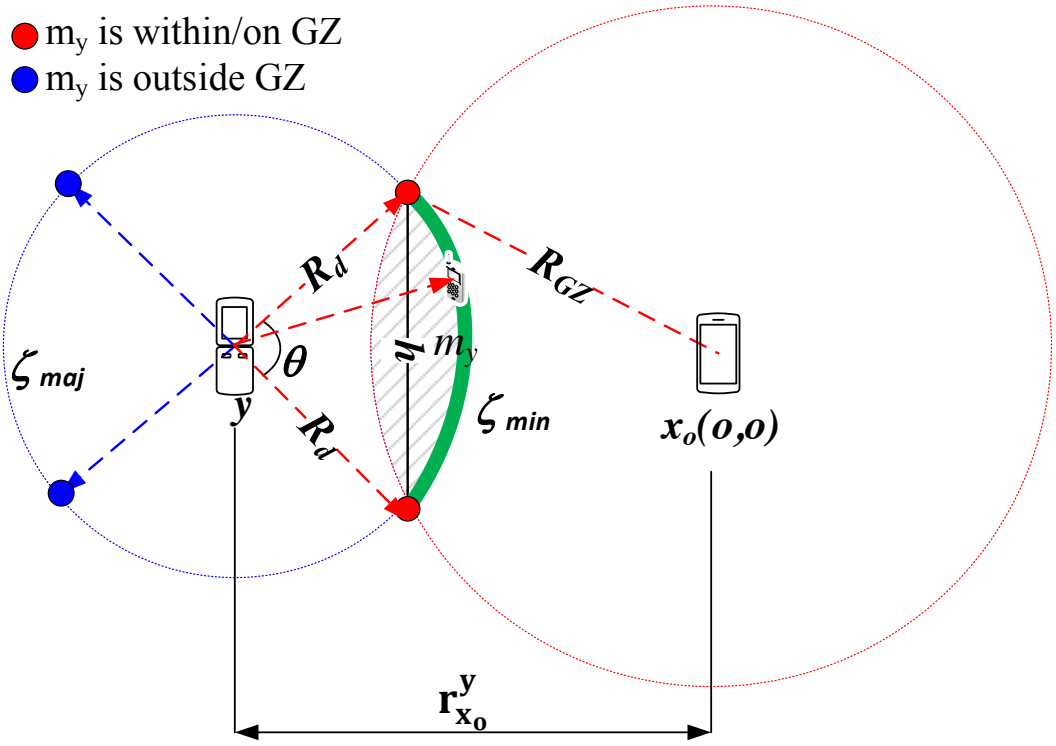

Figure 3.6 : Location of D2D receiver will either be on the length of the minor arc ζ_{min} (green) or on the major arc ζ_{maj} (blue)

disk of radius R_{GZ} and D2D transmitter at distance of $r^y_{x_o}$. We are interested to calculate the minor arc length shown in Fig. 3.6 as ζ_{min}. First, we have to find out the angle θ, for which we need $h/2$ as shown in the figure. From trigonometry and basic circular geometry, the arc length can be found using the following formula depending on the known parameters [106],

$$\zeta_{min} = R_d\theta,$$

Now, h is,

$$h = \frac{1}{r^y_{x_o}}\sqrt{4{r^y_{x_o}}^2 R^2_{GZ} - ({r^y_{x_o}}^2 - R^2_d + R_{GZ})^2}, \tag{3.15}$$

while θ, is

$$\theta(r_{x_o}^{y}, R_d, R_{GZ}) = 2\arcsin\left(\frac{h}{2R_d}\right). \tag{3.16}$$

So, the length of the minor arc will be ,

$$\zeta_{min} = 2R_d \arcsin\left(\frac{\sqrt{4{r_{x_o}^{y}}^2 R_{GZ}^2 - \left({r_{x_o}^{y}}^2 - R_d^2 + R_{GZ}\right)^2}}{2R_d r_{x_o}^{y}}\right). \tag{3.17}$$

Thus, each D2D communication link can operate in the half-duplex mode if its receiver is located on the minor arc ζ_{min} as shown in Fig. 3.3 (d). Equipped with the expression for ζ_{min}, we can now proceed to find the intensity and probability of D2D transmitters which can operate in the HD mode. Based on this probability, the D2D communication pair can still operate in the HD mode as this will not violate the interference protection (IP) given to the primary user, but will increase the spectral efficiency and capacity for D2D users (SUs). The counting measure of D2D users that will operate in HD mode will depend on the D2D receivers which are on the minor arc of the overlapping circle of $b(y, R_d)$.

Lemma 3: Conditioned on primary user x_o at the origin with a guard zone of radius R_{GZ}, the intensity measure of D2D transmitters y that can operate in the half-duplex mode will be,

$$\Lambda_{HD} = \int_{R_{GZ}}^{R_{GZ}+R_d} \lambda_d \zeta_{min}\left(R_{GZ}, R_d, r_{x_o,y}\right) r dr. \tag{3.18}$$

Proof: We can segregate the D2D transmitters y and receivers m_y, which will communicate in the half-duplex mode based on the angle θ or if it lies on ζ_{min}. Now, to calculate the total number of D2D Txs in regions $\mathcal{C}_1$ whose receivers are on ζ_{min}, denoted by subset $|B|$, we have:

$$\mathbb{E}\left\{\Lambda_{|B|}\right\} = \mathbb{E}\left[\sum_{y_i \in \Phi_d} \mathbb{1}_{(R_{GZ}<||Y_i||\leq R_{GZ}+R_d)} . \mathbb{1}_{(\theta_{m_{Y_i}}=\zeta_{min})}\right] \tag{3.19}$$

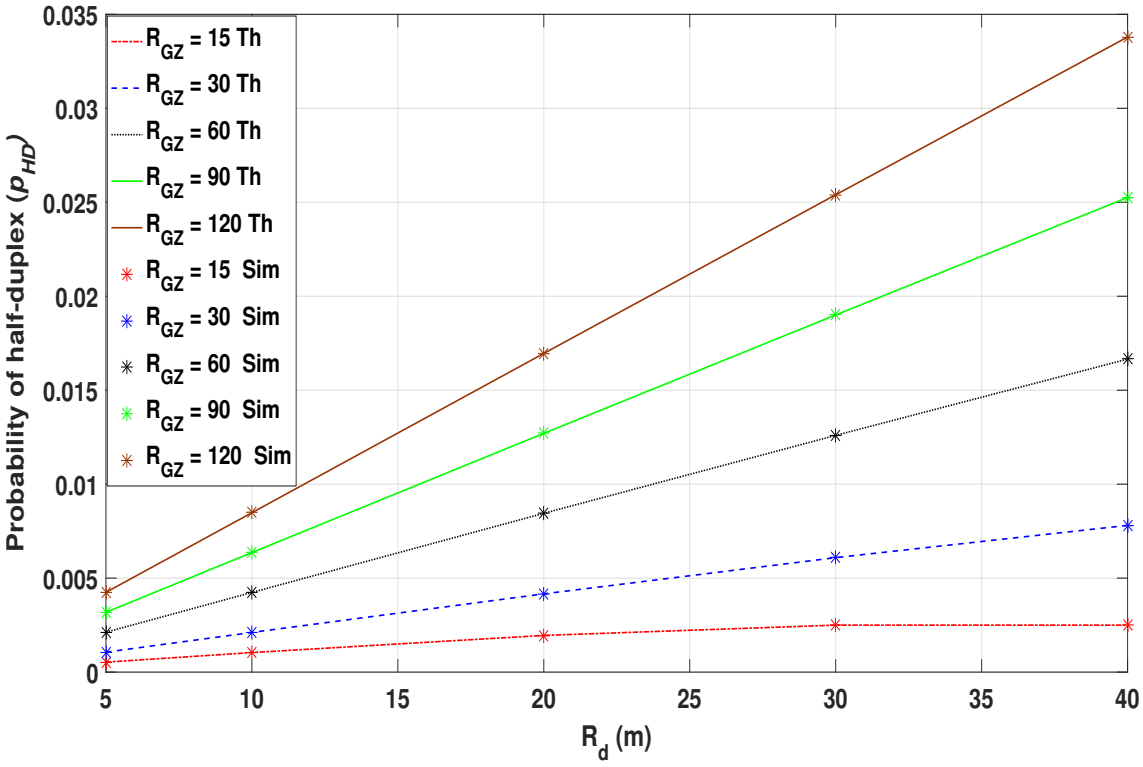

Figure 3.7 : Probability of half-duplex D2D links from Lemma 4 as a function of R_{GZ} and R_d with simulation results

From the application of Campbell theorem, after applying the integrals and converting to polar coordinates we will have the total intensity of users in $|B|$,

$$\lambda_{HD} = \int_{R_{GZ}}^{R_{GZ}+rd} r\lambda_d \zeta_{min} dr. \tag{3.20}$$

Putting in the expression for ζ_{min} completes the proof.

The expression for ζ_{min} is given in Eq. 3.14. Based on this, we can derive the probability of D2D links to be half-duplex mode next.

Lemma 4: Given the intensity measure of D2D users in the half-duplex mode as Λ_{HD}, the probability of the half-duplex mode will be,

$$p_{HD} = \frac{\Lambda_{HD}}{2\pi R_p^2} \tag{3.21}$$

Proof: The probability of half-duplex users is derived by getting the ratio of half-

duplex users (Λ_{HD}) by a total number of D2D users in a given area of interest i.e. total area (πR_p^2). This has further been validated and results are shown in Fig. 3.7. As the Eqs. 3.18 and 3.21 indicate that intensity of users to be in half-duplex mode depends on the width of region $\mathcal{C}_1$, therefore, increasing the increasing R_{GZ} and R_d in turn results in higher p_{HD}. Both theoretical and simulation results are in line with the analytical expressions.

3.4.3 Case 3: D2D pair in full-duplex mode outside the GZ

In this case, a D2D communication pair can share a primary user's spectrum without disrupting its reception. D2D links can operate in the FD mode in two regions ($\mathcal{C}_1$ and $\mathcal{C}_2$ Fig. 3.5), the transmitters and receivers in region $\mathcal{C}_1$, whose receivers are on the major arc of the overlap circles (i.e. outside GZ) and D2D transmitters and receivers in region $\mathcal{C}_2 = b(o, R_{GZ}+R_d)^c$. Depending on the distance of D2D transmitters (y) and receivers (m_y), distance based conditions for D2D users operating in FD mode in regions $\mathcal{C}_1$ and $\mathcal{C}_2$ can be expressed as,

$$\begin{cases} R_{GZ} < r_{x_o,y} < R_{GZ} + R_d & y, m_y \in \mathcal{C}_1 \\ r_{x_o,y} \geq R_{GZ} + R_d & y, m_y \in \mathcal{C}_2. \end{cases}$$

This mechanism of mode selection in turn significantly increases the areal spectral efficiency of SUs as the D2D pairs can use full-duplex capability while protecting the reception of primary users. Since the induced interference from a FD receiver will not disrupt the primary user's transmission, so it can harvest the data-rate gains of FD communication. To characterize the interference field of FD D2D users, we have to consider the interference generated by D2D users in two regions, $\mathcal{C}_1$ and $\mathcal{C}_2$. In terms of the indicator function, we can formulate the counting measure of FD transmitters as,

$$\Lambda_{FD} = \sum_{y_i \in \varphi_d} \mathbb{1}_{(R_{GZ}+R_d<||Y_i||\leq\infty)} + \sum_{y_i \in \varphi_d} \mathbb{1}_{(R_{GZ}<||Y_i||\leq R_{GZ}+R_d)} \mathbb{1}_{(R_{GZ}<||m_{Y_i}||\leq R_{GZ}+R_d)} \tag{3.22}$$

The intensity of D2D transmitters in region $\mathcal{C}_2$ is comparatively easier to formulate; however, the intensity of FD D2D users in region $\mathcal{C}_1$ requires the angle of the major arc of an overlapping circle. Since we have the intensity measure of the D2D transmitters operating in the HD mode, now the receivers of D2D transmitters which will be outside R_{GZ} will be on the major arc of circle $b(y, R_d)$. As the total angle of a circle is 2π, the probability of a D2D communication link in this scenario where D2D Rx will be on the major arc ζ_{maj} (i.e. green arc in Fig. 3.6) is given by:

$$\zeta_{maj} = (2\pi - \theta)R_d. \tag{3.23}$$

where θ is given in Eq. 3.16 as an angle of a receiver with its D2D transmitter, when RX exists on minor arc and operates in the half-duplex mode. Now, the intensity measure of D2D transmitters operating in the FD mode within $\mathcal{C}_1$ with receivers located on the major arc of $b(y, R_d)$ is denoted by $\tilde{\Lambda}_{FD}$,

$$\tilde{\Lambda}_{FD} = 2\lambda_d \int_{R_{GZ}}^{R_{GZ}+rd} (2\pi - \theta(y, R_d, R_{GZ}))\, ydy. \tag{3.24}$$

Thus, the total intensity measure of the D2D transmitters that can operate in full duplex mode can be expressed as the sum of the counting measures of D2D transmitters in regions $\mathcal{C}_1$ and $\mathcal{C}_2$,

$$\Lambda_{FD} = 2\lambda_d \int_{R_{GZ}}^{R_{GZ}+rd} (2\pi - \theta(y, R_d, R_{GZ}))\, ydy + 2\pi\lambda_d \int_{R_{GZ}+R_d}^{\infty} ydy. \tag{3.25}$$

Hence, the probability of these transmitters to be in the FD mode will simply be a normalization of Λ_{FD} over $|A|$, which is evaluated next.

Lemma 5: Conditioned on the circular disk of radius $R_{GZ} + R_d$ at origin o, the probability of a D2D communication link to be in the full-duplex mode in regions

$\mathcal{C}_1$ and $\mathcal{C}_2$ can be expressed as,

$$p_{FD} = \frac{2\pi\lambda_d}{|A|}\left(|A| - \pi(R_{GZ} + R_d)^2\right). \tag{3.26}$$

Proof: To account for a D2D transmitter that will communicate in the full-duplex mode, we have to find the number of transmitters that can communicate in the full-duplex mode in two regions $\mathcal{C}_1$ and $\mathcal{C}_2$. This includes all the transmitters of $\mathcal{C}_2$ $R_{GZ} + R_d < ||y|| < \infty$. Considering subset $B \subset A$, where, $B = \mathcal{C}_1 \cup \mathcal{C}_1$, the expected counting measure of D2D transmitters in $\mathcal{C}_1$,

$$\mathbb{E}\left\{\Lambda_{\mathcal{C}_1}\right\} = 2\pi\lambda_d \int_{R_{GZ}}^{R_{GZ}+R_d} y dy \tag{3.27}$$

Similarly, for counting measure of D2D transmitters in $\mathcal{C}_2$,

$$\mathbb{E}\left\{\Lambda_{\mathcal{C}_2}\right\} = 2\pi\lambda_d \int_{R_{GZ}+R_d}^{\infty} y dy \tag{3.28}$$

From 3.11, the probability of D2D links to be in the full-duplex mode will be,

$$p_{FD}\left(y \in B\right) = \frac{\Lambda_{\mathcal{C}_1} + \Lambda_{\mathcal{C}_2}}{\Lambda_{|A|}} \tag{3.29}$$

Inserting the expressions for the intensity measures into the above equation, we can have the equation for p_{FD}.

The analytical and simulation results for D2D link to be in FD mode are presented in Fig. 3.8. As shown, with the increase in interference protection for cellular user (R_{GZ}), the probability of FD tends to decrease as it eventually decreases the interference from a D2D link by putting more links to either silent or half-duplex mode. Also, p_{FD} is less for higher D2D link distances (R_d) as this yields more D2D links to be in the half-duplex mode in region $\mathcal{C}_1$.

Probability of D2D Rx to be on ζ_{maj} or ζ_{maj}: The pdf of angle θ between D2D Tx and D2D Rx is $1/2\pi$. The probability of D2D Rx being located on either

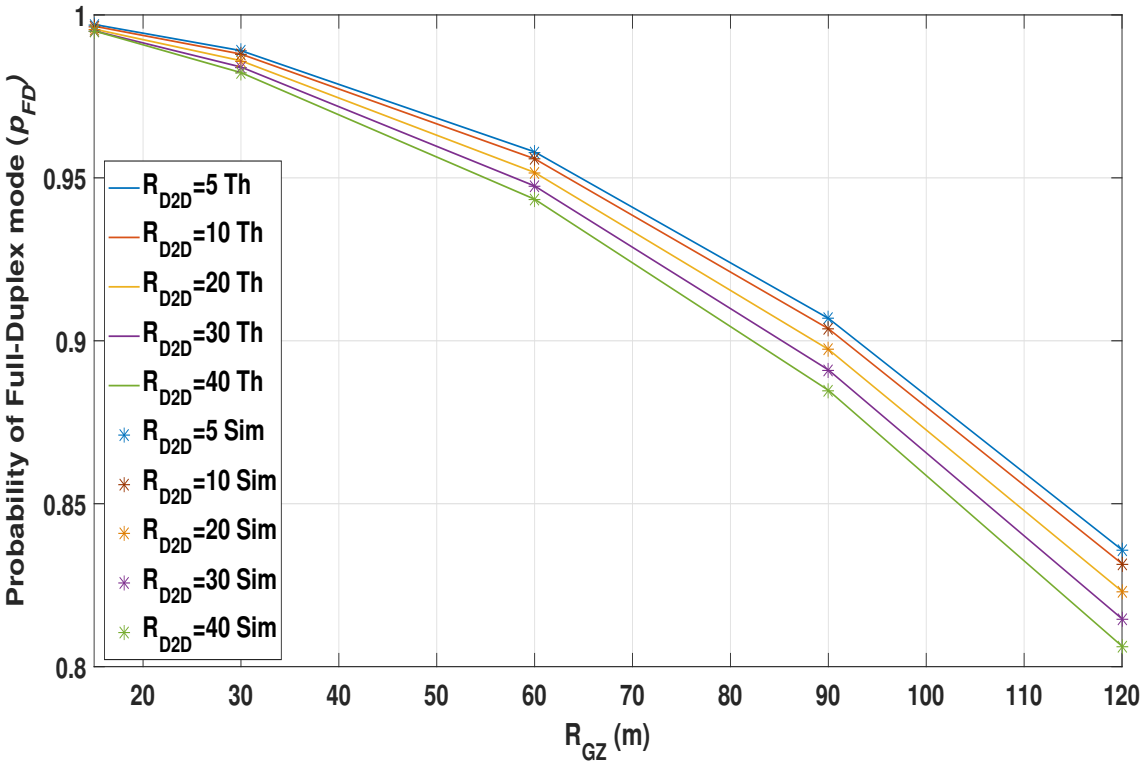

Figure 3.8 : Probability of full-duplex D2D links as a function of R_{GZ} and R_d from Lemma 5 and simulations

ζ_{maj} or ζ_{maj} arc is shown in Fig. 3.9 as a function of D2D Tx distance in $\mathcal{C}_1$. As the transmitter moves away from GZ the probability of D2D link to be in FD mode increases which is shown with the increase of ζ_{maj}. On the other hand, if the D2D Tx is in the vicinity of GZ, then the probability of the link operating in HD mode (Rx on ζ_{min}) is higher which also ensures protection to primary receiver.

As we have now the relative intensities for D2D transmitters in a half-duplex and full-duplex mode so we can assess the interference from these users to primary users when computing the success probability. The interference field for a typical user from full-duplex links will be twice that of Λ_{FD} because of the receivers of active full-duplex D2D links. Hence, the trade-off between capacity of active full-duplex D2D transmitters Λ_{FD}, and protection for a cellular receiver based on guard-zone

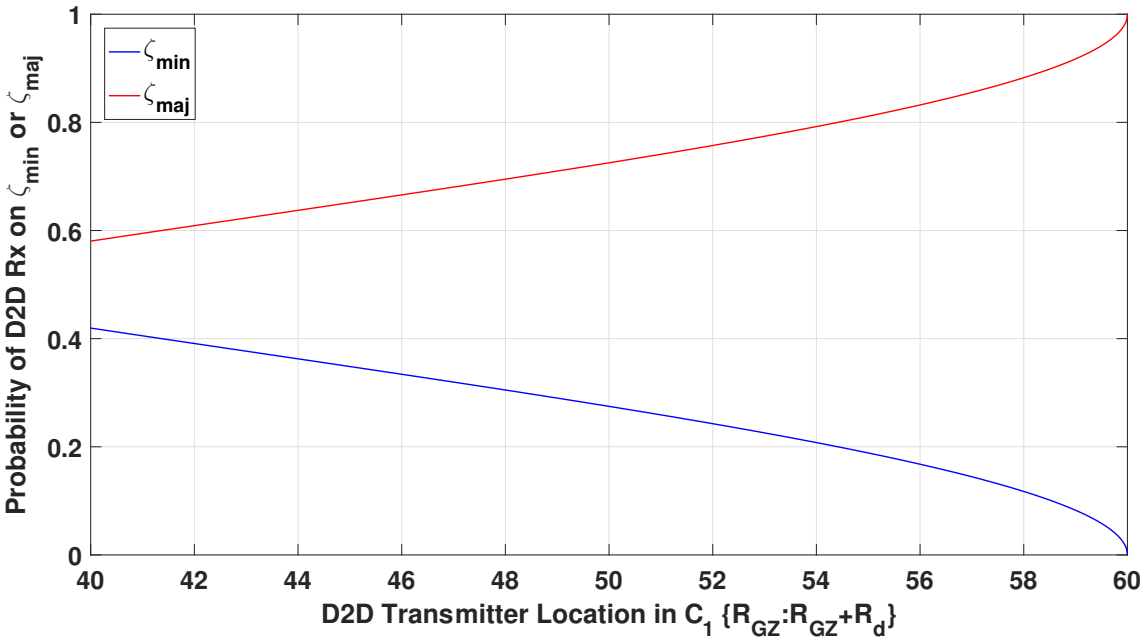

Figure 3.9 : Probability of D2D receiver to be located on either ζ_{min} (HD mode) or on ζ_{maj} (FD mode) as a function of distance of D2D Tx in $\mathcal{C}_1$

radius (R_{GZ}) is an interesting optimization problem to consider.

3.5 Success Probability and SIR Analysis

In this section, we characterize the complementary cumulative distribution function (CCDF) of SIR, which is also known as a complement of the outage probability that can equally be thought of as the average fraction of the network area or users to achieve the target SIR threshold T. The success probability of a typical user is expressed in terms of the Laplace transform of aggregate interference as the channel gains for interfering users follow Rayleigh fading with an exponential distribution i.e. exp(μ). The SIR success probability is a key parameter which is used to further evaluate expressions for the data rate, throughput and Area Spectral Efficiency (ASE). The success probability of a typical user under consideration is given in section 3.3.3.

Approximation: Due to the sophisticated mathematical derivation for expressions

of success probability and loss of analytical tractability, the φ_d is approximated to Φ_d with the hole carved out at origin $b(o, R_{GZ})$. The intensity of D2D transmitters and receivers is represented with λ_d for notational simplicity. For simplicity of analysis, as we have considered single cellular user so, we assume one hole in the PHP and approximate it to PPP beyond that hole, also been done in previous works for similar reasons. The point processes for different users are assumed to be independent of each other to provide the abstract level analysis of the proposed method.

3.5.1 SIR success probability of cellular user

To formulate the success probability of a typical cellular user (x_o) in downlink, we consider a receiver at the origin connected to the base station at distance of R_c with interference protection provided through a circular guard-zone of radius R_{GZ}. The interference field for a typical receiver consists of all of the D2D active users in a cell except the tagged base station. As discussed in section 3.2, conditioned on the critical regions and parameters ($\mathcal{C}_1$, $\mathcal{C}_2$, and $\theta(y, m_y)$), the interference field consists of D2D transmitters in the half-duplex mode (Λ_{HD}) , D2D transmitters ($\Lambda_{FD}(y)$) and receivers ($\Lambda_{FD}(m_y)$) in the full-duplex mode. From 3.18 and 3.25, we can write the interference field for (x_o) as,

$$\Lambda_{IF}^{x_o} = \Lambda_{HD} + \Lambda_{FD}(y) + \Lambda_{FD}(m_y). \tag{3.30}$$

Equipped with the counting measures of interfering users, we can now formulate the success probability of a typical cellular user.

Proposition 1: In a considered network, the success probability of a typical cellular receiver is the Laplace transform of interference from half-duplex and full-duplex

D2D users, which is given by,

$$p_s^{x_o} = \exp(-2\pi\lambda_d \mathcal{H}(\theta, R_d, \alpha_d)) \exp(-2\pi\lambda_d \mathcal{F}_T(\theta, R_d, \alpha_d)) \exp(-2\pi\lambda_{m_d} \mathcal{F}_R(\theta, R_d, \alpha_d)) \tag{3.31}$$

where,

$$\mathcal{H}(\theta, R_d, \alpha_d) = \int_{R_{GZ}}^{R_{GZ}+R_d} \frac{\theta(y, R_d, R_{GZ})}{2\pi(1 + \frac{||y||^{\alpha_d}}{s})} y dy, \tag{3.32}$$

$$\mathcal{F}_T = \int_{R_{GZ}}^{R_{GZ}+R_d} \frac{2\pi - \theta(y, R_d, R_{GZ})}{2\pi(1 + \frac{||y||^{\alpha_d}}{s})} y dy + \int_{R_{GZ}+R_d}^{\infty} \frac{1}{1 + \frac{||y||^{\alpha_d}}{s}} y dy, \tag{3.33}$$

$$\mathcal{F}_R = \int_{R_{GZ}}^{R_{GZ}+R_d} \frac{2\pi - \theta(m_y, R_d, R_{GZ})}{2\pi(1 + \frac{||m_y||^{\alpha_d}}{s})} m_y dm_y + \int_{R_{GZ}+R_d}^{\infty} \frac{1}{1 + \frac{||m_y||^{\alpha_d}}{s}} m_y dm_y, \tag{3.34}$$

and,

$$s = \frac{T R_c^{\alpha_c} P_d}{P_c} \tag{3.35}$$

Proof: The success probability can be expressed by putting Eq. 3.6 in Eq. 3.5,

$$p_s^{x_o} = F^c_{x_o, x_{BS}} > T \frac{\mathcal{I}_{x_o,y} + \mathcal{I}_{x_o,m_y}}{P_c l\left(x_o, x_{BS}\right)} \tag{3.36}$$

where, $l\left(x_o, x_{BS}\right)$ is the path-loss of a typical user to its tagged base station. $\mathcal{I}_{x_o,y}$ is the interference field from all the active D2D transmitters (both in HD and FD mode),

$$\mathcal{I}_{x_o,y} = \sum_{y \epsilon \Phi_d} P_d F^d_{x_o,y} l(x_o, y) 1^{HD}_{m_y,y} + \sum_{y \epsilon \Phi_d} P_d F^d_{x_o,y} l(x_o, y) 1^{FD}_{m_y,y}, \tag{3.37}$$

Also, $\mathcal{I}_{x_o,m_y}$ is the interference from D2D Rxs conditioned on the links in the FD mode,

$$\mathcal{I}_{x_o,m_y} = \sum_{m_y \in \Phi_{m_d}} P_d F^d_{x_o,m_y} l(x_o, m_y) 1^{FD}_{m_y,y} \tag{3.38}$$

Expressing the constants in Eq. 3.36 with s as in Eq. 3.35, the total interference experienced by typical PU (x_o) is originated from three set of users as expressed in Eqs. 3.37 and 3.38. The Laplace transform of these interference terms follows as,

$$\mathcal{L}_{\mathcal{I}}(s) = \mathbb{E}_{\Phi_d,\Phi_{m_d},\theta(HD/FD)}\left(\prod_{y\epsilon\Phi_d}\exp(-sF^d_{x_o,y}l(x_o,y)1^{HD}_{m_y,y})\right), \left(\prod_{y\epsilon\Phi_d}\exp(-sF^d_{x_o,y}l(x_o,y))1^{FD}_{m_y,y}\right)\left(\prod_{y\epsilon\Phi_{m_d}}\exp(-sF^d_{x_o,m_y}l(o,m_y))1^{FD}_{m_y,y}\right) \quad (3.39)$$

Relaxing the inter-dependencies of the point processes we will now characterize the Laplace transform of these terms individually. First, considering the interference from HD D2D transmitters,

$$\mathcal{L}_1(s) = \mathbb{E}_{\Phi_d,HD}\left(\prod_{y\epsilon\Phi_d} exp(-sF^d_{x_o,y}l(x_o,y)1^{HD}_{m_y,y})\right) \quad (3.40)$$

Applying Rayleigh channel distribution (i.e. $F^d_{x_o,y} \sim exp(\mu)$), the PGFL of PPP and conventional stochastic geometry machinery,

$$\mathcal{L}_1(s) = \mathbb{E}_{HD}\left(\int_{\mathbb{R}^2\setminus b(o,R_{GZ})}\frac{1}{1+\frac{||y||^{\alpha_d}}{s}}ydy1^{HD}_{m_y,y}\right) \quad (3.41)$$

As the segregation between HD and FD D2D links is based on angle θ between transmitter and receiver located inside region $\mathcal{C}_1$, we can express the expectation of a transmitter being in the HD mode as,

$$\mathbb{E}_{HD}\left\{1^{HD}_{m_y,y}\right\} = \mathbb{E}_{HD}\left\{\mathbb{1}_{(R_{GZ}<||y||\leq R_{GZ}+R_d)}\mathbb{1}_{||m_y||<R_{GZ}}\right\}. \quad (3.42)$$

Similarly, the expectation measure for D2D transmitters and receivers in the full-duplex mode will be,

$$\mathbb{E}_{FD}\left\{1^{FD}_{m_y,y}\right\} = \mathbb{E}_{FD}\left\{\mathbb{1}_{(R_{GZ}<||y||\leq R_{GZ}+R_d)}.\mathbb{1}_{(R_{GZ}<||m_y||<R_{GZ}+R_d)} + \mathbb{1}_{(R_{GZ}+R_d<||y||\leq\infty)}.\right.$$
$$\left.\mathbb{1}_{(R_{GZ}+R_d<||m_y||\leq\infty)}\right\}. \quad (3.43)$$

These distance based expectation measures can be applied as pdf of the angle (θ) between D2D transmitter and receiver as explained in section 3.2. The pdf of the θ for HD and FD links in $\mathcal{C}_1$ will be,

$$f_{HD}(\theta) = \frac{\theta(y, R_d, R_{GZ})}{2\pi} \tag{3.44}$$

$$f_{FD}(\theta) = \frac{2\pi - \theta(y, R_d, R_{GZ})}{2\pi} \tag{3.45}$$

Applying the expectation for HD in Eq. 3.41 with the pdf of f_{HD}, and converting into polar coordinates,

$$\mathcal{L}_1(s) = \exp\left(-2\pi\lambda_d \int_{R_{GZ}}^{R_{GZ}+R_d} \frac{f_{HD}(\theta)}{1 + \frac{||y||^{\alpha_d}}{s}} y dy\right) \tag{3.46}$$

The inside integral term is denoted by $\mathcal{H}(\theta, R_d, \alpha_d)$. Now, the second interference terms in Eq. 3.39 consist of FD interferers in regions $\mathcal{C}_1$ and $\mathcal{C}_2$. Since all D2D transmitters in $\mathcal{C}_2$ can communicate in FD mode so its Laplace transform will be easier to compute. However, FD users inside $\mathcal{C}_1$ are conditioned on the angle θ of the major arc. Thus, for the FD transmitters in $\mathcal{C}_1$, the pdf of $f_{FD}(\theta)$ will be applied to incorporate the probability of FD mode. Using the standard simplification machinery, the Laplace transform of second term in Eq. 3.39 will be ,

$$\mathcal{L}_2(s) = \exp\left(-2\pi\lambda_d \left(\int_{R_{GZ}}^{R_{GZ}+R_d} \frac{f_{FD}(\theta)}{1 + \frac{||y||^{\alpha_d}}{s}} y dy + \int_{R_{GZ}+R_d}^{\infty} \frac{1}{1 + \frac{||y||^{\alpha_d}}{s}} y dy\right)\right) \tag{3.47}$$

Similarly, the Laplace transforms of third interference terms in Eq. 3.39 can be written as,

$$\mathcal{L}_3(s) = \exp\left(-2\pi\lambda_{m_d} \left(\int_{R_{GZ}}^{R_{GZ}+R_d} \frac{f_{FD}(\theta)}{1 + \frac{||m_y||^{\alpha_d}}{s}} m_y dm_y + \int_{R_{GZ}+R_d}^{\infty} \frac{1}{1 + \frac{||m_y||^{\alpha_d}}{s}} m_y dm_y\right)\right) \tag{3.48}$$

The inside integrals in $\mathcal{L}_2(s)$ and $\mathcal{L}_3(s)$ are denoted by $\mathcal{F}_T(\theta, R_d, \alpha_d)$ and $\mathcal{F}_R(\theta, R_d, \alpha_d)$, respectively. Inserting expressions for $f_{HD}(\theta)$ and $f_{FD}(\theta)$ completes the proof.

3.6 Results and Analysis

In this section, performance analysis of cellular user is done using the system model given in section 3.3.3. Monte-carlo simulations have been used with a large number of iterations and randomness to get the average of performance metric for cellular receiver at the origin. The simulation values of the network configuration parameters are listed in Table 3.2, unless mentioned elsewhere specifically. The probability of success for typical cellular user is evaluated against SIR threshold (TdB) and plotted in result figures.

Table 3.2 : Simulation Parameters and their values

Parameter	**Simulation Values**
λ_d	$\{0.001, 0.005, 0.05, 0.5\} Users/Km^2$
$F_{o,\kappa}$	μ
α_c, α_d	4, 3.7
P_c, P_d	0.6,0.4
β	0.3
T	-20:1:20
R_{GZ}	$\{15, 30, 60, 90\}m$
R_d	$\{10, 20, 30\}m$
R_c	$\{4, 6\}m$

Fig. 3.10 shows preliminary theoretical and simulation results for success probability of a typical cellular user with FD enabled D2D secondary users, HD only D2D users and without any D2D users. As shown, with FD enabled D2D users the success probability of typical receiver/user drops at the cost of improved gains for secondary users. This trade-off needs extensive and further critical analysis to assess

the FD gains for secondary users in cognitive networks, as also highlighted in future research directions in section 6.3. Further insight into this analysis with simulation results are presented in the next section.

Success Probability of Cellular User: An interesting result presented in Fig. 3.11 shows the impact of increasing the D2D user intensity over success probability of a typical cellular receiver. As the intensity (λ_D) of D2D users increases, it increases the probability of full-duplex users in the vicinity of the cellular receiver, hence, contributing to interference. The intensity of FD D2D links increases with the increase in λ_D as also indicated in Eq. 3.25. This factor causes a gradual decrease in success probability of the cellular receiver as shown in Fig. 3.11. From λ_D 0.001 to 0.5, a typical cellular receiver experiences aggressive interference from D2D users in the half-duplex and full-duplex modes, as also highlighted in success probability expression in Eq. 3.31. The key factor in the decline of success probability is the

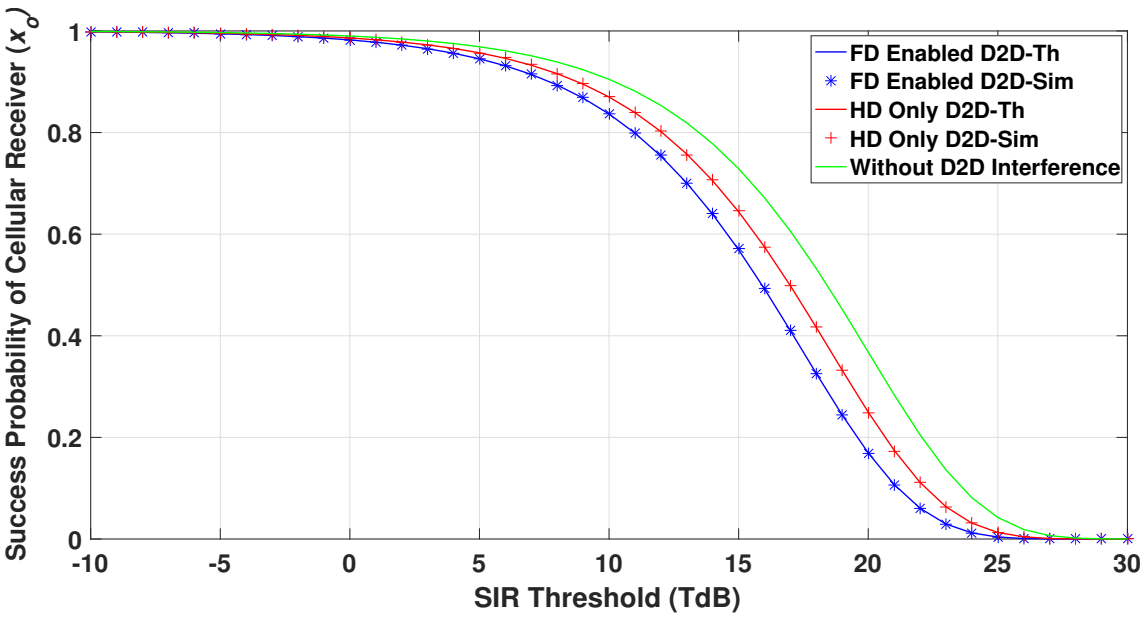

Figure 3.10 : Success probability of typical cellular receiver as a function of SIR threshold. System configuration parameters are λ_d=0.002, P_c=50dBm, P_d=80dBm, α_d=4

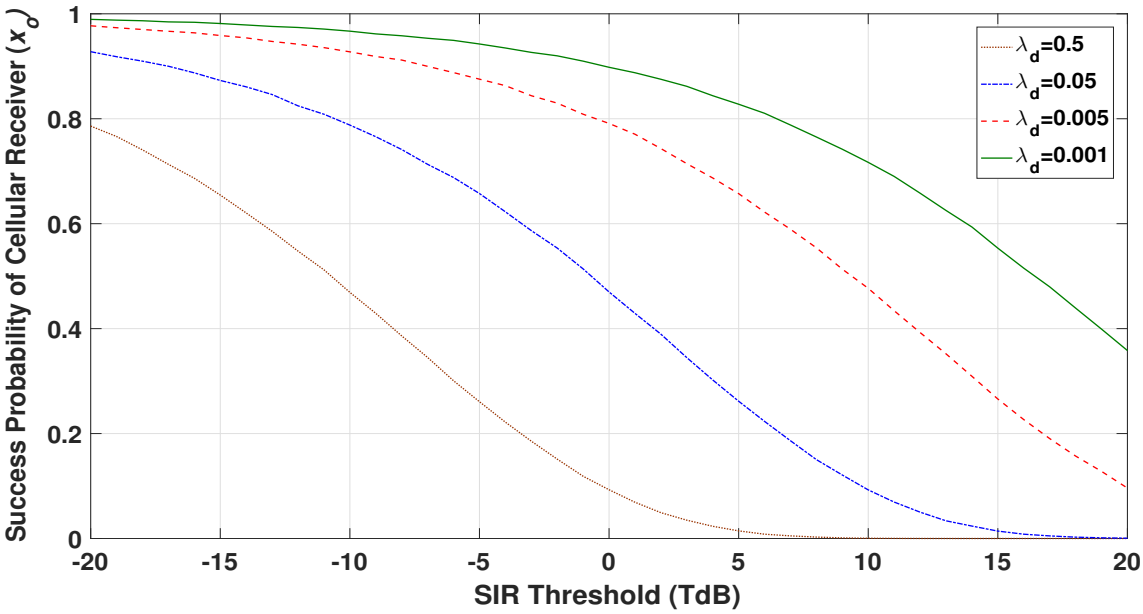

Figure 3.11 : Success probability of a cellular receiver as a function of SIR threshold (TdB) for different λ_D

interference from both D2D transmitters and receivers operating in the full-duplex mode. As given in theoretical expressions, the interference term in Eq. 3.32 shows the impact of HD D2D transmitters on success probability, whereas, Eqs. 3.33 and 3.34 measure the interference from FD D2D transmitters and receivers, respectively. Therefore, a trade-off between success probability and the number of active D2D users is another interesting research direction which will be explored in the future.

The critical parameter R_{GZ} controls the capacity of active D2D links and also protects the cellular user's reception. As shown in Fig. 3.12, a greater guard zone protects cellular users reception from D2D interference by putting more D2D links in the silent mode. This was also expected from theoretical analysis; for instance, the intensity of PHP given in Eq. 3.3 presents the similar notion. Thus, a higher guard zone protection guarantees a higher success probability for a typical cellular user, whereas a smaller guard zone results in an increased interference field from half-duplex transmitters and full-duplex transmitters/receivers, resulting in a lower

success probability of cellular receiver. This parameter can be tuned according to the interference protection required or QoS guarantees for a primary user.

3.7 Summary

In this work, we have presented a comprehensive analysis of a cognitive network where a primary user's reception is protected with guard zones from full-duplex enabled D2D secondary users. Using stochastic geometry tools, the impact of D2D users in the vicinity of an active cellular user is studied. We defined a critical region where D2D link can operate in half-duplex mode if D2D receiver is inside the guard zone and can operate in full-duplex mode if both D2D transmitter and receiver are outside the guard zone. The probabilities of half duplex and full duplex modes are derived and validated through extensive simulation results. The interference to primary user is also characterized from active D2D links in half duplex and full duplex modes. From preliminary analysis and results, it is possible to allow

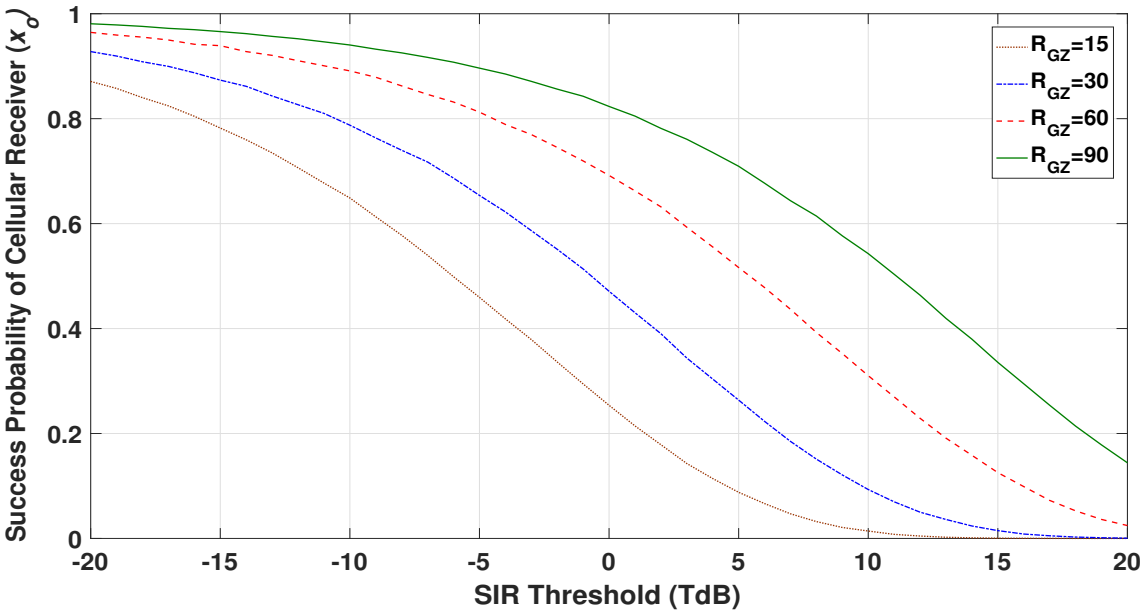

Figure 3.12 : Success probability of a cellular receiver as a function of SIR threshold (TdB) for different R_{GZ}

secondary users in the cognitive setup to harvest the gains of full duplex technology as long as the primary user is guaranteed certain interference protection. The trade-off between D2D network capacity and its impact on success probability of a cellular user is also studied and results are presented. One of the interesting extensions of this work is to find an optimum guard-zone radius which can provide maximum D2D user capacity. Further analysis is also possible by considering multiple concurrent cellular users reception and how it affects the D2D network capacity, which is one of the prospective future research directions we intend to explore.

Chapter 4

Coverage Analysis of D2D Users in Full Duplex D2D Cognitive Network

This chapter presents the stochastic geometry based success probability formulation and analysis for D2D network. Section 4.1 outlines the introduction of the chapter. Section 4.3 presents the system model considered for the simulation setup. Success probability and interference characterization for a D2D link using SG tools are evaluated in section 4.4. Section 4.5 presents key findings from simulations results, followed by the summary of the chapter presented in section 4.6. Parts of the work described in this chapter resulted in Publications [92, 107].

4.1 Introduction

Due to high internet, mobile and broadband speeds with ubiquitous coverage, exponential growth of wireless data has been seen for a recent couple of years. 1000 fold increase in mobile traffic has been seen in this decade so far [108]. Mobile broadband is also considered as the most rapidly increasing market segment with a global penetration of 47% in 2015, a value that has increased 12 times since 2007 [109]. Such an unprecedented increase in mobile broadband subscribers challenges network capacity and data rates. The demand for ubiquitous connectivity and high data rates has motivated network providers and vendors to come up with optimum use of existing resources (spectrum) and the integration of new technologies (Full Duplex, D2D). The development and testing of such solutions are also one of the driving factors for the future generation (5G) of mobile networks. Among these proposals, Cognitive radio, TVWS, CBRS, and multi-Radio Access Technologies

(RATs) coexistence have proven to be an effective solution for spectrum scarcity.

The key idea behind spectrum sharing is the use-it or share-it rule, where primary licensed users can share underutilized spectrum with secondary unlicensed users conditioned on interference protection from secondary users. This sharing is done based on pre-defined conditions for leaving the spectrum for priority users whenever needed and imposing the least interference to primary users as modelled with guard-zones in chapter 3. For detailed benefits of dynamic spectrum sharing and heterogeneous device coexistence, readers are referred to [9].

The D2D communication has shown its considerable potential to elevate the user experience and efficiently improve the network capacity by traffic off-loading from the main network. It is also one of the key enabling technologies in next-generation networks [39]. Importance of short-distance social communications like D2D and potential advantages are also discussed in section 1.2. D2D is a good technology candidate for opportunistic dynamic spectrum sharing without producing harmful aggregate interference to other devices (due to shorter link distances and lower transmit powers). In this thesis, we propose D2D technology as a tier-2 (SU) technology candidate and model the system by characterizing the interference and success probability [33]. Due to strict interference threshold conditions which SU has to comply with for PU transmission protection, D2D has more potential as compared to LTE-LAA and WiFi as the D2D users can communicate in a near distance of Exclusion Zones (EZ). The D2D network has performance advantages as compared to other small cell technologies due to limited interference and near-distant communication between transmitters and receivers.

4.2 Related Works

In the context of dynamic spectrum sharing, recently stochastic geometry modeling and analysis of CBRS has been done in [33]. Authors present a tractable

performance analysis of Spectrum Access System (SAS) by employing EZ for priority access licensed (PAL) users, while general authorized access (GAA) users operate using contention-based channel access mechanism (CSMA). Previously, similar work has been done in the context of cognitive radio where opportunistic spectrum access is exploited. However, unique interference restrictions in EZ of PAL and induced aggregate interference from GAA users makes CBRS systems challenging. For instance, authors in [80] presented a stochastic geometry model to characterize interference from SU to PUs and also in multi-tier networks. A similar approach of employing EZ has been used in [101], SG analysis for co-existence of contention-based (WiFi) and scheduled based (LTE) networks is presented in [34]. Moreover, the SG analysis for interference characterization and expressions for network performance metrics for K-tier heterogeneous cellular networks is presented in [88]. Most of the analysis in this domain uses Matern hardcore process of type-II (MHPP-II) [110] to study the coexistence among licensed (primary) and unlicensed (secondary) users, which are limited to only bi-polar networks. However, due to strict interference limitations on EZ boundaries of PAL, CBRS requires sophisticated analysis to locate operational zones for GAA's operations. Another work in [111] investigates the impact of different coexistence techniques for FD D2D with cellular and WiFi. The proposed work in this chapter analyzes the opportunistic use of D2D devices in the vicinity of EZ's while limiting the induced interference to protect PALs.

Authors in [112] formulated the stochastic-geometry based model of a down-link cellular network with D2D using H-transform theory and coverage-aware power control coupled with opportunistic access is proposed. Another work in [32] presents stochastic geometry based comprehensive and detailed analysis on Full-Duplex communications for cache-enabled D2D networks. Different operating modes, their probabilities and content-based caching have been discussed. Authors in [113] have studied the impact of self-interference suppression for FD radios in opportunistic

spectrum access for overlay and underlying models. Different operating modes and their impact on the performance of primary and secondary users were extensively investigated. Also, an adaptive transmission-reception-sensing based mechanism for FD enabled cognitive radios is proposed in [114]. SG analysis of FD D2D has also been recently studied and performance trade-off has been studied [32]. The initial SG analysis for FD gains was presented in [102]. Another SG approach presented signal to interference and noise ratio (SINR), transmit-power and mode switching (HD/FD) for FD D2D for cellular networks [13]. Interestingly, a similar concept has recently been proposed to use OSA for Machine-Type Communications [115]. Authors in [116,117] also leverage use of SG for performance analysis of an arbitrarily-shaped cognitive network and also study the impact of SU activity protocol. MGF of interference from SU is derived to evaluate the outage probability of the primary user. In this article, performance analysis of a second technology candidate can be equated to use of D2D, Machine-type Devices, and similar stationary users.

4.3 System Model

We consider the same system model described in detail in section 3.3, with small notational changes mentioned herein. This system consideration uses the same methodology of analysis given in section 3.3.4 with typical receiver now D2D receiver placed at the origin and a tagged D2D transmitter at a distance of R_d. Most of the symbols and notation used are given in Table 3.1, unless mentioned otherwise.

4.3.1 Propagation Model

Considering probe D2D received at origin (m_o), with D2D transmitter (y_o) at R_d, the received power from intended link can then be written as,

$$P_r(m_o, y_o) = P_d F^d_{m_o,y_o} l(m_o, y_o), \tag{4.1}$$

where, $l(m_o, y_o)$ represents the distance based path loss which is given by $l(m_o, y_o) = ||m_o - y_o||^{-\alpha_d}$, while, $||.||$ is Euclidean norm operator and F_{m_o,y_o} is the respective channel gain. The process Φ_d is PPP, while φ_d and φ_{m_d} are close approximations to PHP due to the introduction of GZ for cellular users. Such spatial dependency of a thinned process yields analytical complexity and may not result in tractable results. Thus, in literature, such correlations among point processes are approximated to either PPP or PHP (with upper and lower bounds). Similar approximations are adopted in conventional analysis and proven to be accurate. Readers are referred to [13] for comparative analysis of distribution approximations and final results. More details and taxonomy on approximations and different techniques researchers resort to for closed-form expressions are summarized in [36].

The set of interfering field (intensity of interfering users) constitutes active D2D users in HD/FD mode and active cellular users, represented as:

$$\lambda_{IF} = p_{FD}\tilde{\lambda}_d \mathbb{1}^{FD}_{y,m_y} \cap p_{HD}\tilde{\lambda}_d \cap \mathcal{C}^c(x, R_{GZ}) \cap \lambda_c \tag{4.2}$$

where, $\mathcal{C}(x, R_{GZ})$ represent the GZ protection which is a circular disk of radius R_{GZ}, centered at location of cellular receiver denoted by x. Depending on the number of active cellular users, total area covered by these GZ's is given in Eq. 3.1. Here, λ_c denotes the intensity of cellular base stations (transmitter) which are Poisson distributed with process Φ_c. Moreover, to model the state of D2D link, i.e., HD or FD, we assign mark $s(y)$ for each communication link between D2D receiver ($m_y \in \varphi_{m_d}$) and D2D transmitter ($y \in \varphi_d$). The D2D communication pair (m_y, y) is assigned an independently chosen link state of being in silent, half-duplex or full-duplex mode with probability p_{sil}, p_{HD} or p_{FD}, respectively, such that $p_{sil} + p_{HD} + p_{FD} = 1$. Unlike, in Chapter 3, where the probability of being in silent, HD and FD D2D users was derived based on the locations of D2D users in critical regions, here we aim to evaluate the impact of HD and FD users by varying the p_{HD} and p_{FD}. The self-interference leakage in FD links is considered to be imperfect with

a residual self-interference-to-power-ratio (SIPR) β. The value of β ranges from 0 to 1 for perfect and imperfect SIPR, respectively. When a D2D link is in the FD mode, induced interference from the D2D receivers also adds up to aggregate interference to a typical receiver and constitutes PHP of intensity $\tilde{\lambda}_d$, given in Eq. 3.3. That is a trade-off or the cost of FD operation at the benefit of increased capacity and data rates.

Now, the SIR at a typical receiver is the ratio of the intended received signal power to total interference power from the rest of users. The interference term ($\mathcal{I}_{m_o,y\setminus y_o}$) represents the interference received from all active D2D transmitters ($y \in \varphi_d$) except from intended transmitter i.e. y_o. Thus, we can write SIR of probe D2D receiver as follows,

$$SIR^d_{m_o} = \frac{P_d F^d_{m_o,y_o} l\left(m_o, y_o\right)}{\mathcal{I}_{m_o,x} + \mathcal{I}_{m_o,y\setminus y_o} + \mathcal{I}_{m_o,m_y}\mathbb{1}^{FD}_{m_y,y} + \beta P_d \mathbb{1}^{FD}_{m_o,y_o}}. \tag{4.3}$$

The last term in the above equation is due to SIPR from the antenna of the typical receiver if it is operating in the full-duplex mode and will be 0 in the case when the typical link is in the half-duplex mode. The impact of this leakage in context of β is also investigated and results are discussed in section 4.5.

4.3.2 Performance Metrics

The typical user can successfully communicate with the tagged transmitter, if SIR is greater than a certain SIR threshold T, also known as success or coverage probability. The success probability is a key parameter which is used to further evaluate expressions for the data rate, throughput and Area Spectral Efficiency (ASE). The probability of success for a typical D2D link between receiver and transmitter can be written as,

$$p^{m_o}_s(T) \triangleq \mathbb{P}(SIR^d_{m_o} > T) \tag{4.4}$$

4.4 Success Probability of Typical D2D User

In this section, we will characterize the interference experienced by a typical D2D receiver. This interference consists of active cellular user, HD D2D transmitters and FD D2D receivers. Using key stochastic geometry tools as given in sub-section 2.5.3, we will eventually derive the success probability of D2D receiver. Considering the presented system model and a typical receiver with a tagged transmitter at the origin, the Signal to Interference Ratio (SIR) for D2D receiver can be written respectively as:

$$SIR^{d}_{m_o} = \frac{P_d F^{d}_{m_o,y_o} l\left(m_o, y_o\right)}{\mathcal{I}_{m_o,x} + \mathcal{I}_{m_o,y\setminus y_o} + \mathcal{I}_{m_o,m_y}\mathbb{1}^{FD}_{m_y,y} + \beta P_d \mathbb{1}^{FD}_{m_o,y_o}}, \tag{4.5}$$

where

$$\mathcal{I}_{m_o,x} = \sum_{x\in\Phi_c} P_c F^{c}_{m_o,x} l(m_o, x), \tag{4.6}$$

is the interference received at a typical user from cellular base station (transmitter). This interference will be higher for more BS and cellular users according to their distribution. The second interference term in Eq. 4.5 represents interference at a typical user from all the other D2D transmitters (operating in the HD mode with probability p_{HD}).

$$\mathcal{I}_{m_o,y} = \sum_{y\in\varphi_d/y_o} P_d F^{d}_{m_o,y} l(m_o, y) \tag{4.7}$$

Now, the D2D receivers of D2D links in FD mode also produce interference for a typical receiver, which is the cost (trade-off) of FD operation. The intensity of FD links is randomly assigned with probability p_{FD}.

$$\mathcal{I}_{m_o,m_y} = \sum_{m_y\in\varphi_{m_d}} P_d F^{d}_{m_o,m_y} l(m_o, m_y)\mathbb{1}^{FD}_{y,m_y} \tag{4.8}$$

$\mathcal{I}$ is defined by the network topology and MAC protocol in use by users of different technologies (cellular/D2D). Interference characterization in stochastic geometry is captured by the location of interferers (using point processes) and the random channel gains $F_{y_o,(x/y/m_y)}$. Thus, interference can be formulated by its pdf (or its cdf). However, a closed-form expression for the pdf of aggregate interference in large-scale networks is not possible, so, $\mathcal{I}_{agg}$ is calculated by taking the Laplace transform of the pdf. Alternatively, Characteristic function and moment generation functions are also trivial stochastic geometry tools to characterize $\mathcal{I}_{agg}$ [80]. In the next part of this section, we derive the success probability of a typical D2D receiver using Laplace transform of aggregate interference in a similar manner as we derived for cellular user in section 3.5. To evaluate the success probability of a typical D2D receiver, inserting Eq. 4.5 in Eq. 4.4 gives,

$$p_s^{m_o}(T) = \mathbb{P}\left(\frac{P_d F^d_{m_o,y_o} l\left(m_o, y_o\right)}{\underset{m_o,x}{\mathcal{I}} + \underset{m_o,y\setminus y_o}{\mathcal{I}} + \underset{m_o,m_y}{\mathcal{I}} + \beta P_d \mathbb{1}^{FD}_{m_o,y_o}} > T\right) \tag{4.9}$$

The link distance between a typical SU (D2D) and its transmitter is $l\left(y_o, m_{y_o}\right)$; hence, the distance based path-loss will be $R_d^{-\alpha_d}$. Simplifying the above expression to apply i.i.d Rayleigh fading, we will have,

$$p_s^{m_o} = \mathbb{P}\Big\{F^d_{y_o}, m_{y_o} > T\frac{\mathcal{I}_{m_o,x} + \mathcal{I}_{m_o,y\setminus y_o} + \mathcal{I}_{m_o,m_y} + \beta P_d \mathbb{1}^{FD}_{m_o,m_{y_o}}}{P_d R_d^{-\alpha_d}}\Big\} \tag{4.10}$$

Considering an i.i.d Rayleigh fading channel, we simplify the above equation for the Laplace transform. As $F^d_{y_o}, m_{y_o} = \exp(1)$ is channel fading/gain during transmission from the tagged transmitter to a typical receiver, applying the expectation of randomness for PPP and PHP, we have

$$p_s^{m_o}(T) = \mathbb{E}_{\Phi_c,\varphi_d,\varphi_{m_d}}\Big\{\exp -s\Big(\mathcal{I}_{y_o,x} + \mathcal{I}_{y_o,y} + \mathcal{I}_{y_o,m_y/m_{y_o}} + \beta P_d \mathbb{1}^{FD}_{y_o,m_{y_o}}\Big)\Big\} \tag{4.11}$$

Using the properties of exponential independence of expectation, and converting the summation to a product for the generalized expression, gives

$$p_s^{m_o} = \exp\left(-s(\beta P_d \mathbb{1}^{FD}_{y_o,m_{y_o}}) \prod_{\kappa\in\Phi_c,\varphi_d,\varphi_{m_d}} \mathcal{L}_{I_k}(s\mathcal{I}_{y_o,\kappa})\right) \tag{4.12}$$

Laplace transform of interference fields from cellular, HD and FD users will be evaluated in future work along with the validation of the simulation results.

4.5 Results and Analysis

In this section, we present extensive simulation results, detailed discussions and analysis of the D2D network performance. We investigate the impact of different network configuration ($R_{GZ}, R_d, \lambda_c, p_{FD}, \lambda_d$) parameters on the performance of D2D users. Monte-Carlo simulations with high iterations have been used to average out the performance from different network realizations and results are presented. Fig. 4.1 presents one of the emulated network realization considered in a simulation setup with 1, 2 and 3 active cellular users with their guard zones for illustrative purpose. The D2D users are not allowed to transmit inside the GZs. Moreover, the state of the D2D link is chosen from random probability (mark $s(y)$) of being in silent (p_{sil}), HD (p_{HD}) or FD (p_{FD}) mode.

We have two different types of simulation sets and results; interestingly, the same trends have been observed for different simulation setups. The first simulation setup details and system model are given in Table 3.2 and results are presented and discussed first. The second simulation setup and parameter values are given in Table 4.1 and results are presented and discussed in the second half of this section.

Success Probability ($p_s^{m_o}$) as a function of Guard-zone radius (R_{GZ}) and D2D link distance (R_d): The simulation results for the success probability of a typical D2D receiver as a function of R_{GZ} and R_d are shown in Fig. 4.2 and 4.3, respectively. The typical link is operating in HD mode. As R_{GZ} increases, the

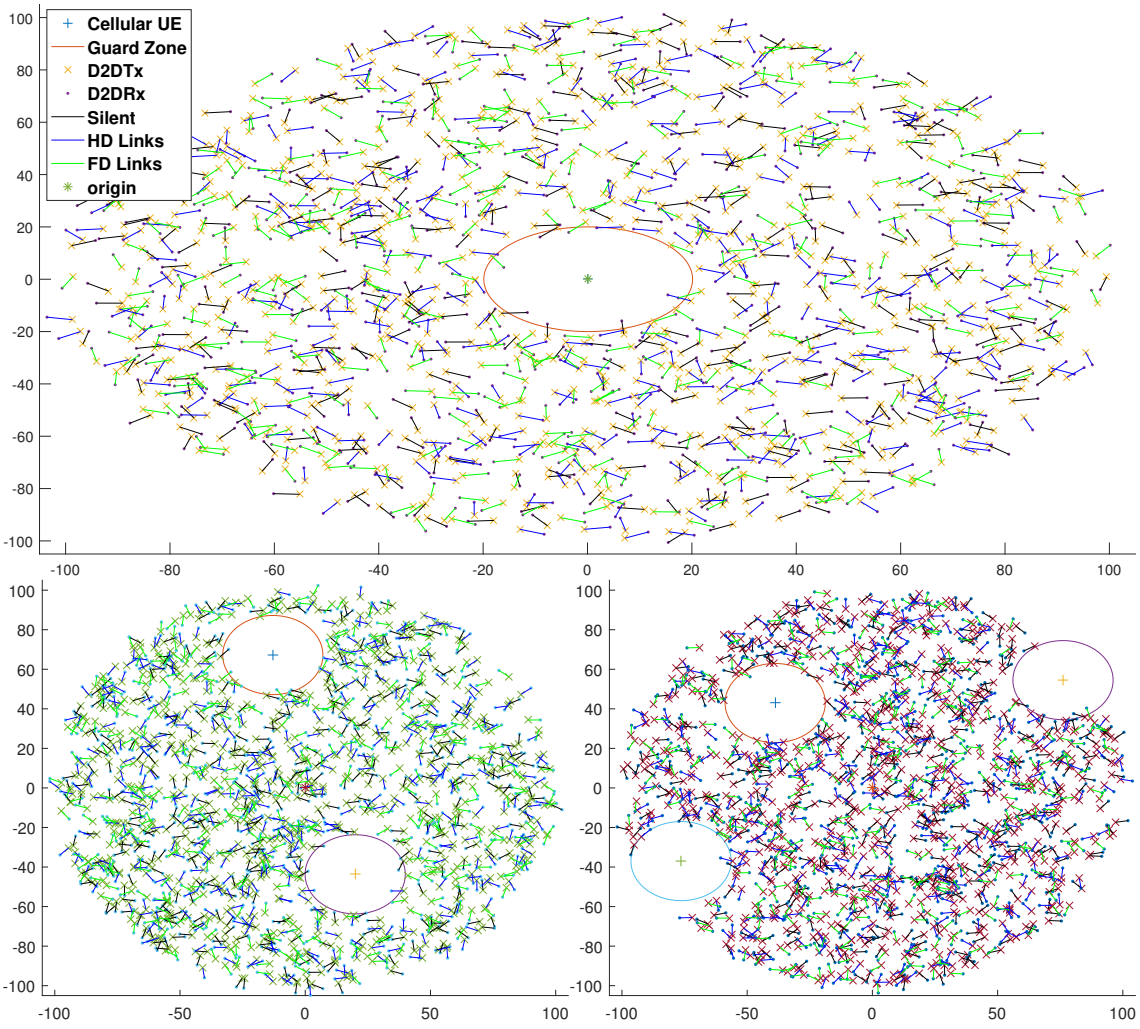

Figure 4.1 : Simulation model for FD enabled D2D cognitive networks with 1,2 and 3 active cellular users. D2D link states are randomly chosen with probabilities p_{sil},p_{HD} and p_{FD} for silent, HD and FD D2D link between transmitter and receiver.

Table 4.1 : Simulation Parameters and their values

Parameter	**Simulation Values**
λ_c	$\{0.32, 0.096, 0.20, 0.29, 0.40\} Users/Km^2$
λ_d	$\{0.003, 0.009, 0.05, 0.1\} Users/Km^2$
R_{GZ}	$\{10, 20, 40, 60, 80\} m$
α_c, α_d	4,3
P_c, P_d	1,0.05
β	0.3
R_d	$\{3, 5, 7, 9\} m$
p_{FD}	0,0.3,0.5,0.9
T	-20:1:20

success probability of the D2D link also increases due to the fact that a higher guard zone protection for a cellular user results in a reduced interference field from active D2D users. Stringent GZ protection causes more D2D links to be in silent mode and reduces the capacity of secondary operation i.e. D2D in this case. Another factor is a distance of the cellular receiver from a typical D2D link as if it is in the vicinity then it will put the dominant D2D interferers in the silent mode. Therefore, the optimal size of the guard zone balances the performance trade-off between the success probability of cellular and D2D users.

Another critical factor affecting the performance of the success probability of a typical D2D link is the D2D link distance (R_d) as shown in Fig. 4.3. As R_d increases, the success probability decreases due to the fact that this will result in an increase in half-duplex D2D links rather than the full-duplex D2D links. So, the interference field will contain more HD transmitters rather than FD transmitters and receivers,

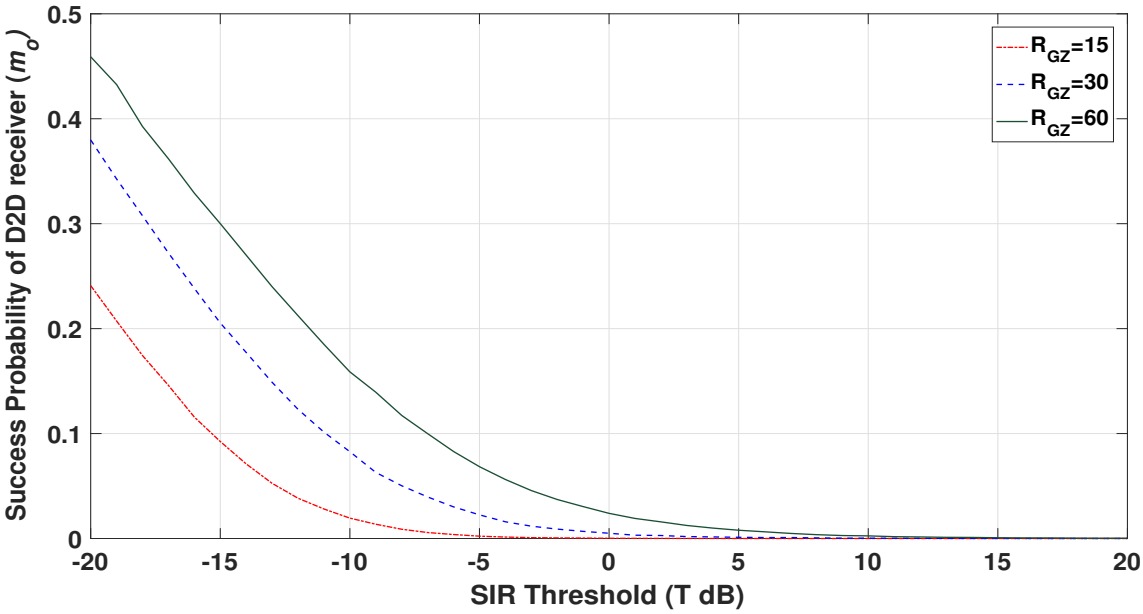

Figure 4.2 : Success probability of a D2D receiver as a function of SIR threshold (TdB) for different R_{GZ}

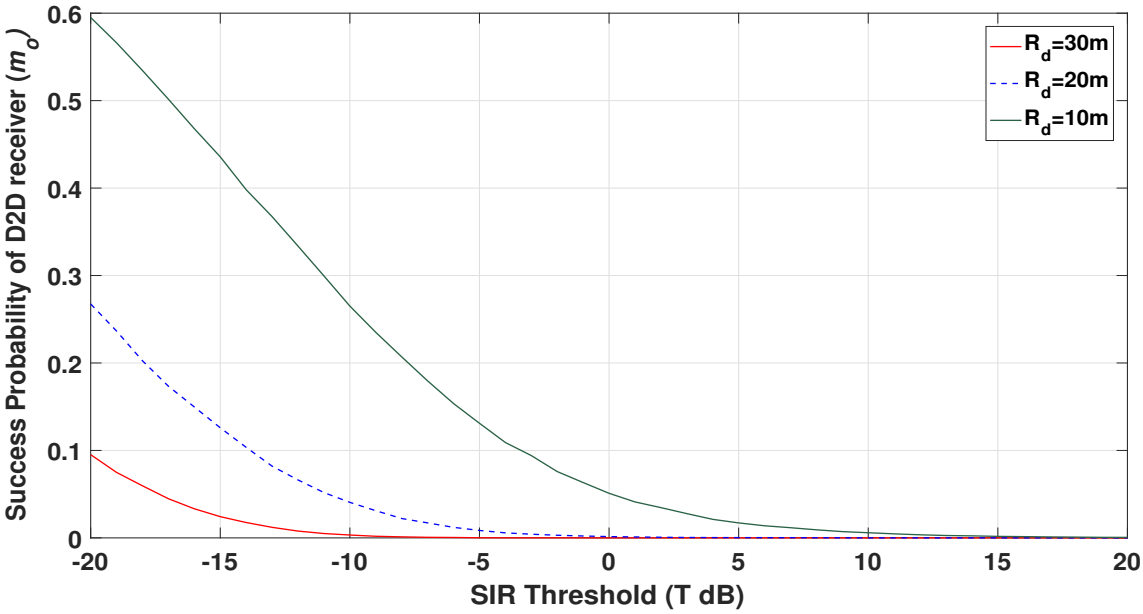

Figure 4.3 : Success probability of a D2D receiver as a function of SIR threshold (TdB) for different R_d

hence, less interference with higher R_d. This is in correlation with the overlap area shown in Fig. 3.5, decreasing the probability of the full-duplex D2D links.

According to the simulation configuration parameters given in Table 4.1, we will now present further analysis on the performance of the D2D network. Previously, we assessed the impact of having one active/schedule cellular user. Now, we will increase the number of simultaneously active cellular users which will increase the interference for the typical D2D receiver. Also, further results are presented, for instance, increasing D2D link distance (R_d) and step-wise increase from lenient to stringent guard-zone protection (R_{GZ}) for cellular user. Also, the impact of increasing the probability of FD users (p_{FD}), and D2D users intensity (λ_d) is evaluated and discussion on results is presented.

Impact of Cellular user intensity (λ_c): An interesting result which is useful for cognitive networks, is presented in Fig. 4.4. As the cellular users transmit with comparatively higher power then the D2D user, and their GZ also has impact on D2D network capacity, an increase in λ_C causes a decrease in $p_s^{m_o}$ of a typical D2D receiver as shown in Fig. 4.4. Also shown in Fig. 4.1, as the cellular user intensity is increased, due to the fact that $P_c >> P_d$ (Table 4.1), the typical D2D receiver experiences very high interference from cellular network and hence, causing performance degradation. Also, from Eq. 4.11, the interference field of cellular users ($\mathcal{I}_{y_o,x}$) increases, causing $SIR_{m_o^d}$ to fall below the threshold T, which in turn causes down-gradation for $p_s^{m_o}$.

Impact of D2D user intensity (λ_d) and FD probability (p_{FD}): The Fig. 4.5 shows that increasing the number of D2D users also limits the coverage/success probability of the D2D receiver. We can only push the limited number of D2D users to be active before we start loosing the optimum gains. As we increase the λ_d, it also increases the λ_{m_d}, which means a greater number of active D2D receivers.

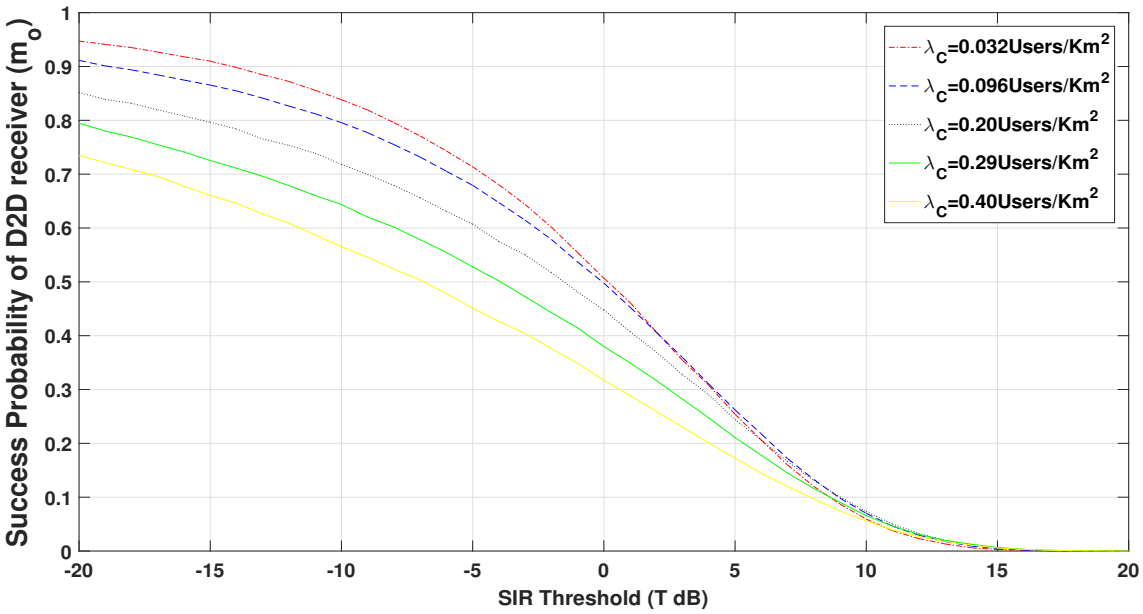

Figure 4.4 : Success probability of a D2D receiver as a function of SIR threshold (TdB) for different λ_c

In general, this increases the number of active FD receivers in the network, which induces more interference. A similar trend will be followed when we directly increase the probability of active D2D receivers by increasing the p_{FD}, and results are shown in Fig. 4.6. The performance of D2D network in Fig. 4.5 is also in line with the analytical analysis. For instance, the interference field in Eq. 4.2 depends on the intensity of D2D users, also in Eq. 4.7 and in Eq. 4.11, the $p_s^{m_o}$ depends on the interference originated from the number of D2D receivers in FD mode denoted by $\mathcal{I}_{y_o,m_y}$. Although the gains from FD operation are quite interesting, it also causes an increased interference for active links in the network (for both cellular and D2D user). Thus, there should be an optimal number of active D2D users in FD mode which is indicated as our future research direction to explore in section 6.3. Another compromising approach to tackle the FD interference is to shorten the D2D link distance (R_d) as this will limit the interference in the spatial domain and increases the efficient spectrum utilization.

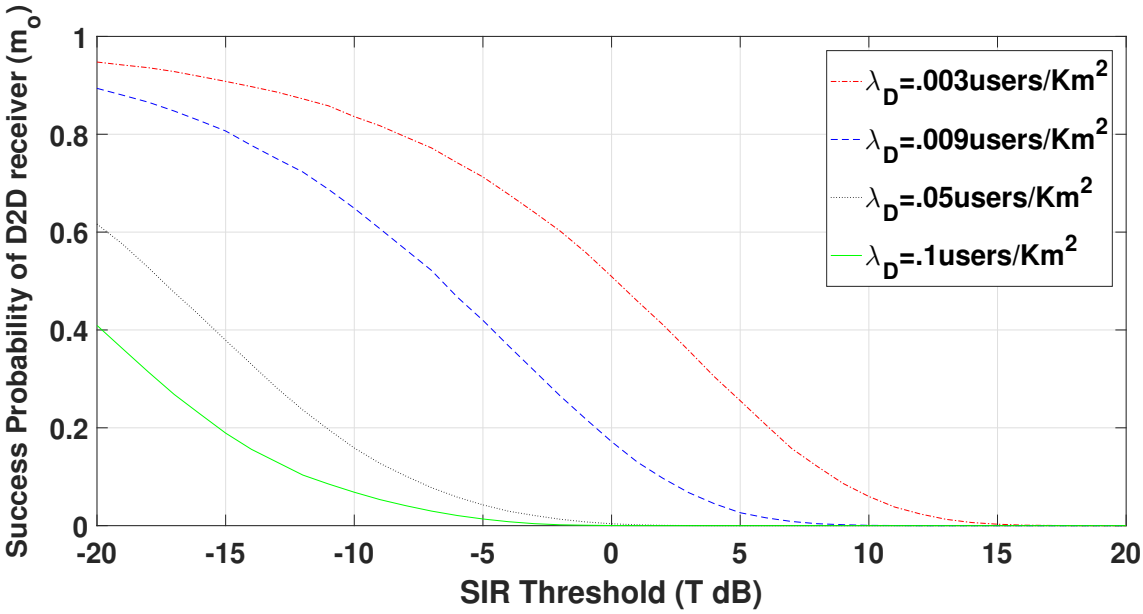

Figure 4.5 : Success probability of a D2D receiver as a function of SIR threshold (TdB) for different λ_d

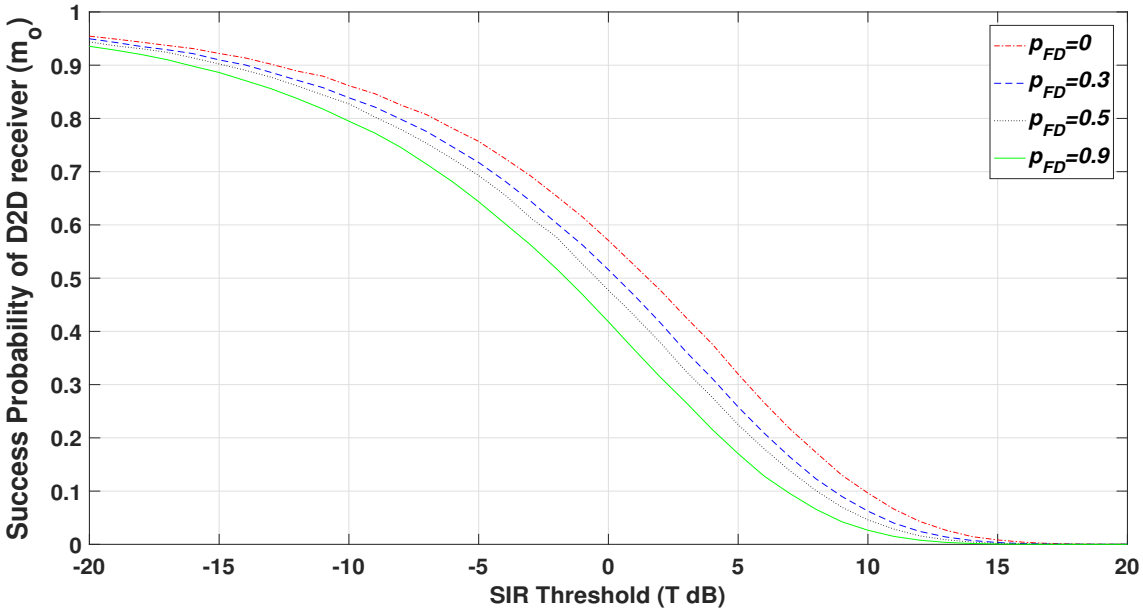

Figure 4.6 : Success probability of a D2D receiver as a function of SIR threshold (TdB) for different p_{FD}

Impact of D2D link distance (R_d) and Guard Zone radius (R_{GZ}): We ran further simulations according to network configuration parameters given in Table 4.1 and studied the impact of different D2D link distance and guard-zone radius values on overall coverage probability of D2D network. The results are shown in Fig. 4.7 (a) and (b), respectively. A similar trend has been observed as in Figs. 4.2 and 4.3. The gradual increase in D2D link distance R_d results in decrease in $p_s^{m_o}$. This is due to the fact that higher link distance will have more spatial interference as compared to smaller R_d. It is noted that smaller D2D link distances also better suit ultra-dense and urban scenarios as it can increase the network capacity of secondary users. This can also be related to the pdf of link distance based on social-interaction which is given in Eq. 3.7. Also, in Fig. 4.7 (b), as we impose more stringent protection for cellular receiver (i.e. bigger GZ), this in turn increases the coverage probability of D2D network. As only one cellular user is active then the interference is caused by only one receiver, unlike the result in Fig. 4.4, where each cellular user is protected by GZ. As the radius of GZ increases, more D2D links fall within the GZ and hence remain in silent mode. So, the increase in GZ radius in turn decreases the interference for the typical D2D receiver, increases the protection for cellular receiver and also increases the success probability for D2D receiver ($p_s^{m_o}$) as shown in Fig. 4.7 (b).

4.6 Summary

In this chapter, we have presented a stochastic geometry based performance analysis of FD D2D network while protecting cellular users communication with guard zones. PPP reflects the cellular user distribution, while D2D users reflects a close approximation of PHP. The success probability for a typical D2D user is evaluated for different system parameters, yielding insightful results to capture the performance of Full Duplex technology in D2D while abiding by the interference protection of

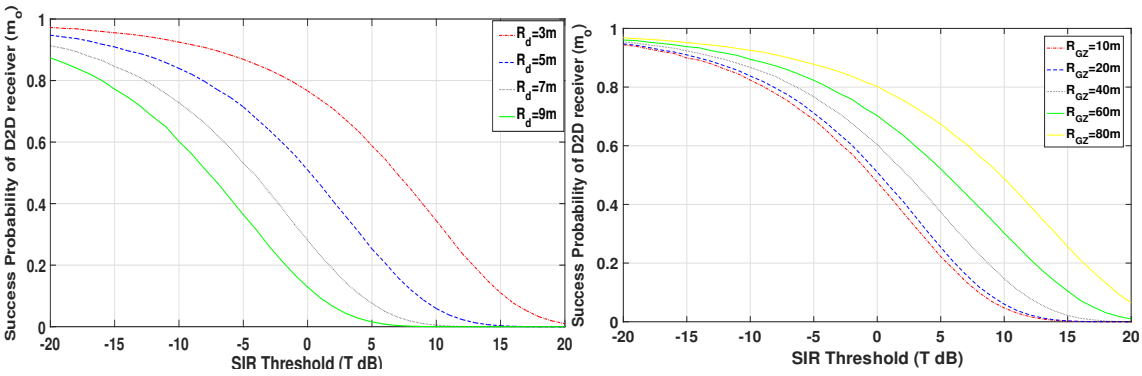

(a) (b)

Figure 4.7 : Success probability of a D2D receiver as a function of SIR threshold (TdB) for different (a) R_d and (b) R_{GZ}.

cellular users. The results have shown the potential of the FD technology, if the D2D link state (HD/FD) is chosen based on aggregate interference. Moreover, an interesting observation based on a shorter D2D link-distance has shown a significant increase in the success probability. Also, the intensity of FD users can be allowed to communicate as long as the success probability of other users is not severely degraded. Until now, we have not considered any medium access protocol for coexistence of D2D with cellular users due to tractability of analytical analysis. In next chapter, we are going to evaluate different medium access protocols for coexistence of different Radio Access Technologies.

Chapter 5

Coexistence Analysis of LTE, Full Duplex D2D and WiFi

In previous chapters so far, the emphasis was on design, modeling and analysis of FD enabled cognitive network in licensed or semi licensed spectrum sharing frameworks using stochastic geometry. In this chapter, we investigate different coexistence techniques (discussed in section 2.4.2) for multi-RATs (like WiFi, LTE-U, LTE-LAA, and FD D2D) in unlicensed bands. Before 5G, WiFi has been the dominant and unchallenged technology in unlicensed bands and recently mobile operators have also targeted these bands for communication. The major challenge was fair and peaceful coexistence among scheduled and random MAC based technologies. This drove the need for critical evaluation of coexistence spectrum sharing methods and also is the theme of this chapter. We start with the basic introduction and related works in this context in section 5.1. Then, we first present the analysis of different LTE transmission/coexistence techniques on FD D2D in section 5.2. System model, transmission techniques and their impact on the performance of FD D2D network are studied, results are presented and analysis is given in section 5.2. Following this, we also present Network Simulator (ns-3) based simulation results for the coexistence of WiFi and LTE in unlicensed spectrum in section 5.3. Finally, the chapter summary is given in section 5.4. Parts of the work described in this chapter resulted in Publication [111].

5.1 Introduction and Related Work

Dynamic spectrum allocation has brought forth a multifold increase in network capacity and throughput. Moreover, the latest developments of reduction in residual self-interference-to-power ratio (SIPR) techniques enable in-band full-duplex (FD) communications in which a transceiver can transmit and receive simultaneously on the same frequency channel and even using the same antennas. That in-band FD capability has the potential of doubling the spectral efficiency of all existing wireless systems. However, a trivial integration of FD into existing communications paradigms would result in excessive network interference [118]. In fact, the advantage of FD depends on whether SIPR is perfect or imperfect as well as having a meticulous network design as discussed in [119]. Similarly, D2D is also proven to be a potential candidate to augment the capacity of cellular networks [120]; however, this is at the expense of introducing additional network interference. Different network models of cellular and D2D communications can be envisioned based on the centralized or distributed D2D communications scenarios. Also, the coexistence of D2D and LTE in unlicensed spectrum is envisioned to ease and offload the network congestion from the main cellular network [120, 121].

The networks ultra-densification using small cells over unlicensed or shared spectrum with D2D connectivity is one of the key communications paradigms for 5G [39, 122]. In this work, we consider the potential integration of FD capability to this scenario, while using different transmission techniques for LTE. We observe that due to the higher interference from in-band FD communications as well as D2D, FD-capable D2D devices may wish to opportunistically switch between Half-Duplex (HD) and FD modes. LTE and overlay FD D2D communications were previously studied with imperfect SIPR and varying distance distributions between D2D nodes in [13]. The authors in this work used a stochastic geometry analysis, Monte-Carlo

and discrete link-level ns-3 simulator for feasibility study of coexistence of different radio access technologies.

The stochastic geometry and random graph theory has emerged as a powerful tool to study key network parameters [123]. Thanks to its mathematical tractability, it has also been used for analysis of heterogeneous networks (HetNets) [88] and the performance study of different coexistence techniques in spectrum sharing between LTE-LAA and WiFi [88]. A baseline model for throughput analysis of HD or FD systems and the impact of SIPR have recently been reported using stochastic geometry [118]. This analysis is further extended to model the performance of a LTE network with HD or FD D2D in the licensed bands [13]. However, to the best of our knowledge, none of these works have considered the impact of LTE in unlicensed bands with the legacy coexistence techniques for HD or FD D2D communications.

The coexistence between LTE-LAA [50] and WiFi has been extensively investigated since its proposal [34]. Coexistence techniques for LAA and WiFi include listen-before talk (LBT) and Discontinuous Transmission (DTX). For instance, authors in [124] employed these methodologies along with Q-learning for an efficient co-existence of WiFi and LAA. The real-time test-bed results are also reported for LAA and WiFi coexistence in [52]. Stochastic geometry analysis of the state-of-the-art coexistence approaches for LAA and WiFi is presented in [34]. Researchers also have developed discrete link-level ns-3 module dedicated to study the coexistence of LTE-unlicensed and WiFi [125]. The preliminary results were presented for discussion with cooperation from the WiFi Alliance in 3GPP TSG RAN working group meeting in November, 2015 [126]. Detailed description of ns-3 module, configuration parameters, and design were given in [127].

The existing literature provides a good insight for coexistence analysis between WiFi and LTE-LAA, however, the impact of state-of-the-art coexistence techniques

on FD enabled D2D users in unlicensed bands needs to be investigated. Moreover, the impact of SIPR for FD D2D modes also needs to be incorporated for critical analysis. This work presents detailed analysis of SIPR effect and coexistence techniques used by LTE on D2D network on unlicensed bands using stochastic geometry. Also, we use ns-3 simulator to extensively study the impact of different coexistence methods for LTE-unlicensed and WiFi in time-domain.

5.2 Impact of LTE transmission techniques on FD D2D

This section presents analysis of the impact of using different transmission techniques for LTE on FD enabled D2D users.

5.2.1 System Model

The system model in this chapter also follows the PP distribution for LTE and D2D users. To avoid the repetition and due to space constraints, in general, the system model for spatial distribution, connectivity, propagation assumptions, notations, symbols and distribution of emulated setup is similar to the one given in 4.3. The considered system model realization with LTE and D2D users is also shown in Fig. 5.1 using Voronoi tessellation.

5.2.2 LTE Transmission Techniques

In this work, we consider three different scenarios based on the transmission method employed by LTE and we study its impact on FD D2D transmissions. In the first scenario, LTE transmits continuously without any protocol modifications and D2D pair communicates either in HD or FD mode with probability p_{HD} or p_{FD}, respectively. When in the HD mode, the value of β is varied to assess the impact of SIPR for baseline results. In the second scenario, LTE uses a duty cycle based transmission pattern for η fraction of time, whereas the other devices in the

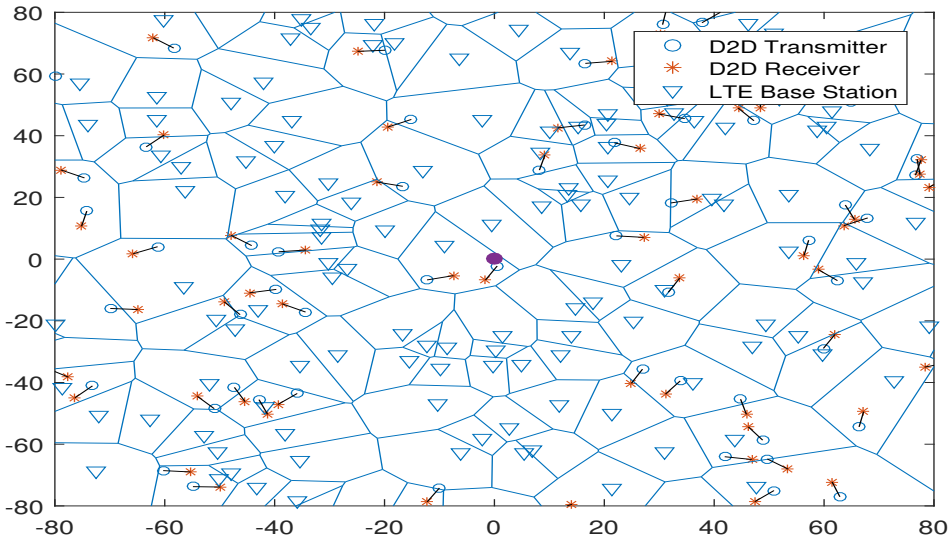

Figure 5.1 : Realization of network model with LTE users and D2D links nodes using Voronoi tessellation.

medium transmit for $1-\eta$ time. In the third scenario, LTE devices use the LBT mechanism for channel access, where each node uses the aggregated energy detection (Γ_{ed}) in the medium and transmits only if the Γ_{ed} value is below a threshold. To implement LTE-LBT, PPP $\Phi_x = \{x_i, m(x_i)\}$ on $\mathbb{R}^2$ is considered , where each point x_i is assigned with mark $m(x_i)$. This mark represents each point of the random back-off timer which is uniformly distributed between $(0, 1)$. This back-off timer indicates the aggressiveness of LTE nodes for accessing the channel. Due to the difference in transmit powers and path loss, D2D nodes and the LTE nodes have different impacts on success probability (p_s).

5.2.3 Performance metric

Since both D2D and LTE nodes form a homogenous PPP, we perform our analysis by considering a receiver (m_o) at the origin as it is equally applicable for all the other nodes in the network due to the motion invariance and translation property

of PPP. The analysis is performed by considering full buffer downlink traffic only. Moreover, D2D nodes are always communicating whereas LTE nodes employ one of the coexistence mechanism to share the medium with D2D. We denote the set of system parameters $(\lambda_L, \beta, \alpha)$ as the network configuration. In the considered network scenario, a transmission attempt from all other nodes to a tagged node (at origin) is considered successful, if its $SIR^d_{m_o}$ (given in Eq. 4.3) is greater than threshold T. As a performance metric, we have considered success probability for transmission of typical D2D link and this is given in Eq. 4.4.

5.2.4 Results and Analysis

This section presents simulation results for network configuration parameters and discussions on presented results. The network configuration and simulation parameters, notations and values are given in Table 5.1. The baseline performance comparison analysis of HD-only, FD enabled and simple LTE network is presented in Fig. 3.10. Thus, we move on to the main results of this section.

Continuous LTE Transmissions

In Fig. 5.2, the success probability of typical D2D user $p_s^{m_o}$ is shown when LTE users transmit continuously without employing any coexistence protocol or in other words, without caring for competing users from other RAT i.e. D2D. When intensity (λ_L) of LTE users is increased that further increases the successful transmissions and higher medium occupancy for LTE users. This behavior can be explained by the fact that the higher transmission intensity of the LTE nodes increases the interference floor for the D2D pair. To overcome this interference floor, the D2D pair should increase its transmit power for successful transmission. However, increasing power is not a viable solution since it will affect the LTE users in return in the uplink. One possible solution to this problem is to shift the D2D transmission on to some other frequency band as discussed in section 2.4.2 or employ a frequency hopping

Table 5.1 : Simulation Parameters and Network Configuration

Parameter	**Simulation Values**
LTE power (P_L)	1
D2D power (P_D)	0.005
LTE user intensity (λ_L)	0.005
D2D user intensity (λ_D)	$2^*\lambda_L$
Path-loss component for D2D (α_d)	3
Path-loss component for LTE (α_L)	4
SIR Threshold (T)	-20:1:20
Plane Radius (R_c)	100m
D2D Link Distance (R_D)	$R_P/20$
SIPR (β)	0-1
Energy detection threshold (Γ_{ed})	-72dBm, -77dBm,-82dBm
Duty Cycle (η)	0.33, 0.5, 0.7 (33%,50%,70%)

technique when one band is aggressively used by LTE as discussed in section 2.4.2.

When LTE transmits continuously, we also investigate the impact of different SIPR (β) values on performance of D2D success probability as shown in Fig. 5.3. This result shows how much self-interference due to FD operation effects the $p_s^{m_o}$. The SIPR is varied from β=0, β=0.3 to β=0.7, while other network configuration parameters are λ_d=0.01, λ_L=0.005 and p_{FD}=0.5. As we observe from the results, with the shift from perfect to imperfect SIPR, a typical receiver has to face now extra interference from D2D receivers operating in FD mode. It can be observed in Fig. 5.3 that for the low SIR regimes there is much less effect of SIPR on $p_s^{m_o}$. On the other hand, for higher SIR values the impact of SIPR is prominent. So for D2D,

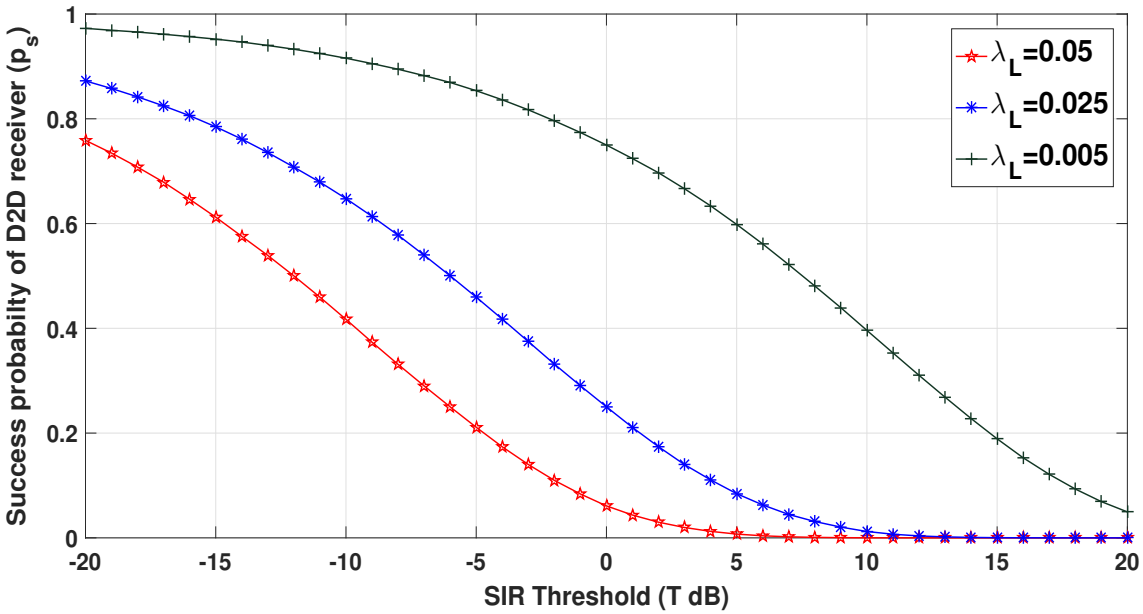

Figure 5.2 : Success probability of typical D2D user as a function of SIR threshold over different intensity of LTE users ($_L$).

in order to operate at higher SIR values, almost perfect SIPR is required which can be achieved due to advancement of signal processing and chip designing techniques. Thus, better SIPR elevates the advantages of FD technology and elevates the overall performance of the system it is integrated in.

LTE with Discontinuous Transmissions (DTX)

The simple method for LTE to ensure fairness and peaceful coexistence with technologies like WiFi/D2D is to employ duty-cycle based transmissions. To ensure fairness, the duty-cycle period (η) can be adjusted according to the traffic conditions and the medium utilization by other technology candidates. For instance, Fig. 5.4 shows the impact of the LTE duty cycle on D2D success probability. The duty cycle period or amount of time LTE transmits is varied from η=33%, η=50%, η=67% to η=80%. As LTE transmits for a higher fraction of the time, the success probability of D2D degrades due to an increase in number of LTE users transmitting and higher

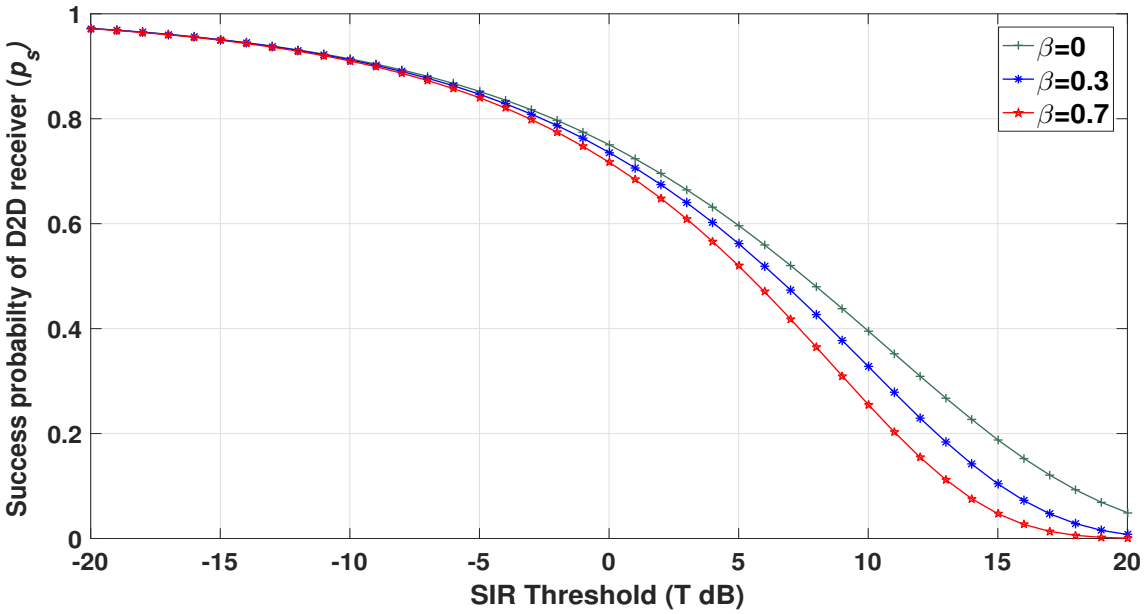

Figure 5.3 : Success probability of typical D2D user as a function of SIR threshold for different values of SIPR (β).

collisions with D2D packets. As seen in the previous results, D2D network performance declines if LTE transmits for a longer period or the number of UEs tends to increase as shown in Fig. 5.2.

The LTE network does not guard or care for D2D communications as it transmits with the same power for η fraction of time. Specially, the LTE nodes transmitting in the vicinity of D2D communication degrade their performance. Therefore, from the results we conclude that the LTE nodes near the D2D nodes must use some sensing based mechanism to protect D2D nodes from strong interference. The duty-cycle based DTX method might work well with the coexistence of inter-technology contenders where different LTE operators agree on DTX period, but this does not suit well for multi-RAT coexistence scenarios. Thus, for such scenarios, sensing based mechanisms are preferred with careful selection of energy sensing thresholds, which is investigated next.

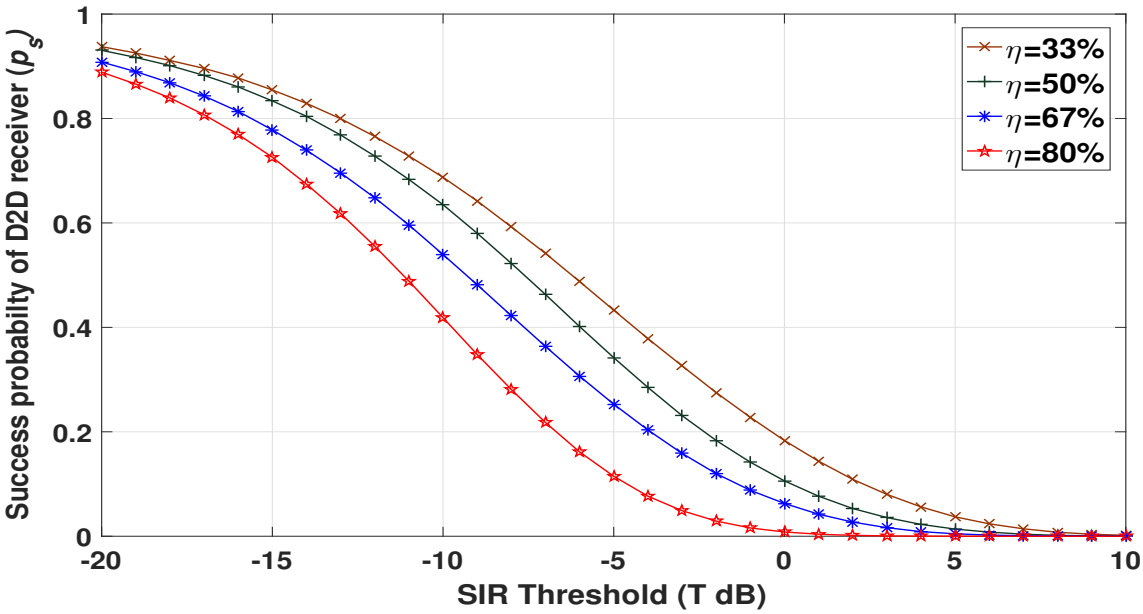

Figure 5.4 : Success probability of typical D2D user as a function of SIR threshold over different duty-cycle (η) values of LTE DTX.

LTE Listen-before-Talk (LBT) with Contention Window (0,1)

Besides DTX, listen before talk (LBT) with a random back off is another coexistence mechanism based on energy detection (Γ_{ed}) in the medium. Each node has a random back off timer between (0,1), which identifies how often the node senses the channel. Fig. 5.5a shows the impact of different energy detection thresholds (Γ_{ed}) for channel sensing on the success probability of the D2D nodes. For lower Γ_{ed} values, the number of LTE nodes accessing the channel increases, which in turn impacts the D2D nodes and their success probability decreases. An interesting observation from this result is that D2D communication is guarded by the LTE LBT transmission type. The LTE nodes in the vicinity of D2D pairs will guard D2D communication by not accessing the channel; however when the ED threshold is significantly reduced to -10dBm then the success probability of the D2D nodes starts to drop. Result comparison in Figures 5.5a and 5.5b shows how perfect (β=0) and almost imperfect (β=0.7) SIPR significantly impacts the performance of the D2D

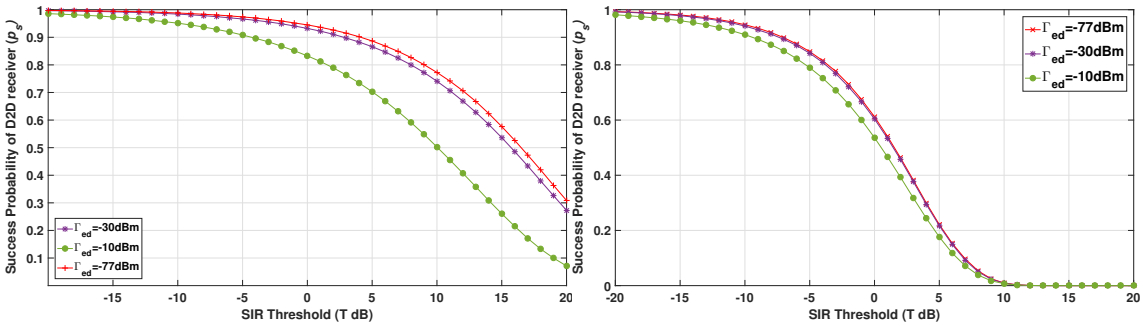

(a) (b)

Figure 5.5 : Success probability of typical D2D user as a function of SIR threshold for different energy detection threshold values with SIPR (a)β=0 (b)β=0.7

network. Due to the increased residual SIPR, D2D communication suffers from severe interference from its own transmissions and from the LTE devices collectively. Therefore, the performance gain of FD communication is limited to the amount of SIPR. Therefore, the benefits of FD technology could only be practically gained once the SIPR is reduced. Hence, LTE-LBT better guards D2D transmissions at the cost of the coverage outage of the nodes near D2D pairs. Based on mission-critical applications, D2D communication can be guarded by nearby LTE nodes and the optimum ED threshold can be selected to find the acceptable trade-off. The intuitive notion from the results indicates that although FD D2D may disrupt network performance due to an increased aggregate interference, performance gains can be achieved by carefully adjusting the power levels of the D2D and HD/FD mode selection for the D2D nodes. We aim to characterize this tradeoff between spectral efficiency, interference impact and network throughput in future work by using a mathematical model.

5.2.5 Conclusions

In this section, the impact of different LTE transmission methods over HD and FD D2D networks is analyzed by using stochastic geometry analysis and simulations. The success probability for D2D nodes is numerically evaluated for scenarios when LTE nodes transmit continuously, employ discontinuous transmission or use the listen-before-talk mechanism. Moreover, the impact of self-interference-to-power ratio (SIPR) on D2D success probability is evaluated. The LTE network is protected from D2D interference, whereas, the D2D success probability can be improved by carefully adjusting the transmit power and the modes of transmission. Also, near to perfect SIPR results in a higher success probability for the D2D nodes without impacting the LTE network significantly. Thus, FD technology gains can be harvested for short-distance communications like D2D if SIPR is under 0.5, otherwise, higher interference causes more transmission failures. Moreover, LTE-LBT better guards D2D pair communication by silencing the nearby nodes, however the energy detection threshold (Γ_{ed}) can be tuned accordingly to meet a trade-off for success probability of D2D and LTE transmissions. The next section discusses a coexistence study among LTE and WiFi in unlicensed spectrum, which is one of the well debated and increasingly explored research problems when LTE was proposed to share unlicensed spectrum with the most dominant incumbent i.e. WiFi.

5.3 LTE and WiFi Coexistence

Recently, standardization and development activities for use of LTE in unlicensed spectrum has attracted great attention from research, industry and regulatory bodies. Due to new spectrum opportunities in the 5GHz band and scarcity of licensed spectrum, vendors and Mobile Network Operators (MNO) have been supporting the deployment of LTE in unlicensed spectrum since 2014. However, polite incumbents like WiFi are concerned about peaceful, fair and harmless coex-

istence with LTE-unlicensed. Federal Communications Commission (FCC) is also investigating technical reports on the performance of LTE technologies in unlicensed spectrum and their coexistence with incumbent technologies. Initially, LTE-U forum proposed initial specifications for deployment of LTE in unlicensed (LTE-U) using Carrier Sense Adaptive Transmission (CSAT) coexistence mechanism to be deployed in regions which do not require listen-before-talk (LBT). The 3rd Generation Partnership Project (3GPP) also proposed different scenarios and requirements for Licensed Assisted Access-LTE (LAA-LTE) in Release 13. The initial proposal requires control signaling via a licensed anchor and provides Supplement Downlink (SDL) in unlicensed spectrum. Very recently variants of this technology are also being proposed to achieve optimum performance and spectral efficiency using LTE supported technology with WiFi-like deployment. For instance, a variant of such technology is MulteFire [128].

Despite growing activities in development and deployment of LTE in unlicensed spectrum there exist many challenging research questions voiced by WiFi Alliance which require critical in-depth evaluation of fair, peaceful and optimum coexistence of LTE in unlicensed spectrum. The 3GPP, Wi-Fi alliance and other stake-holders are working closely to address these challenges. Also, different MAC protocols are under consideration for LTE. Wifi is random access while LTE is a scheduled system which makes it more difficult to achieve certain performance and coexistence trade-off. Moreover, factors like channel occupancy, traffic intensity, energy detection threshold, user intensity per cell also impact the overall performance of the system. However, our scope in this work was limited to the study of duty-cycle based coexistence mechanism.

The WiFi has proven to be an efficient system in unlicensed spectrum for almost a decade, however its performance starts to degrade with the increase in number of users and competing access points. Unlike LTE which is a scheduled system,

WiFi is a contention based system for medium access. Therefore, LTE has no intra-system contention operating in a multi-operator environment. In terms of control signals (CS), LTE has better CS optimization than WiFi. LTE has also support for seamless handover and service continuity when a user leaves one cell and joins another. Moreover, LTE has centralized architecture were eNB controls channel access decisions. In contrast, WiFi system relies on the decentralized channel access mechanism based on CSMA protocol. However, CSMA/CS protocol has proved to be an efficient way of sharing common medium and spectrum for multiple devices in an uncoordinated fashion.

Before stepping into these unlicensed bands for mobile communications, there is a major challenge of peaceful and fair coexistence for new technologies with incumbents. The main incumbent technology in 5GHz spectrum is WiFi. Combined and harmonious operation of WiFi and LTE in the same unlicensed frequency bands was one of the very popular research topics among the research community, as it may provide a practical solution to address spectrum shortage and capacity constraints.

Unlike licensed bands, communication in unlicensed spectrum must follow regional regulatory requirements to avoid interference with adjacent devices using the same spectrum. Due to no exclusive licensing, these bands can be used by any technology until they follow regulatory requirements. These requirements may also vary for different bands within 5GHz spectrum. For instance, in the US and EU UNII-2 bands (5260-5320) require dynamic frequency selection (DFS) capabilities to avoid interference with Radar. So, if Radar signals are detected than a device operating in this spectrum must leave the channel and shift to some other available frequency channel.

The prime concern for success of either LTE-U or LAA is their peaceful and fair coexistence with incumbent technologies in unlicensed spectrum (WiFi). Fair and

equal medium sharing is required for successful coexistence among all devices operating in unlicensed spectrum. This coexistence can be made possible by using channel sensing and medium access protocols which also consider on-going transmissions and provide equal opportunity to other transceivers as well without any interference. Researchers are urging the development of a single global solution allowing compliance with all regulatory regimes. In efforts to achieve this, few coexistence techniques have been proposed in literature.

In literature, recently there have been a few proposals on coexistence techniques claiming fair medium access with minimum interference to adjacent stations. Existing approaches can be categorized based on their methodology i.e. channel selection based, duty-cycling and listen-before-talk (LBT). A hybrid combination of these approached has also been proposed for acceptable trade-off between performance and cost incurred.

5.3.1 Simulation Setup and System Model

We used link-level network simulator ns-3 with an under-development (in 2016) module for simulations of LTE and WiFi coexistence [125], following a 3GPP indoor scenario as given in TR36.889, Release 13. The preliminary results were presented for discussion with cooperation from WiFi Alliance in 3GPP TSG RAN working group meeting in November, 2015 [126]. To study the coexistence effect of LTE in unlicensed (LTE-U) and WiFi in an indoor scenario, 4 cells of each technology (Wifi and LTE-U) with 5users/cell are deployed. Total number of AP/eNB is 8 and number of users is 40. The small cells of each operator are equally spaced and centred along the shorter dimension of the building. The distance between two closest nodes from two operators is random. The set of small cells for both operators is centred along the longer dimension of the building. The system requirements are according to description given in TR36.889 released and maintained by 3GPP as part of release

13. Each simulation was run for 2s of data transfer and 15s overall. Three different scenarios are considered for comparative performance analysis study: firstly two WiFi networks are deployed, then the second WiFi device is replaced with an LTE device, and lastly two LTE devices are deployed. The metric of fairness as defined by 3GPP is that any other device operating in unlicensed spectrum should not impact performance of WiFi more than any other WiFi in the vicinity. The details of simulation scenarios, and ns-3 LTE/WiFi coexistence model is given in [127]. Typical realization of simulation model for indoor scenarios is shown in Fig. 5.6, where operator A and operator B can be LTE or WiFi.

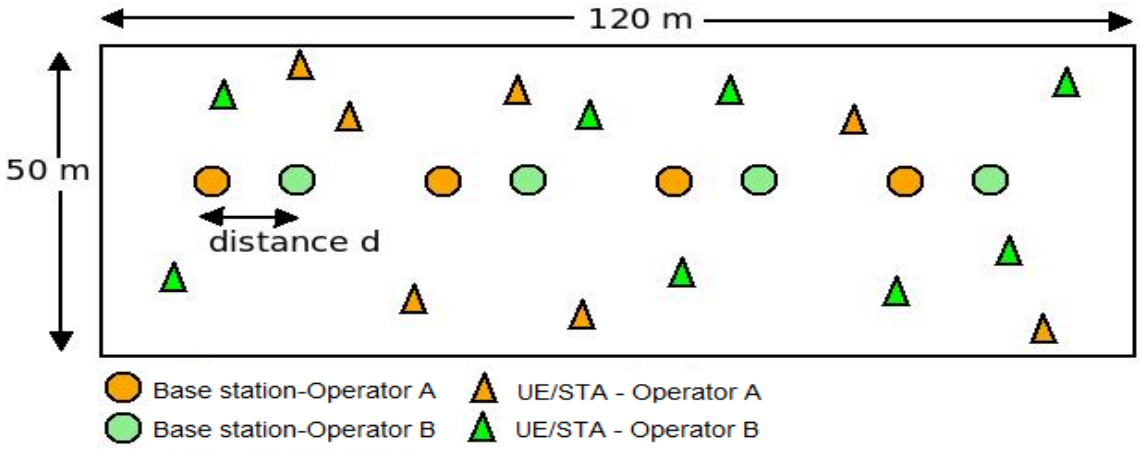

Figure 5.6 : Illustration of indoor simulation scenario in ns3 module for LTE and WiFi coexistence [126].

The first set of simulation scenarios evaluated the impact of varying duty-cycle over user throughput. Duty-cycle for LTE is implemented using Almost Blank Sub-frames (ABS) over 40 LTE sub-frames (i.e. 40ms). For instance, in the first set of experiments, duty-cycle is set to 100% which means LTE will transmit without any silent or ABS frames. In contrast, the 50% duty cycle period will include almost half (22 ms of 40 ms Tx time) ABS frames and in the other half LTE will transmit. So, WiFi will be able to transmit during the time period in which LTE is on silent mode.

UDP traffic is used where each packet is comprised of 1000bytes. The resulting rate is expected to saturate the channel as maximum data rate is divided by the average number of actual UEs per cell. Table 1 shows ABS patterns for different duty-cycles of LTE. For instance, duty cycle 1 means LTE will transmit without employing any ABS or silent sub-frames, whereas, duty cycle 0 all of LTE sub frames will be blank except for two sub frames which are reserved for Master Information Block (MIB) and System Information Block (SIB1) transmissions. In all simulations, full buffer UDP traffic conditions are considered. Final average user throughput is reported.

5.3.2 Results and Analysis

WiFi and WiFi network coexistence: Firstly, both operators A and B are WiFi Access Points (APs) competing for channel access to allow their STAs to download the data. Operator A has 1 STA, while the number of STAs for operator B have been increased from 1 to 8 and the average user throughput is shown in Fig. 5.7. As WiFi employs CSMA/CA, which is a soft sensing based channel access mechanism, this encourages fair and peaceful coexistence among other competing devices in the medium. The offered throughput is equally dsitributed among the

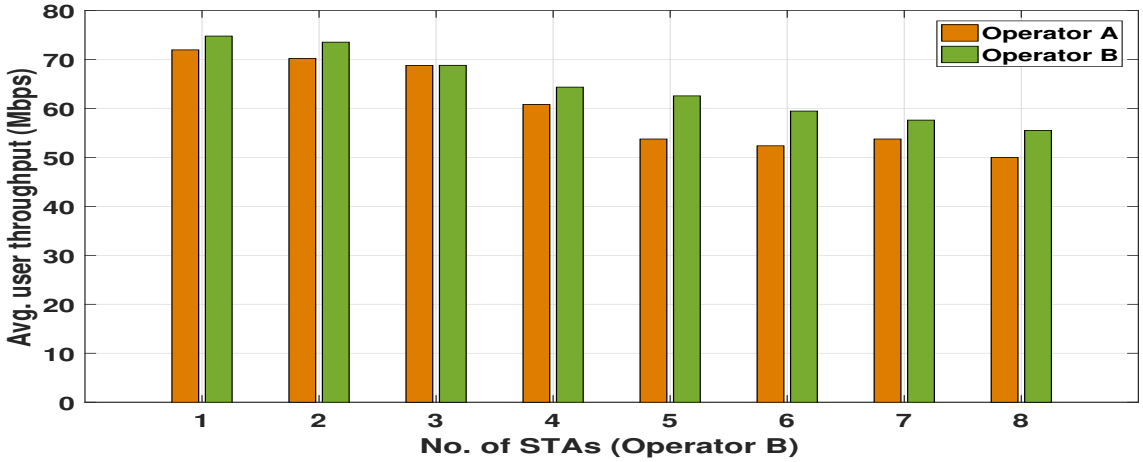

Figure 5.7 : Average user throughput of user as a function of increasing number of stations of Operator B.

competing users. For instance, as the number of STAs for a second WiFi operator starts increasing in Fig. 5.7, the aggregate throughput for Operators B's STAs is almost the same as that of Operator A's STA. When any other device like LTE is deployed in the same scenarios without any channel sharing mechanism, it highly disrupts WiFi transmissions by blocking its channel access. However, such negative impact on WiFi can be mitigated by introducing a duty-cycle period for LTE to share the medium among LTE and WiFi. In the next section, we will study the effect of different duty cycle periods for WiFi and LTE network performance.

LTE-U duty-cycle based coexistence with WiFi: Now, we study the coexistence scenario where WiFi (Operator A) and LTE-U (Operator B) share the unlicensed spectrum where LTE-U employs a duty-cycle (η) based coexistence mechanism. The results of this simulation scenario are shown in Fig. 5.8. Duty cycle (η) for LTE-U is varied from 0 to 1 with different ABS patterns. For instance, duty cycle 0 means that almost all of LTE sub-frames are muted to allow WiFi transmissions, interference free. Only control frames such as MIB and SIB1 are transmitted. Alternatively, duty cycle 1 means LTE constantly transmits without any blank or silent sub-frames. In this scenario, CSMA/CA of WiFi block its channel access as LTE is transmitting all the time. This leads to an LTE dominant environment, which is unfair channel utilization among a diverse set of technologies operating in the same location. This is expected and confirms the results that have been shown in the literature and also in numerical results presented in the previous section. The notable observation from results in Fig. 5.8 is that maximum achievable UE throughput at 100% duty cycle is about 12.2Mbps, while maximum achievable throughput by WiFi STAs at 0% duty cycle is about 11.8Mbps. The politeness factor of CSMA/CA in WiFi standard forces its devices to listen, wait and back-off before transmitting, yielding a decrease in throughput, whereas LTE instantly transmits without any backoff which causes collisions for WiFi packets still not transmitted. This happens

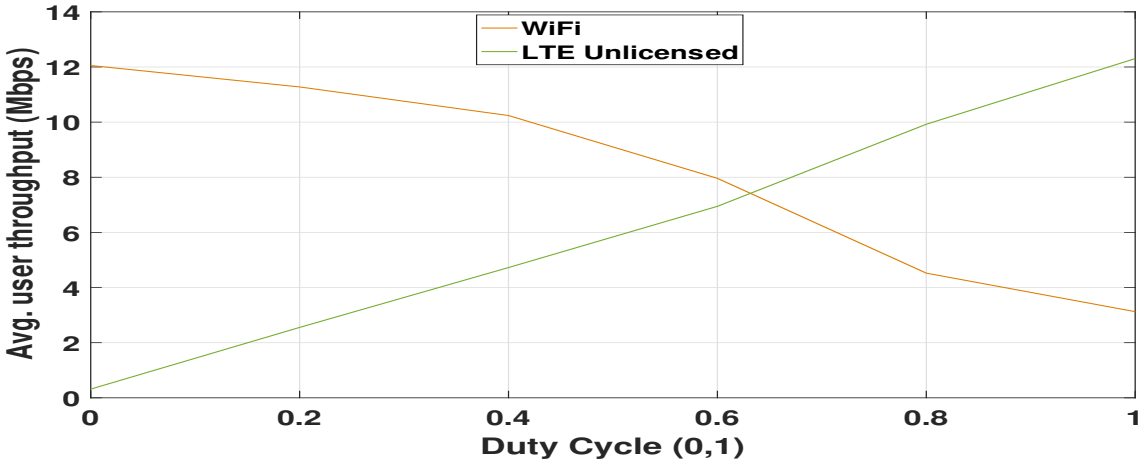

Figure 5.8 : Average user throughput of WiFi and LTE users in unlicensed spectrum as a function of different duty cycle (η) values.

in every transition period from WiFi to LTE transmissions and may cause significant loss in throughput for WiFi. For fair sharing, we see that when duty cycle period is 0.5 (50%) both LTE and WiFi almost achieve equal throughput i.e. 6.6Mbps each. Next, we increase the number of cells for each technology and study how it will impact the coexistence of LTE-U and WiFi.

LTE-U and WiFi coexistence with fixed duty-cycle: The number of cells for each technology (WiFi and LTE) are increased to study its impact on user throughput while keeping the duty-cycle fixed to 0.5 and the results are shown in Fig. 5.9. The η of 0.5 allows WiFi to utilize the medium at least 50% of the time without any disruptions or interference from LTE-U. As shown in Fig. 5.9, WiFi users have higher throughput because of less interference and reduced packet collisions due to LTEs abrupt transmissions. The increase in number of cells increases interference and packet collisions for WiFi, hence this results in decreases in throughput. Also, due to no back-off mechanism, LTE-U sudden transmissions may result in collision with WiFi's in the air packets, hence disrupting the WiFi performance. Overall, if LTE-U also employs some kind of random backoff before instantly transmitting

then it may improve the WiFi performance at duty-cyle of 0.5.

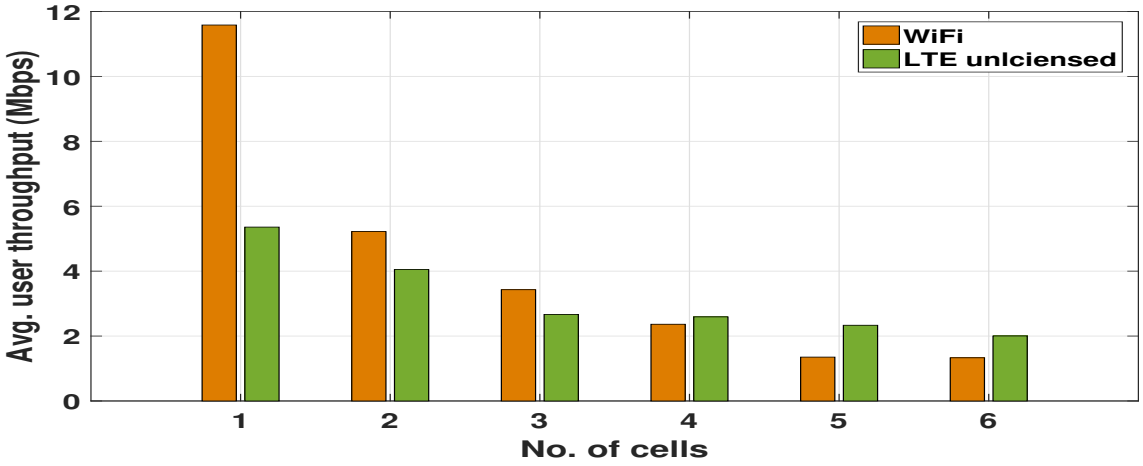

Figure 5.9 : Average user throughput of WiFi and LTE-U users as a function of increasing number of cells while η=0.5.

An efficient interference mitigation algorithms of LTE as compared to WiFi outperforms WiFi performance in densely deployed high interference situations. WiFi is susceptible to interference and performance degradation in high load conditions, while LTE has more advanced interference mitigation techniques. The politeness factor of CSMA/CA protocol of WiFi also contributes towards its lesser throughput as compared to duty cycled LTE. An increased back-off and repeated transmissions from WiFi also results in reduced throughput especially in dense and crowded networks.

LTE-U and LTE-U coexistence with duty-cycle: Both operator A and B are LTE-U base stations which employ a duty-cycle base coexistence mechanism for spectrum sharing. As shown in Fig. 5.10, the maximum achievable UE throughput for both operators in 100% duty cycle is 1.2 for operator A and 1.8 for operator B. In this case, both operators transmits simultaneously which causes packet loss due to collisions. This throughput can be increased if the LBT mechanism is employed. Sudden increase in UE throughput at 100% duty cycle is due to the absence of any

muting or blank sub-frames. The reason for non-zero throughput in results is due to the factor that control frames are still transmitted even when the duty cycle is 0, which means all frames are blank or silent. Therefore, as shown in Fig. 5.10 with increase of η from 0.2 to 1 also increases in the throughput of respective users as both operators get to access the medium more often.

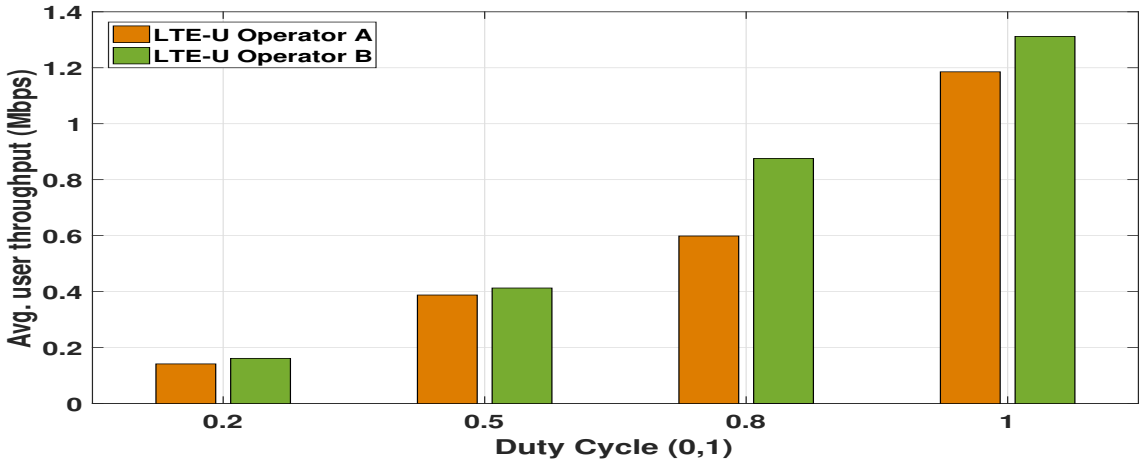

Figure 5.10 : Two LTE-U operators coexisting in unlicensed spectrum with different duty-cycle values.

These results show that LTE should also follow some sensing based listen-before-talk (LBT) coexistence mechanism as well, to coexist peacefully and fairly with WiFi. Only duty cycling is not good enough for LTE to operate without causing a problem to incumbent technologies. Duty-cycle based coexistence could be an acceptable solution when both operators are from LTE-U and employ duty-cycle to share the spectrum equally. The consistency or fairness for channel access cannot be guaranteed when both operators are transmitting without any duty cycle. Fair performance can be achieved when the transmitting device listens for on-going transmissions before contending for channel access. Duty cycle method falls under the category of time-sharing coexistence techniques. Other methods include frequency hopping or sensing based-techniques, which have previously been well discussed in

section 2.4.2 and also numerically evaluated in section 5.2. Time-sharing alone is not sufficient to guarantee fair and peaceful sharing among different technologies operating in the same spectrum and in the same location. Thus, sensing based or hybrid coexistence mechanism are viable solutions for inter and intra technology coexistence in unlicensed spectrum.

5.4 Summary

In this chapter we discussed the comparative performance analysis of coexistence methods for different technologies, mainly for WiFi and LTE in unlicensed spectrum. We used stochastic geometry based Monte-Carlo Simulation and link-level ns3 simulations for feasibility of coexistence among different RATs. The first section also employed FD enabled D2D to study how FD operation affects different coexistence methods employed by LTE. Duty-cycle based discontinuous transmissions for LTE and sensing based LBT access methods were investigated for different duty-cycle (η) and energy detection (Γ_{ed}) threshold values, respectively. SIPR factor is critical in gaining the full advantage of FD technology as it has significant impact on the performance of both the LTE and D2D network. In the second section, we discussed ns3 based simulation results for LTE and WiFi coexistence. Sensing based hybrid coexistence mechanism on the same standard of politeness as WiFi's CSMA is the recommended solution for any incoming RAT to share the spectrum with incumbents.

Chapter 6

Conclusions and Future Work

This chapter summarizes the key contributions made by this research study and highlights the possible future directions to extend this work. The first section presents the abstract level summarization of research work conducted and presented in this dissertation. The second section presents the key contributions made, followed by future research directions to address the emerging research problems in a related field.

6.1 Research Summary

This work started with a comprehensive literature review and taxonomy of key enabling technologies and spectrum sharing frameworks in 5G, a glimpse of which is included with illustrations in Chapter 1. We then critically assessed existing state-of-the-art works using stochastic geometry and other system evaluations tools, discussed advantages, shortcomings and key features in Chapter 2. The main focus of this analysis was to investigate the integration of different technology candidates with legacy technologies and outline the performance trade-offs of this integration. For instance, FD radios have been envisioned to elevate the data rates for smarter end devices. Enabling FD radios in D2D can elevate the performance gains for short-range communications by doubling the data rates while limiting the interference due to short D2D link distances. A feasibility study of FD enabled D2D cognitive networks and the impact of induced interference on the performance of primary users is undertaken in Chapter 3. The limits on FD D2D users ability to successfully communicate by ensuring stringent protections to a primary user

are shown in Chapter 4. Also in this chapter, the dependence of different network configuration parameters on the performance of the D2D network was studied and discussed using numerical simulation. We then investigated in Chapter 5 the performance of different transmission techniques for LTE users and how they impacts on a FD enabled D2Ds performance which is opportunistically sharing the spectrum. Furthermore in Chapter 5 we briefly discussed ns-3-based simulation results for LTE and WiFi coexistence in the sub6GHz band. Finally, the abstract level conclusions are drawn in this chapter below along with possible future research topics to be explored.

6.2 Contributions

The main contribution of the thesis can be summarized as follows,

- We formulated the integration model of a FD enabled D2D cognitive network using stochastic geometry tools for network realization. The stochastic geometry framework concerning an optimal mode selection for D2D users enabled with half-duplex and full-duplex capabilities is proposed, and at the same time protecting receptions of primary users. Specifically, each primary user reception is protected and D2D users opt for a mode based on their proximity to primary users.

- We propose a novel mechanism for mode selection by D2D devices depending on receivers vicinity to PUs guard zones while ensuring this does not impact on the PUs reception for dynamic spectrum sharing frameworks. The proposed mode selection mechanism encourages primary licensees to allow SU operation either in HD or FD modes, as long as the SUs provide agreed-upon interference protection to PUs.

- We derived quantified performance gains for opportunistic spectrum use, com-

plemented by FD radios in terms of probability of successful receptions by both cellular and D2D users. Using the expressions for coverage probabilities, we also present insights into different GZ radius values and their impact on SUs communication. The induced interference from FD use of D2D devices and overall aggregate interference is characterized. The trade-off between interference introduced by FD operation and spectral efficiency due to FD is critically investigated. The simulations results were in line with the analytical expressions derived through stochastic geometry machinery.

- The link distance for D2D communication pair plays a vital role in the aggregate interference. It is evident from simulation results and analytical formulations that shorter link distances limit the impact of induced interference, consequently allowing frequency reuse for other D2D pairs in the spatial domain. We have evaluated the improvement in network capacity for a different distribution of D2D link distances.

- The protection for primary users is ensured through GZs, but how much will it affect the SUs capacity? The impact of stringent or lenient protection for the primary user on the capacity of SUs is thoroughly investigated.

- We evaluated a comparative performance analysis of the main coexistence methods for multiple RATs operating in unlicensed spectrum. We have discussed the impact of different LTE transmission techniques on FD D2D and evaluated the tolerance of D2D users for aggressive transmission by LTE.

- The coexistence of LTE-unlicensed and the most dominant incumbent (WiFi) with polite coexistence approach (CSMA/CA) is studied, where LTE uses a duty-cycle based spectrum sharing method. Furthermore we discussed ns-3 based simulation results of LTE-unlicensed and WiFi coexistence while allowing LTE to transmit with different duty-cycle patterns in an opportunity to

coexist fairly with WiFi.

6.3 Future Work

The research conducted in this thesis can be extended to address various research questions. Efficient spectrum utilization remains a hot research topic and with numerous devices contending for shared spectrum resources, novel approaches to spectrum sharing are needed. Depending on the insights generated and findings from this research, we highlight the following potential research directions to be explored in the future:

- One of the interesting extensions of this work is to use the proposed stochastic geometry model presented in Chapter 3 to discover an optimum guard-zone radius which can provide maximum D2D user capacity. While protecting the primary user receptions with a stringent guard zone, the capacity of secondary users can be increased by carefully assessing the induced interference.

- This work mainly focused on the integration of FD, and D2D in existing cellular networks. This work can be extended to investigate the feasibility of different MAC and physical layer aspects of FD technology. An interesting research problem would be to investigate the performance of different MAC layer designs for FD systems and how they impact on the fairness of medium use with incumbents.

- Currently, the derived formulation for performance metrics in Chapter 3 assumes scheduled LTE transmission for a single user to keep the tractability of the analysis. The model can be extended by considering multiple concurrent cellular users reception and how it affects the D2D network capacity.

- Performance analysis of different LTE transmission techniques has been presented in Chapter 5. An interesting research topic would be to assess the

impact of different medium access control (MAC) mechanisms employed by secondary technology candidates. Rise of FD radios for smarter end devices will require efficient MAC protocols to coexist peacefully with other competitors using the same spectrum.

- The locations of primary and secondary users can be modeled with more appropriate random point processes. Fitting point processes according to users location requires pdf of contact distance distributions, but it might complicate the derivation for expressions of key performance metrics. The dependence among those point processes makes it challenging to capture, yet more realistic insights into system performance can be obtained. Such analysis and research in the future will lead to fruitful contributions.

Bibliography

[1] J. G. Andrews, S. Buzzi, W. Choi, S. V. Hanly, A. Lozano, A. C. Soong, and J. C. Zhang, "What will 5G be?," *IEEE Journal on selected areas in communications*, vol. 32, no. 6, pp. 1065–1082, 2014.

[2] A. Gupta and R. K. Jha, "A survey of 5G network: Architecture and emerging technologies," *IEEE access*, vol. 3, pp. 1206–1232, 2015.

[3] N. Solutions and Networks, "White paper: How can mobile networks deliver 1000 times more capacity by 2020?," white paper, Nokia Networks Insight Newsletter, 2013.

[4] D. J. Law, W. W. Diab, A. Healey, S. B. Carlson, and V. Maguire, "IEEE Industry Connections Ethernet Bandwidth Assessment," report, IEEE802.3 Working Group, July 2012.

[5] C. V. N. Index, "Global Mobile Data Traffic Forecast Update 20142019," white paper, Cisco, February 2015.

[6] G. PPP, "5G Vision: the next generation of communication networks and services," tech. rep., The 5G infrastructure public private partnership, 2015.

[7] S. Yrjölä, P. Ahokangas, and M. Matinmikko, "Evaluation of recent spectrum sharing concepts from business model scalability point of view," in *IEEE International Symposium on Dynamic Spectrum Access Networks (DySPAN)*, pp. 241–250, 2015.

[8] Qualcomm Technologies Inc., "Spectrum for 4G and 5G," whitepaper, San Diego, CA, USA, December 2017.

[9] I. F. Akyildiz, W.-Y. Lee, M. C. Vuran, and S. Mohanty, "NeXt generation/dynamic spectrum access/cognitive radio wireless networks: A survey," *Computer Networks*, vol. 50, no. 13, pp. 2127 – 2159, 2006.

[10] F. Boccardi, R. W. Heath, A. Lozano, T. L. Marzetta, and P. Popovski, "Five disruptive technology directions for 5G," *IEEE Communications Magazine*, vol. 52, no. 2, pp. 74–80, 2014.

[11] E. Hossain and M. Hasan, "5G cellular: key enabling technologies and research challenges," *IEEE Instrumentation and Measurement Magazine*, vol. 18, no. 3, pp. 11–21, 2015.

[12] X. Zhang, W. Cheng, and H. Zhang, "Full-duplex transmission in PHY and MAC layers for 5G mobile wireless networks," *IEEE Wireless Communications*, vol. 22, no. 5, pp. 112–121, 2015.

[13] K. S. Ali, H. ElSawy, M. Alouini, A. Khavasi, and J. Suk, "Modeling Cellular Networks With Full-Duplex D2D Communication: A Stochastic Geometry Approach," *IEEE Transactions on Communications*, vol. 64, no. 10, p. 4409, 2016.

[14] S. Kim and W. Stark, "Full duplex device to device communication in cellular networks," in *International Conference on Computing, Networking and Communications (ICNC)*, pp. 721–725, 2014.

[15] K. T. Hemachandra, N. Rajatheva, and M. Latva-aho, "Sum-rate analysis for full-duplex underlay device-to-device networks," in *IEEE Wireless Communications and Networking Conference (WCNC)*, pp. 514–519, 2014.

[16] S. Ali, N. Rajatheva, and M. Latva-aho, "Full duplex device-to-device communication in cellular networks," in *2014 European Conference on Networks and Communications (EuCNC)*, pp. 1–5, IEEE, 2014.

[17] M. Amjad, F. Akhtar, M. H. Rehmani, M. Reisslein, and T. Umer, "Full-duplex communication in cognitive radio networks: A survey," *IEEE Communications Surveys & Tutorials*, vol. 19, no. 4, pp. 2158–2191, 2017.

[18] Y. Liao, L. Song, Z. Han, and Y. Li, "Full duplex cognitive radio: a new design paradigm for enhancing spectrum usage," *IEEE Communications Magazine*, vol. 53, no. 5, pp. 138–145, 2015.

[19] G. Zheng, I. Krikidis, and B. orn Ottersten, "Full-duplex cooperative cognitive radio with transmit imperfections," *IEEE Transactions on Wireless Communications*, vol. 12, no. 5, pp. 2498–2511, 2013.

[20] Y. Wang, J. Li, L. Huang, Y. Jing, A. Georgakopoulos, and P. Demestichas, "5G mobile: Spectrum broadening to higher-frequency bands to support high data rates," *IEEE Vehicular technology magazine*, vol. 9, no. 3, pp. 39–46, 2014.

[21] T. S. Rappaport, S. Sun, R. Mayzus, H. Zhao, Y. Azar, K. Wang, G. N. Wong, J. K. Schulz, M. Samimi, and F. Gutierrez, "Millimeter wave mobile communications for 5G cellular: It will work!," *IEEE access*, vol. 1, pp. 335–349, 2013.

[22] M. J. Marcus, "5G and" IMT for 2020 and beyond"[Spectrum Policy and Regulatory Issues]," *IEEE Wireless Communications*, vol. 22, no. 4, pp. 2–3, 2015.

[23] 3GPP, "Technical Specification Group Radio Access Network; Evolved Universal Terrestrial Radio Access (E-UTRA); User Equipment (UE) radio trans-

mission and reception (Release 10) ," tech. rep., TS 36.101 V10.19.0, June, 2011.

[24] G. Boudreau, J. Panicker, N. Guo, R. Chang, N. Wang, and S. Vrzic, "Interference coordination and cancellation for 4G networks," *IEEE Communications Magazine*, vol. 47, no. 4, pp. 74–81, 2009.

[25] J. A. Hoffmeyer, "Regulatory and standardization aspects of DSA technologies-global requirements and perspective," in *First IEEE International Symposium on New Frontiers in Dynamic Spectrum Access Networks (DySPAN)*, pp. 700–705, 2005.

[26] J. An, K. Yang, J. Wu, N. Ye, S. Guo, and Z. Liao, "Achieving sustainable ultra-dense heterogeneous networks for 5G," *IEEE Communications Magazine*, vol. 55, no. 12, pp. 84–90, 2017.

[27] T. Nakamura, S. Nagata, A. Benjebbour, Y. Kishiyama, T. Hai, S. Xiaodong, Y. Ning, and L. Nan, "Trends in small cell enhancements in LTE advanced," *IEEE Communications Magazine*, vol. 51, no. 2, pp. 98–105, 2013.

[28] M. Haenggi, J. G. Andrews, F. Baccelli, O. Dousse, and M. Franceschetti, "Stochastic geometry and random graphs for the analysis and design of wireless networks," *IEEE Journal on Selected Areas in Communications*, vol. 27, no. 7, pp. 1029–1046, 2009.

[29] J. G. Andrews, A. K. Gupta, and H. S. Dhillon, "A primer on cellular network analysis using stochastic geometry," *arXiv preprint arXiv:1604.03183*, 2016.

[30] J. G. Andrews, F. Baccelli, and R. K. Ganti, "A tractable approach to coverage and rate in cellular networks," *IEEE Transactions on communications*, vol. 59, no. 11, pp. 3122–3134, 2011.

[31] I. Trigui and S. Affes, "Unified analysis and optimization of D2D communications in cellular Networks over fading channels," *IEEE Transactions on Communications*, vol. 67, no. 1, pp. 724–736, 2019.

[32] M. Naslcheraghi, M. Afshang, and H. S. Dhillon, "Modeling and performance analysis of full-duplex communications in cache-enabled D2D networks," in *IEEE International Conference on Communications (ICC)*, pp. 1–6, 2018.

[33] P. Parida, H. S. Dhillon, and P. Nuggehalli, "Stochastic geometry-based modeling and analysis of citizens broadband radio service system," *IEEE Access*, vol. 5, pp. 7326–7349, 2017.

[34] Y. Li, F. Baccelli, J. G. Andrews, T. D. Novlan, and J. C. Zhang, "Modeling and analyzing the coexistence of Wi-Fi and LTE in unlicensed spectrum," *IEEE Transactions on Wireless Communications*, vol. 15, no. 9, pp. 6310–6326, 2016.

[35] N. Deng, W. Zhou, and M. Haenggi, "Heterogeneous cellular network models with dependence," *IEEE Journal on selected Areas in Communications*, vol. 33, no. 10, pp. 2167–2181, 2015.

[36] H. ElSawy, E. Hossain, and M. Haenggi, "Stochastic geometry for modeling, analysis, and design of multi-tier and cognitive cellular wireless networks: A survey," *IEEE Communications Surveys & Tutorials*, vol. 15, no. 3, pp. 996–1019, 2013.

[37] K. Ali, *Modeling, Analysis, and Design of 5G Networks using Stochastic Geometry*. PhD thesis, King Abdullah University of Science and Technology, Thuwal, Kingdom of Saudi Arabia, 2018.

[38] Y. Mehmood, N. Haider, M. Imran, A. Timm-Giel, and M. Guizani, "M2M Communications in 5G: State-of-the-Art Architecture, Recent Advances, and

Research Challenges," *IEEE Communications Magazine*, vol. 55, pp. 194–201, Sep. 2017.

[39] I. F. Akyildiz, S. Nie, S.-C. Lin, and M. Chandrasekaran, "5G roadmap: 10 key enabling technologies," *Computer Networks*, vol. 106, pp. 17–48, 2016.

[40] R. H. Tehrani, S. Vahid, D. Triantafyllopoulou, H. Lee, and K. Moessner, "Licensed spectrum sharing schemes for mobile operators: A survey and outlook.," *IEEE Communications Surveys and Tutorials*, vol. 18, no. 4, pp. 2591–2623, 2016.

[41] M. D. Mueck, S. Srikanteswara, and B. Badic, "Spectrum sharing: Licensed shared access (LSA) and spectrum access system (SAS)," *Intel White Paper*, 2015.

[42] ETSI, "Reconfigurable Radio Systems (RRS); System architecture and high level procedures for operation of Licensed Shared Access (LSA) in the 2300 MHz-2400 MHz band," *ETSI Technical Report*, 2015.

[43] M. Palola, M. Matinmikko, J. Prokkola, M. Mustonen, M. Heikkila, T. Kippola, S. Yrjola, V. Hartikainen, L. Tudose, A. Kivinen, *et al.*, "Live field trial of Licensed Shared Access (LSA) concept using LTE network in 2.3 GHz band," in *IEEE International Symposium on Dynamic Spectrum Access Networks (DYSPAN)*, pp. 38–47, 2014.

[44] J. Fang, T. Lin, C. Chang, C. Yang, H. Su, C. Lu, B. Wang, C. Hung, P. Chiu, M. Wang, *et al.*, "Licensed shared access by mobile networks: Proof-of-concept demonstration over ViSSA platform," in *IEEE/IFIP Network Operations and Management Symposium (NOMS)*, pp. 1–2, 2018.

[45] P. Ahokangas, M. Matinmikko, S. Yrjola, M. Mustonen, H. Posti, E. Luttinen, and A. Kivimaki, "Business models for mobile network operators in Licensed

Shared Access (LSA)," in *IEEE International Symposium on Dynamic Spectrum Access Networks (DYSPAN)*, pp. 263–270, 2014.

[46] X. Ding, C.-H. Liu, L.-C. Wang, and X. Zhao, "Coexisting Success and Throughput of Multi-RAT Wireless Networks with Unlicensed Band Access," *IEEE Wireless Communications Letters*, vol. PP, no. 99, pp. 1–1, 2015.

[47] J. Jeongho, N. Huaning, Q. C. Li, A. Papathanassiou, and W. Geng, "LTE in the unlicensed spectrum: Evaluating coexistence mechanisms," in *IEEE Globecom Workshops (GC Wkshps), 2014*, pp. 740–745.

[48] M. I. Rahman, A. Behravan, H. Koorapaty, J. Sachs, and K. Balachandran, "License-exempt LTE systems for secondary spectrum usage: Scenarios and first assessment," in *IEEE Symposium on New Frontiers in Dynamic Spectrum Access Networks (DySPAN)*, pp. 349–358.

[49] Alcatel-Lucent, Ericsson, Q. I. Technologies, Verizon, and S. Electronics, "LTE-U Technical Report Coexistence Study for LTE-U SDL V1.0," technical report, LTE-U Forum, February 2015.

[50] R. Ratasuk, N. Mangalvedhe, and A. Ghosh, "LTE in unlicensed spectrum using licensed-assisted access," in *Globecom Workshops (GC Wkshps), 2014*, pp. 746–751.

[51] X. Yang, Y. Rui, C. Qimei, and Y. Guanding, "Joint licensed and unlicensed spectrum allocation for unlicensed LTE," in *IEEE 26th Annual International Symposium on Personal, Indoor, and Mobile Radio Communications (PIMRC)*, pp. 1912–1917.

[52] J. Yubing, S. Chao-Fang, B. Krishnaswamy, and R. Sivakumar, "Coexistence of Wi-Fi and LAA-LTE: Experimental evaluation, analysis and insights,"

in *IEEE International Conference on Communication Workshop (ICCW)*, pp. 2325–2331.

[53] A. Al-Dulaimi, S. Al-Rubaye, Q. Ni, and E. Sousa, "5G communications race: Pursuit of more capacity triggers LTE in unlicensed band," *IEEE Vehicular Technology Magazine*, vol. 10, no. 1, pp. 43–51, 2015.

[54] ETSI, "Broadband Radio Access Networks (BRAN); 5 GHz high performance RLAN," report, ETSI, 2012. (2012-06), EN 301 893 V1.7.1.

[55] A. K. Sadek, "Carrier sense adaptive transmission (CSAT) coordination in unlicensed spectrum," June 11 2015. US Patent App. 14/566,068.

[56] M. Hirzallah, W. Afifi, and M. Krunz, "Full-duplex-based rate/mode adaptation strategies for Wi-Fi/LTE-U coexistence: A POMDP approach," *IEEE Journal on Selected Areas in Communications*, vol. 35, no. 1, pp. 20–29, 2016.

[57] Y. Jian, U. P. Moravapalle, C.-F. Shih, and R. Sivakumar, "Duet: An adaptive algorithm for the coexistence of LTE-U and WiFi in Unlicensed spectrum," in *International Conference on Computing, Networking and Communications (ICNC)*, pp. 19–25, IEEE, 2017.

[58] S. S. Sagari, "Coexistence of LTE and WiFi heterogeneous networks via inter network coordination," in *Proceedings of the 2014 workshop on PhD forum*, pp. 1–2, ACM, 2014.

[59] S. Sagari, I. Seskar, and D. Raychaudhuri, "Modeling the coexistence of LTE and WiFi heterogeneous networks in dense deployment scenarios," in *2015 IEEE international conference on communication workshop (ICCW)*, pp. 2301–2306, IEEE, 2015.

[60] A. M. Cavalcante, E. Almeida, R. D. Vieira, S. Choudhury, E. Tuomaala,

K. Doppler, F. Chaves, R. C. Paiva, and F. Abinader, "Performance evaluation of LTE and Wi-Fi coexistence in unlicensed bands," in *2013 IEEE 77th Vehicular Technology Conference (VTC Spring)*, pp. 1–6, IEEE, 2013.

[61] T. Nihtilä, V. Tykhomyrov, O. Alanen, M. A. Uusitalo, A. Sorri, M. Moisio, S. Iraji, R. Ratasuk, and N. Mangalvedhe, "System performance of LTE and IEEE 802.11 coexisting on a shared frequency band," in *2013 IEEE Wireless Communications and Networking Conference (WCNC)*, pp. 1038–1043, IEEE, 2013.

[62] E. Almeida, A. M. Cavalcante, R. C. Paiva, F. S. Chaves, F. M. Abinader, R. D. Vieira, S. Choudhury, E. Tuomaala, and K. Doppler, "Enabling LTE/WiFi coexistence by LTE blank subframe allocation," in *2013 IEEE International Conference on Communications (ICC)*, pp. 5083–5088, IEEE, 2013.

[63] I.-K. Fu and W. Plumb, "Method of in-device interference mitigation for cellular, bluetooth, WiFi, and satellite systems coexistence," Jan. 26 2016. US Patent 9,246,603.

[64] Q. Ye, M. Al-Shalash, C. Caramanis, and J. G. Andrews, "Resource optimization in device-to-device cellular systems using time-frequency hopping," *IEEE Transactions on Wireless Communications*, vol. 13, no. 10, pp. 5467–5480, 2014.

[65] F. Belghoul, T. Tabet, and D. Zhang, "Method and apparatus for frequency hopping coexistence in unlicensed radio frequency bands for mobile devices," Jan. 3 2017. US Patent 9,537,642.

[66] E. ETSI, "301 893 v1. 8.1 (2015-03). Broadband Radio Access Networks (BRAN); 5 GHz high performance RLAN; Harmonized EN covering the es-

sential requirements of article 3.2 of the R&TTE Directive," *Harmonized European Standard*, 2015.

[67] Y. Li, J. Zheng, and Q. Li, "Enhanced listen-before-talk scheme for frequency reuse of licensed-assisted access using LTE," in *IEEE 26th Annual International Symposium on Personal, Indoor, and Mobile Radio Communications (PIMRC)*, pp. 1918–1923, 2015.

[68] C. Cano, D. J. Leith, A. Garcia-Saavedra, and P. Serrano, "Fair coexistence of scheduled and random access wireless networks: Unlicensed LTE/WiFi," *IEEE/ACM Transactions on Networking*, vol. 25, no. 6, pp. 3267–3281, 2017.

[69] C. Chen, R. Ratasuk, and A. Ghosh, "Downlink Performance Analysis of LTE and WiFi Coexistence in Unlicensed Bands with a Simple Listen-Before-Talk Scheme," in *IEEE 81st Vehicular Technology Conference (VTC Spring)*, pp. 1–5.

[70] C. K. Kim, C. S. Yang, and C. G. Kang, "Adaptive listen-before-talk (LBT) scheme for LTE and Wi-Fi systems coexisting in unlicensed band," in *2016 13th IEEE Annual Consumer Communications & Networking Conference (CCNC)*, pp. 589–594, IEEE, 2016.

[71] A. D. Wyner, "Shannon-theoretic approach to a gaussian cellular multiple-access channel," *IEEE Transactions on Information Theory*, vol. 40, no. 6, pp. 1713–1727, 1994.

[72] K. S. Gilhousen, I. M. Jacobs, R. Padovani, A. J. Viterbi, L. A. Weaver, and C. E. Wheatley, "On the capacity of a cellular CDMA system," *IEEE transactions on vehicular technology*, vol. 40, no. 2, pp. 303–312, 1991.

[73] M.-S. Alouini and A. J. Goldsmith, "Area spectral efficiency of cellular mobile radio systems," *IEEE Transactions on vehicular technology*, vol. 48, no. 4,

pp. 1047–1066, 1999.

[74] J.-P. Linnartz, "Exact analysis of the outage probability in multiple-user mobile radio," *IEEE transactions on communications*, vol. 40, no. 1, pp. 20–23, 1992.

[75] S. N. Chiu, D. Stoyan, W. S. Kendall, and J. Mecke, *Stochastic geometry and its applications*. John Wiley & Sons, 2013.

[76] M. Haenggi, *Stochastic Geometry for Wireless Networks*. Cambridge University Press, 2012.

[77] H. ElSawy, A. Sultan-Salem, M.-S. Alouini, and M. Z. Win, "Modeling and analysis of cellular networks using stochastic geometry: A tutorial," *IEEE Communications Surveys & Tutorials*, vol. 19, no. 1, pp. 167–203, 2016.

[78] A. Ali, "Load-aware modelling in cellular networks with repulsively deployed base stations," Master's thesis, Macquarie University, Australia, 2015.

[79] F. Baccelli, B. Błaszczyszyn, *et al.*, "Stochastic geometry and wireless networks: Volume II Applications," *Foundations and Trends® in Networking*, vol. 4, no. 1–2, pp. 1–312, 2010.

[80] H. ElSawy, E. Hossain, and M. Haenggi, "Stochastic geometry for modeling, analysis, and design of multi-tier and cognitive cellular wireless networks: A survey," *IEEE Communications Surveys Tutorials*, vol. 15, no. 3, pp. 996–1019, 2013.

[81] W. Kendall, J. Mecke, and D. Stoyan, "Stochastic geometry and its applications," 1995.

[82] F. Baccelli, M. Klein, M. Lebourges, and S. Zuyev, "Stochastic geometry and architecture of communication networks," *Telecommunication Systems*, vol. 7,

no. 1-3, pp. 209–227, 1997.

[83] S. Weber, J. G. Andrews, and N. Jindal, "Transmission capacity: applying stochastic geometry to uncoordinated ad hoc networks," *IEEE Journal on Sel. Areas in Communications*, 2008.

[84] M. Haenggi, "On distances in uniformly random networks," *IEEE Transactions on Information Theory*, vol. 51, no. 10, pp. 3584–3586, 2005.

[85] F. Baccelli and B. Błaszczyszyn, "Stochastic Geometry and Wireless Networks, Volume ITheory, of Foundations and Trends in Networking," 2009.

[86] M. Z. Win, P. C. Pinto, and L. A. Shepp, "A mathematical theory of network interference and its applications," *Proceedings of the IEEE*, vol. 97, no. 2, pp. 205–230, 2009.

[87] S. Weber, J. G. Andrews, and N. Jindal, "An overview of the transmission capacity of wireless networks," *IEEE Transactions on Communications*, vol. 58, no. 12, pp. 3593–3604, 2010.

[88] H. S. Dhillon, R. K. Ganti, F. Baccelli, and J. G. Andrews, "Modeling and analysis of K-tier downlink heterogeneous cellular networks," *IEEE Journal on Selected Areas in Communications*, vol. 30, no. 3, pp. 550–560, 2012.

[89] M. Haenggi, "User point processes in cellular networks," *IEEE Wireless Communications Letters*, vol. 6, no. 2, pp. 258–261, 2017.

[90] S. S. Kalamkar and M. Haenggi, "The spatial outage capacity of wireless networks," *IEEE Transactions on Wireless Communications*, vol. 17, no. 6, pp. 3709–3722, 2018.

[91] H. Chen, L. Liu, H. S. Dhillon, and Y. Yi, "QoS-Aware D2D Cellular Networks with Spatial Spectrum Sensing: A Stochastic Geometry View," *IEEE*

Transactions on Communications, 2018.

[92] N. Haider, A. Ali, C. Suarez-Rodriguez, and E. Dutkiewicz, "Optimal Mode Selection for Full-Duplex Enabled D2D Cognitive Networks," *IEEE Access*, vol. 7, pp. 57298–57311, 2019.

[93] J. M. Peha, "Approaches to spectrum sharing," *IEEE Communications magazine*, vol. 43, no. 2, pp. 10–12, 2005.

[94] K. Khan and A. Jamalipour, "Coverage Analysis for Multi-Request Association Model (MRAM) in a Caching Ultra-Dense Network," *IEEE Transactions on Vehicular Technology*, pp. 1–1, 2019.

[95] J. Lee and T. Q. Quek, "Device-to-device communication in wireless mobile social networks," in *IEEE 79th Vehicular Technology Conference (VTC Spring)*, pp. 1–5, 2014.

[96] N. T. Viet and F. Baccelli, "Stochastic modeling of carrier sensing based cognitive radio networks," in *Proceedings of the 8th International Symposium on Modeling and Optimization in Mobile, Ad Hoc and Wireless Networks (WiOpt)*, pp. 472–480, 2010.

[97] A. Ali and A. Hasan, "Stochastic geometry of thinned nodes in ad hoc networks," in *9th IEEE International Bhurban Conference on Applied Sciences and Technology (IBCAST)*, pp. 431–435, 2012.

[98] C. Lee and M. Haenggi, "Interference and outage in Poisson cognitive networks," *IEEE Transactions on Wireless Communications*, vol. 11, no. 4, pp. 1392–1401, 2012.

[99] M. M. Deshmukh, S. Zafaruddin, A. Mihovska, and R. Prasad, "Stochastic-Geometry Based Characterization of Aggregate Interference in TVWS Cognitive Radio Networks," *IEEE Systems Journal*, 2019.

[100] L. Vijayandran, P. Dharmawansa, T. Ekman, and C. Tellambura, "Analysis of aggregate interference and primary system performance in finite area cognitive radio networks," *IEEE Transactions on Communications*, vol. 60, no. 7, pp. 1811–1822, 2012.

[101] A. Hasan and A. Ali, "Guard zone-based scheduling in ad hoc networks," *Computer Communications*, vol. 56, pp. 89 – 97, 2015.

[102] Z. Tong and M. Haenggi, "Throughput analysis for full-duplex wireless networks with imperfect self-interference cancellation," *IEEE Transactions on Communications*, vol. 63, no. 11, pp. 4490–4500, 2015.

[103] Z. Yazdanshenasan, H. S. Dhillon, M. Afshang, and P. H. J. Chong, "Poisson hole process: Theory and applications to wireless networks," *IEEE Transactions on Wireless Communications*, vol. 15, no. 11, pp. 7531–7546, 2016.

[104] J. Lee and T. Q. S. Quek, "Device-to-Device Communication in Wireless Mobile Social Networks," in *2014 IEEE 79th Vehicular Technology Conference (VTC Spring)*, pp. 1–5, May 2014.

[105] H. ElSawy, E. Hossain, and M.-S. Alouini, "Analytical modeling of mode selection and power control for underlay D2D communication in cellular networks," *IEEE Transactions on Communications*, vol. 62, no. 11, pp. 4147–4161, 2014.

[106] "Circle." http://www.ambrsoft.com/TrigoCalc/Sphere/Arc_htm. *Accessed* : 29 − 12 − 2018.

[107] N. Haider, A. Ali, Y. He, and E. Dutkiewicz, "Performance Analysis of Full Duplex D2D in Opportunistic Spectrum Access," in *2018 18th International Symposium on Communications and Information Technologies (ISCIT)*, pp. 32–37, IEEE, 2018.

[108] UMTS Forum, "Mobile traffic forecasts: 2010-2020 report," report, January 2011. UMTS Forum Report # 44.

[109] ITU, "ITU ICT Facts and Figures The world in 2015," report, International Telecommunications Unit ITU, 2015.

[110] H. Q. Nguyen, F. Baccelli, and D. Kofman, "A stochastic geometry analysis of dense IEEE 802.11 networks," in *26th IEEE International Conference on Computer Communications (INFOCOM)*, pp. 1199–1207, 2007.

[111] N. Haider, E. Dutkiewicz, D. N. Nguyen, M. Mueck, and S. Srikanteswarae, "The Impact on Full Duplex D2D Communication of Different LTE Transmission Techniques," in *2017 IEEE 85th Vehicular Technology Conference (VTC Spring)*, pp. 1–5, June 2017.

[112] I. Trigui and S. Affes, "Unified analysis and optimization of D2D communications in cellular Networks over fading channels," *IEEE Transactions on Communications*, vol. 67, no. 1, pp. 724–736, 2018.

[113] W. Afifi and M. Krunz, "Incorporating self-interference suppression for full-duplex operation in opportunistic spectrum access systems," *IEEE Transactions on Wireless Communications*, vol. 14, no. 4, pp. 2180–2191, 2014.

[114] W. Afifi and M. Krunz, "Adaptive transmission-reception-sensing strategy for cognitive radios with full-duplex capabilities," in *2014 IEEE International Symposium on Dynamic Spectrum Access Networks (DYSPAN)*, pp. 149–160, IEEE, 2014.

[115] B. A. Jayawickrama, Y. He, E. Dutkiewicz, and M. D. Mueck, "Scalable Spectrum Access System for Massive Machine Type Communication," *IEEE Network*, pp. 1–7, 2018.

[116] J. Guo, S. Durrani, and X. Zhou, "Performance analysis of arbitrarily-shaped underlay cognitive networks: Effects of secondary user activity protocols," *IEEE Transactions on Communications*, vol. 63, no. 2, pp. 376–389, 2015.

[117] J. Guo, S. Durrani, and X. Zhou, "Characterization of aggregate interference in arbitrarily-shaped underlay cognitive networks," in *IEEE Global Communications Conference*, pp. 961–966, 2014.

[118] Z. Tong and M. Haenggi, "Throughput analysis for full-duplex wireless networks with imperfect self-interference cancellation," *IEEE Transactions on Communications*, vol. 63, no. 11, pp. 4490–4500, 2015.

[119] D. N. Nguyen and M. Krunz, "Be responsible: A novel communications scheme for full-duplex MIMO radios," in *2015 IEEE Conference on Computer Communications (INFOCOM)*, pp. 1733–1741, IEEE, 2015.

[120] Y. Wu, W. Guo, H. Yuan, L. Li, S. Wang, X. Chu, and J. Zhang, "Device-to-device meets LTE-unlicensed," *IEEE Communications Magazine*, vol. 54, no. 5, pp. 154–159, 2016.

[121] Q. Chen, G. Yu, A. Maaref, G. Y. Li, and A. Huang, "Rethinking mobile data offloading for lte in unlicensed spectrum," *IEEE Transactions on Wireless Communications*, vol. 15, no. 7, pp. 4987–5000, 2016.

[122] H. Zhang, X. Chu, W. Guo, and S. Wang, "Coexistence of Wi-Fi and heterogeneous small cell networks sharing unlicensed spectrum," *IEEE Communications Magazine*, vol. 53, no. 3, pp. 158–164, 2015.

[123] M. Haenggi, J. G. Andrews, F. Baccelli, O. Dousse, and M. Franceschetti, "Stochastic geometry and random graphs for the analysis and design of wireless networks," *IEEE Journal on Selected Areas in Communications*, vol. 27, no. 7, pp. 1029–1046, 2009.

[124] A. Galanopoulos, F. Foukalas, and T. A. Tsiftsis, "Efficient Coexistence of LTE With WiFi in the Licensed and Unlicensed Spectrum Aggregation," *IEEE Transactions on Cognitive Communications and Networking*, vol. 2, no. 2, pp. 129–140, 2016.

[125] T. Henderson, "LTE LBT Wi-Fi Coexistence Module," *ns-3 project, Tech. Rep*, vol. 2, 2016.

[126] B. Bojovic, L. Giupponi, T. R. Henderson, and M. Miozzo, "Coexistence simulation results for DL only LAA, Document for: Discussion and Decision," report, 3rd Generation Partnership Project, November 2015 2015.

[127] L. Giupponi, T. Henderson, B. Bojovic, and M. Miozzo, "Simulating LTE and Wi-Fi coexistence in unlicensed spectrum with NS-3," *arXiv preprint arXiv:1604.06826*, 2016.

[128] M. Alliance, "Multefire release 1.0 technical paper: A new way to wireless," *White paper, January*, 2017.